APPLICATION OF MODELING AND ANALYTICAL METHODS FOR CHARACTERIZING AQUATIC TOXICITY AND TOXICOKINETICS OF PETROLEUM SUBSTANCES

by

Aaron David Redman

A dissertation submitted to the Faculty of the University of Delaware in partial fulfillment of the requirements for the degree of Doctor of Philosophy in Civil Engineering

Spring 2018

APPLICATION OF MODELING AND ANALYTICAL METHODS FOR CHARACTERIZING AQUATIC TOXICITY AND TOXICOKINETICS OF PETROLEUM SUBSTANCES

by

Aaron David Redman

Approved: _____
Sue McNeil, Ph.D.
Chair of the Department of Civil and Environmental Engineering

Approved: _____
Babatunde Ogunnaike, Ph.D.
Dean of the College of Engineering

Approved: _____
Ann L. Ardis, Ph.D.
Senior Vice Provost for Graduate and Professional Education

I certify that I have read this dissertation and that in my opinion it meets the academic and professional standard required by the University as a dissertation for the degree of Doctor of Philosophy.

Signed: _____

Dominic M. Di Toro, Ph.D.
Professor in charge of dissertation

I certify that I have read this dissertation and that in my opinion it meets the academic and professional standard required by the University as a dissertation for the degree of Doctor of Philosophy.

Signed: _____

Pei Chiu, Ph.D.
Member of dissertation committee

I certify that I have read this dissertation and that in my opinion it meets the academic and professional standard required by the University as a dissertation for the degree of Doctor of Philosophy.

Signed: _____

Jonathan H. Cohen, Ph.D.
Member of dissertation committee

I certify that I have read this dissertation and that in my opinion it meets the academic and professional standard required by the University as a dissertation for the degree of Doctor of Philosophy.

Signed: _____

William Stubblefield, Ph.D.
Member of dissertation committee

ACKNOWLEDGMENTS

Thank you first to my wife, Debbie, and my children for their love and support that gave me the motivation to finish this degree. Also, thank you for my co-workers at ExxonMobil for their technical and moral support that greatly improved the quality of the work presented here. And thank you to my advisor, Professor Di Toro, and to Kathy Werrell for making this ride as smooth as possible.

TABLE OF CONTENTS

Appendix

LIST OF TABLES

LIST OF FIGURES

INTRODUCTION

Petroleum substances such as crude oils, solvents, and fuels are complex materials comprised of dozens to several thousand individual constituents, whose physicochemical properties span several orders of magnitude. This translates into a mixture of constituents with widely variable toxicity, all present at different concentrations. Further, various exposure systems are used to perform toxicity tests (e.g., oiled gravel, with dispersant, etc), which can alter the results [1].

This results in conflicting conclusions and inconsistent interpretation of toxicity studies on petroleum substances. There is a need for a conceptual and quantitative framework for evaluating risks and hazards of petroleum substances. These challenges were addressed with the development of the hydrocarbon block method (HBM), which divided up a petroleum substance into narrowly defined blocks of constituents with similar properties [2].

Since this initial work advances in the analytical characterization have the potential to refine risk assessments. Development of two dimensional GC methods (GCxGC) provides more comprehensive characterization of the chemical class and mass distribution within a substance. The initial HBM work was extended to accommodate this improved analytical methods for hazard assessment [3] and risk assessment [4].

The modeling provides a mechanistic connection between the composition and the toxicity. However, the GCxGC data that is commonly used in the present work is not widely available to the general research community. Therefore, an analytical tool

has been developed to measure bioavailable hydrocarbons. This is based on the commonly available solid phase microextration (SPME) methods using siloxane polymer-coated fibers. These methods have been modified for measurement of bioavailable hydrocarbons, which can be related to toxicity [5]. The fibers provide an analytical analog to a toxic unit (TU), which characterize the sum of the fractional toxicity of all the hydrocarbon constituents present in an exposure.

The modeling and analytical tools typically are used to analyze results of steady state exposures. In the environment, however, exposures can vary in time and space such as during an oil spill, or downstream from an outfall, or a contaminated site. Only recently have time variable tools been developed for these scenarios [6, 7] with limited application to oil spill scenarios [8, 9]. This remains an open field of research and will be addressed in the final third of this research proposal.

There are three main research themes in this dissertation proposal. These all address the various research areas discussed above. The major research theme is refined hazard and risk assessment of petroleum substances. The components of this research will provide stronger scientific basis and guidance to the research community and will support setting scientifically sound environmental criteria.

The first chapter is based on a paper published in *Chemosphere* [10]summarizes an analysis of a large library of internal SPME data to validate use of this method to measure bioavailable hydrocarbons. The SPME method provides a holistic measurement of the overall exposure and is compared to observed toxicity for a wide variety of substances, and test species. The SPME method is an operationally method (e.g., equilibration time, fiber-water volumes, etc) with a mechanistic basis using the observed correlation between the SPME measurement and toxicity. This

was done by comparing SPME measurements to predicted toxic units using the PETROTOX modeling framework. This analysis shows a consistent log-linear relationship between accumulation in target lipid and SPME across all substance classes and confirms the utility of the SPME method for risk assessment work for both laboratory and field work. The fiber-based effect levels were compared to lipid-based effect levels using empirical measurements and single- and polyparameter models.

The second chapter is published in *Environmental Toxicology and Chemistry* [11] that characterizes the role of droplet oil in aquatic exposures. This is an issue that is important during oil spill damage assessments [12]. Chapter one presents results of experimental work where exposures were prepared with a gradient of droplet exposures. The results were analyzed using the state of the art analytical tools discussed above (PETROTOX [3] and SPME [5]). The main conclusion is that dissolved hydrocarbons are the primary toxicant and that the direct impact of droplet oil is minimal.

The third chapter addressed adaptation of existing time variable damage models for prediction of toxicity of complex petroleum substances. This project involved a modeling analysis of existing data as well as some experimental data to support initial model development. Most applications of this modeling framework in the literature are for single chemicals. This work calibrated this model to available single chemical data and evaluated the variation in these parameters against $\log K_{OW}$, organism weight, and test temperature. The existing data are generally from standard toxicity tests with constant exposures. However, observations of toxicity are collected at intermediate time steps. These data will help establish the damage-repair

relationships for individual chemicals across a range of physicochemical properties, which supports modeling of the complex substance toxicity data.

Chapter 1

TECHNICAL BASIS FOR USING PASSIVE SAMPLING AS A BIOMIMETIC EXTRACTION PROCEDURE TO ASSESS BIOAVAILABILITY AND PREDICT TOXICITY OF PETROLEUM SUBSTANCES

1.1 Abstract

Solid-phase microextraction fibers coated with polydimethylsiloxane (PDMS) provide a convenient passive sampling format to characterize bioavailability of petroleum substances. Hydrocarbons absorb onto PDMS in proportion to both freely dissolved concentrations and partitioning properties of the individual constituents, which parallels the mechanistic basis used to predict aquatic toxicity in the PETROTOX model. When deployed in a non-depletive manner, combining SPME with thermal desorption and quantification using gas chromatography-flame ionization creates a biomimetic extraction (BE) procedure that has the potential to simplify aquatic hazard assessments of petroleum substances since the total moles of all hydrocarbons sorbed to the fiber can be related to toxic thresholds in target lipid of aquatic organisms. The objective of this work is to describe the technical basis for applying BE measurements to predict toxicity of petroleum substances. Critical BE-based PDMS concentrations corresponding to adverse effects were empirically derived from toxicity tests on different petroleum substances with multiple test species. The resulting species sensitivity distribution (SSD) of PDMS effect concentrations was then compared and found consistent with the previously reported target lipid-based SSD. Further, BE data collected on samples of aqueous media dosed with a wide

range of petroleum substances were highly correlated to predicted toxic units derived using the PETROTOX model. These findings provide justification for applying BE in environmental hazard and risk evaluations of petroleum substances and related mixtures.

1.2 Introduction

Environmental contaminants often occur as mixtures, which complicate risk and hazard assessments due to the variable toxicity and physicochemical properties of the individual constituents in the mixture. Petroleum substances are an important class of contaminants due to their wide-spread use in commercial products and chemical intermediates but also due to anthropogenic and natural releases of hydrocarbons through seeps or deposits and combustion [13, 14]. The hydrocarbon constituents in petroleum substances have a wide range in physicochemical properties including water solubility and vapor pressure [15, 16]. These properties span several orders of magnitude for individual constituents even within the same petroleum substance. Further, the abundance of constituents within a substance can vary based on the source of crude oil, refinery processes (e.g., distillation), and natural weathering processes once substances are emitted into the environment.

One approach to address this complexity is to use coupled fate and effects models that account for the complex composition of a petroleum substance as well as the differential physicochemical properties of the individual constituents within the substance. The hydrocarbon block method is an example of this approach, which reduces the complexity of petroleum substances into more narrowly-defined blocks, or pseudoconstituents [2]. The compositional data is used to determine the mole fraction of a given block and the dissolution is computed using Raoult's Law [17]. The

toxicity of the dissolved pseudoconstituents is determined using critical body burden models, such as the Target Lipid Model (TLM) [18-20]. The TLM simulates the accumulation of hydrocarbon into a hypothetical target lipid phase and toxicity occurs when the sum of all accumulated hydrocarbons exceed a critical threshold in this phase. This modeling approach has been formalized in the PETROTOX model which provides a predictive tool to estimate aquatic toxicity of petroleum substances based on substance composition [3, 21].

The complexity inherent in evaluating the toxicity of petroleum substances is one reason bulk exposure metrics, such as total polycyclic aromatic hydrocarbons (TPAH) or total petroleum hydrocarbon (TPH), serve as imprecise hazard assessment metrics [1]. The practical challenge, however, is that detailed compositional analysis of dissolved hydrocarbon constituents is often not available to support an improved technical basis for quantitative risk assessment. Therefore, a need exists for a convenient analytical measurement that directly quantifies the bioavailability of all petroleum hydrocarbons that can contribute to toxicity. The growing application of passive sampling methods for environmental monitoring [22] and hazard assessment of physically and chemically dispersed oils [5] provides further motivation for evaluating the technical basis of this analytical approach. Solid phase microextraction (SPME) provides a convenient passive sampling format that can support hazard and risk assessment by providing measurements of freely dissolved contaminants [22]. Individual constituents partition to polydimethysiloxane (PDMS) coated fibers in proportion to substance partitioning properties and abundance in the exposure media, which is analogous to the fundamental concepts (e.g., accumulation in target lipid) used in the PETROTOX model.

Most applications of SPME to environmental media characterize the concentrations of individual constituents [22, 23]. For exposures to petroleum substances, many unresolved constituents can contribute to aquatic toxicity [24], which are not captured in GC-MS analysis which quantifies only a limited set of individual hydrocarbon analytes. SPME-based methods that employ GC-FID provide a potential solution since the molar response of diverse hydrocarbons is similar based on quantification with flame ionization detection [14]. Thus, by measuring the total molar accumulation of hydrocarbons on fiber PDMS, a surrogate measurement of total petroleum hydrocarbon bioavailability is provided. The particular application of SPME in the present work is performed in a non-depletive manner by employing a low PDMS-water ratio so that the accumulation on the fiber does not significantly reduce exposure concentrations, a so-called biomimetic extraction (BE) [5]. This design is consistent with the intent of aquatic hazard testing, where uptake of chemicals by test organisms are not expected to deplete the exposure concentrations.

The goal of this work is to extend the validation of the BE method [5, 25-28] for use in hazard assessments of petroleum substances through analysis of toxicity data sets including a broader diversity of test species and petroleum substances. Validation was done in successive steps. First, empirical BE-based critical effect concentrations were derived that correspond to observed acute and sublethal effects (e.g., LC50, EC50). The BE critical effect concentrations derived from paired toxicity test and BE data for different petroleum substances were then compared to target-lipid based effect concentrations obtained via application of the TLM. Second, BE measurements collected on samples of aqueous media dosed with a wide range of petroleum substances were compared for consistency with PETROTOX model

predictions. Lastly, polyparameter linear free energy relationships (ppLFER) were then applied to gain further insights on the comparative partitioning behavior of different hydrocarbon classes between target lipid and the surrogate PDMS phase.

1.3 Materials And Methods

A dataset of consistent, high quality ecotoxicity, BE, and substance compositional data are used as the basis for analysis in the present study. The BE method is based on more than 20 years of development and application [5, 26, 29]. The validation datasets include hundreds of individual BE measurements across 16 major classes of substances (Table 1) and for 11 test organisms including juvenile and fish embryos, marine and freshwater invertebrates, and algae. The present study builds on a prior toxicity modeling analysis [21] by relating many of those same published data to corresponding BE measurements performed in one laboratory (e.g., ExxonMobil Biomedical Sciences, Inc, Annandale, New Jersey USA).

Passive sampling methods

Automated BE-SPME analysis was performed on a Perkin Elmer Autosystem gas chromatograph with flame ionization detector (GC-FID). The GC was equipped with a 15 m x 0.53 mm id capillary column with 1.5 µm Rtx-1 stationary phase (Restek) or equivalent and interfaced with a Gerstel (CTC Analytics) MultiPurpose Sampler (MPS) configured for automated SPME injections. The GC inlet was maintained at 280^{o}C and contained an empty 1 mm id (narrow bore) liner (no glass wool). Automated SPME fiber injections were made in the splitless mode with a split time of three minutes. The carrier gas was helium at a constant flow rate of 17 mL/min. The GC oven was temperature programed from 40^{o}C for three minutes up to

300°C at a rate of 45°C/minute. The FID temperature was 300°C and the detector signal attenuation was -3.

Water samples were placed in ca. 20 mL glass vials with no headspace and sealed with Teflon® faced septum screw caps. Samples were automatically extracted with a 1 cm, 30 µm polydimethylsiloxane (0.132 µL PDMS) SPME fiber (Supelco) for 100 minutes at 30°C with orbital agitation at 250 rpm prior to injection. The fiber was automatically thermally desorbed for three minutes directly in the GC injection port. The SPME fiber was thermally cleaned for at least sixty minutes at 280°C in the SPME fiber backout accessory or injection port prior to initiation of the SPME sample sequence. Blank, temperature-programmed GC runs were also acquired prior to the sample sequence to ensure that a clean chromatographic baseline was achieved. A single SPME fiber was used for each sample sequence.

The BE method was calibrated by making 0.5 µL liquid (solvent) injections using the air-gap technique. A series of aromatic hydrocarbon standards (toluene, o-xylene, 2-methylnaphthalene, 2,3-dimethylnaphthalene and 9-methylanthracene) in dichloromethane were manually injected. The FID detector provides uniform response between chemical classes such that both aromatic and aliphatic hydrocarbons have similar response factors [5]. Therefore, the aromatic standards are considered sufficiently representative of the mixtures of hydrocarbons that absorb to the SPME fibers. The instrument conditions were exactly the same as those used to analyze the SPME fiber extracts, except that the splitless injection split time was reduced to one minute to accommodate the solvent peak. Calibration was performed at three concentration levels, of 2,3-dimethylnaphthalene, (approximately 20, 100 and 200 µg/mL) corresponding to on-column amounts of approximately 0.06, 0.3 and 0.6

nanomoles. The average molar response factor of 2,3-dimethylnaphthalene was used to convert the measured GC-FID response (total integrated area) to nanomoles of organic constituents on the PDMS fiber. Where necessary, SPME sample chromatograms were digitally background corrected by subtraction with a blank GC chromatographic run, to account for column bleed. Chromatograms were acquired and processed using Perkin Elmer TotalChrom chromatographic software. Integration parameters were optimized specifically for each sample type to integrate the area under the curve attributable to the SPME extracted sample.

As the automated SPME extraction was performed at 30°C, a temperature correction factor of 1.08 was applied to normalize results to a previously applied manual technique where extraction took place at room temperature (22°C). Temperature corrected BE results were then normalized to the volume of PDMS on the fiber and reported as micromoles (µmol) as 2,3-dimethylnaphthalene / milliliter (mL) PDMS. The detection limit for the automated BE method is approximately 0.5 µmol as 2,3-dimethylnaphthalene / milliliter (mL) PDMS. For the automated BE application, the ratio of PDMS to water sample is approximately 6.6×10^{-6} v/v.

The early application of BE (e.g., the manual method) involved equilibrating short lengths (1 cm) of 100 µm PDMS-coated fibers into a petroleum hydrocarbon contaminated water sample [5]. The fibers were placed in 140 mL amber glass vials containing the water sample and magnetic stir bar. The samples were stirred for 24 hours, which was sufficient to reach >80% of equilibrium for hydrocarbons up to logK_{OW} 5.5. The total concentration of hydrocarbons in the PDMS was determined by dividing the measured nmoles of hydrocarbons by the PDMS volume (0.612 µL, PDMS:water 4.4×10^{-6} v/v). The detection limit for this method is approximately 0.5

µmol/mL PDMS. Parallel testing showed both methods achieve similar results that are within a factor of two (Figure S1).

Additional data were collected for *Hyalella azteca* exposures to PAH-contaminated sediments. The sediments were equilibrated for 14 days using 3 cm lengths of SPME fibers, with 10 µm PDMS coating to ensure equilibrium was achieved. The toxicity assay evaluated 10 d survival of the amphipod in different sediments using the 10 µm BE measurements as the common exposure metric. Additional details are given in Mayer et al [22].

An important general consideration with the BE method is that measurements of the total moles on the fiber are assumed to reflect the degree of bioconcentration by an organism. BE measurements do not necessarily compare directly to the measured or inferred critical body burdens due to the differences in the rate and extent of partitioning between lipid-water or PDMS-water phases as well as other biological processes such as biotransformation. Therefore, the BE measurements are considered a surrogate for bioavailable hydrocarbons that correlate to internal concentrations and hence predicted toxicity.

Ecotoxicity methods

Standard test guidelines were used to develop the toxicity data analyzed in the present study. The original studies have been summarized in other publications, which are listed in Table 1. Briefly, the tests utilized daily renewals of water accommodated fractions (WAFs) using the variable loading approach [30, 31]. The exposure and WAF preparation chambers were kept sealed to minimize losses from volatilization. Observations of toxicity (e.g., mortality, growth, or reproduction) were collected daily. The BE measurements were collected on fresh WAF test media for each treatment level. In some cases BE measurements were collected on old test

solutions, and showed declines typically less than 2- fold (data not shown) through losses to biodegradation or volatilization. Most of the toxicity data have been published elsewhere (Table 1) and all followed general principles of good laboratory practice [32]. All tests had acceptable control performance and water quality (pH, dissolved oxygen, conductivity).

Data analysis

The BE test data were evaluated in two ways. The first approach was to compare BE measurements on a range of substances and loadings to the predicted toxicity using PETROTOX [3, 21]. Predicted toxic units (TU) were computed for each treatment level and compared to the corresponding BE measurement. This comparison included BE measurements that were taken in WAF screening studies that were not part of a toxicity test.

The PETROTOX model first calculates the profile of dissolved constituents based on the detailed substance composition and tested loading. The predicted dissolved concentrations are then converted to toxic units by normalization to the inherent effect concentrations (e.g., LC50) for each constituent, *i* (Eqn 1).

$$TU = \sum C_{W,i} / LC50_i \quad (1)$$

Effects are predicted using the TLM for acute endpoints (e.g., LC50) and chronic effects (e.g., EC10) using the median of compiled acute to chronic ratios [20].

$$LC50_i = k_{TL,i} * C^*_{TL} \quad (2)$$

where accumulation in target lipid (e.g., the assumed site of action) is modeled using the lipid-water partition coefficient (k_{TL}) for a given constituent, *i*. The TUs scale according to the critical target lipid body burden (µmol/g lipid, C^*_{TL}), which represents the sensitivity of the test species. The sum of the individual TUs represents the overall toxicity for a given exposure (i.e. loading) to a given substance. Assuming strict additive toxicity of hydrocarbons, the loading that is predicted to cause a 50% response (i.e. LL50 or EL50) corresponds to a predicted total TU=1.

TUs are a reflection of the collective accumulation of different petroleum hydrocarbons in the target lipid. The BE measurements and TUs reflect the dissolved phase exposure and are expected to correlate. In order to maintain a common basis for comparison with BE data, the predicted TUs were based on a critical target lipid body burden (CTLBB) of a median sensitivity organism, 116 µmol/g lipid [20]. The resulting TUs were converted to target lipid concentrations by combining Eqn 1 and 2, i.e. multiplying the sum TU by the median C^*_{TL}. This step was performed to facilitate comparison between PETROTOX predictions and passive sampling measurements since predicted target lipid concentrations are intuitively more directly comparable to BE-based PDMS concentrations than TUs.

Given variability in the parameters used to calculate TUs, and inferred C_{TL}, as well as in the BE measurements, a Deming-style regression was applied [33] using least squares to determine the error between the model estimate and data where the error is based on the orthogonal distance between data and model. This assumes that the error in the TU predictions is similar to the error in the BE measurements, which is supported by the similar standard errors on the C^*_{TL} in the TLM- [20] and BE-based critical PDMS effect concentrations (Table 2). The initial BE measurements were

used for comparison to the model predictions since the PETROTOX model assumes equilibrium, and no losses that would reduce actual test exposures.

The second approach involved using BE data as the common exposure metric across test substances to support dose-response analysis of organism-specific endpoints. Critical BE concentrations were derived for a variety of acute and chronic endpoints. BE concentrations at 50% mortality (LC50) were determined for most organisms (Table 1) in short term exposures (e.g., 2 to 4 d), and median inhibition of growth was determined for algae. Chronic endpoints included 20% inhibition of growth for algae at 72 h, 4-d deformities for fish embryos, 21-d reproduction for *D. magna*, and 28-d growth inhibition for *O. mykiss*. The 20% effect level was chosen to represent dose-related effects that were consistently above the variability of control and low dose treatments. Dose-response analysis was conducting using the MASS package, and the glm and dose.p function in R [34]. Use on initial BE measurements in this analysis may slightly overstate average exposures and introduce a small bias (e.g., <2-fold) in the derived critical BE concentrations.

Once the critical BE concentrations for acute and chronic data were determined acute to chronic ratios were derived and compared to other compilations [20, 35]. Further, the distribution of acute critical BE concentrations were compared to target lipid-based critical effect concentrations derived previously from the TLM [20] using single hydrocarbon toxicity test data.

Comparing fiber-lipid partition coefficients

The different partitioning properties of hydrocarbons from water to PDMS and target lipid phases were evaluated with ppLFER to characterize the chemical property features that control the observed partitioning processes. The general form of the polyparameter LFER model is given by:

$$\log K = eE + sS + aA + bB + vV + c \quad (3)$$

where the lower case parameters (esabv) correspond to the solvent system (e.g., target lipid-water), and the upper case parameters (ESABV) are the solute interaction terms. The parameter *E* is excess molar refractivity, *S* is polarizability, *A* is the ability to donate a hydrogen bond, *B* is the ability to accept a hydrogen bond, and *V* is the molar volume and, *c*, is a constant. Modeling with ppLFER is widely applied to partitioning data and is described in more detail elsewhere [36-38].

Existing ppLFERs for PDMS-water [39] and target lipid-water [40] were applied to PETROTOX predicted exposures for a medium crude oil across a range of loadings (0.5 – 500 mg/L). The range of illustrative oil loadings span acute to chronic effects and a wide composition range of constituent hydrocarbons found in many petroleum substances. The simulated dissolved profiles provided a basis for evaluating trends in partitioning across hydrocarbon classes and carbon number. Additional details of the ppLFER analysis are given in the SI.

1.4 Results And Discussion

BE vs predicted target lipid concentrations

The objective of this work is to describe the technical basis for applying BE measurements in toxicity prediction of petroleum substances. Comparison of BE measurements and predicted CTL includes 436 data points (280 quantifiable measurements, and 156 measurements below the detection limit), and includes 95 substances from 15 major classes (Table 1).

Figure 1 demonstrates a log-linear trend of C_{TL} between about 10 and 1200 µmol/g lipid. Assuming a typical critical body burden of 120, this corresponds to TUs of 0.1 and 10, for BE measurements between <0.5 to 1000 mM. Thus, BE measurements bracket the range where toxicity is expected to be observed. BE data at or below the method detection limit, around 0.5 mM, were plotted with '<' symbols.

The resulting log-log regression of the quantifiable BE measurements has a slope of 0.64 (95% confidence interval, CI, 0.60 – 0.68) and an intercept of 1.35 (CI 1.30-1.40) (Eqn 8) with a root mean square error (RMSE) of 0.17.

$$\log C_{TL} = 0.64 \log BE + 1.35 \quad (4)$$

The values below the detection limit were not used in the regression. However, non-detectable BE are associated with low C_{TL}, both of which would provide an indication of low potential toxicity.

This analysis demonstrates that BE measurements are correlated with TU predictions, supporting use as a surrogate analytical measurement of bioavailability. This relationship quantitatively links the concentrations in PDMS and target lipid. Note, the slope is not unity, reflecting non-linearity in the BE-C_{TL} response that is discussed in the *Fiber-Lipid partition coefficients* section below. The next step in the analysis was to verify the utility of the BE measurements as an exposure metric for characterizing toxicity thresholds.

Dose Response Analysis

Datasets for individual species were evaluated by comparing the paired observed acute or chronic effects to BE measurements. The goal of this analysis step

is to confirm that BE measurements provide a consistent exposure metric across substance types and treatments for expressing toxicity endpoints. Prior work indicated that BE measurements obtained with different thicknesses of PDMS were comparable (Figure S1) so all BE data were used to derive critical BE concentrations for a given species/endpoint.

Acute toxicity data are well described by the BE measurements for ten different species (Figure 2) including invertebrates, algae, juvenile fish (*O. mykiss*), and fish embryos (*D. rerio*). The BE-based dose response data appear well behaved and are generally steep slope consistent with the acute toxicity pattern of nonpolar organics [41]. The BE measurements appear to provide a consistent exposure metric across different test substances for a given species based on the range of confidence intervals about critical BE concentrations (Table 2). Therefore, as predicted from the observed correlation between target lipid and PDMS partitioning, BE measurements appear to provide a reasonable surrogate for characterizing aquatic exposures of petroleum substances that describe observed toxicity.

Use of BE as the exposure metric for chronic and sub-chronic data shows similar patterns (Figure 3) as the acute data. There are four species with BE-based dose responses: *D. magna*, *O. mykiss*, *P. subcapitata*, and *D. rerio* embryos, based on 21-d reproduction, 28-d growth, EC20 on 3-d growth rate, and 4-d spinal deformities, respectively. The dose responses for *O. mykiss, P. subcapitata,* and *D. rerio* are quite good following exposures to gas oils, weathered, and fresh oils, which are similar to the acute datasets.

The *D. magna* dataset (n=31) generally show low chronic effects (<10%) at low BE measurements (<3 mM). The highest effect of 26% inhibition occurred at BE

measurement of 7.2 mM. One study with a lubricant base oil (LBO, *n*=3) showed 15-21% inhibition of reproduction at 21 days at BE < 1 mM. Further inspection revealed that the treatments, which were exposures to a single high loading (1000 mg/L) for each substance, had observed reproduction of 98-105 neonates per female compared to a control of 125 neonates per female with a coefficient of variation (CV) of 36%. Typical control performance varies from 100-135 neonates per female with typical CV of 15% (range 5 – 24%). The treatments are all within the range of variability of the controls, and the low BE and low TUs (<0.01), suggests that the observed effects are unlikely attributable to the petroleum related hydrocarbons comprising this substance. It is also possible that the presence of additives or impurities, not captured by the BE measurement, could explain this discrepancy.

BE-based species sensitivity distribution (SSD)

The BE measurements are proposed as a surrogate measurement of bioavailable hydrocarbons in exposures to complex petroleum substances. The strong correlation between BE and C_{TL} (Figure 1) supports this hypothesis. Further support is found in comparing the critical BE concentrations to CTLBBs derived from the TLM [20]. The TLM has been applied to more than 40 species and the resulting SSD is assumed to represent the general range of expected sensitivity of organisms from a variety of environmental compartments.

The TLM-derived SSD range from 24.5 to 500 µmol/g lipid with a median of 116 µmol/g lipid, and a standard deviation of 0.33 of the log transformed CTLBBs. The acute critical BE concentrations (Table 2, Figure 4) range from 13.6 to 240 mM PDMS with a median value of 37 mM and a standard deviation of 0.40 on log-transformed values. The individual estimates have an average standard error on the

log critical BE estimates of 0.14, which is similar to the standard errors estimated for TLM-derived CTLBBs for individual species consistent with the assumptions of the Deming regression. The most sensitive critical BE concentration was observed for algae, followed by mysids, followed by daphnids. Fish endpoints (both juvenile and embryo) are found in the middle of the sensitivity distribution with the marine annelid appearing as the least sensitive species.

The standard deviations of log CTLBB and log critical BE SSD are nearly identical suggesting the two distributions capture the expected range of aquatic organism sensitivity further supporting the hypothesis that BE is a surrogate measurement of bioavailable hydrocarbons. However, the means are clearly offset, which implies differences in target lipid-water (K_{LW}) and PDMS-coated fiber-water (K_{FW}) partition coefficients. Empirical K_{FW} in literature are lower by about 0.5 log units [42-46]. An adjustment of this magnitude places the BE-based SSD within the range of CTLBBs. The BE SSD appears to be log-normally distributed based on normality tests (Shapiro-Wilke test, p-value 0.67) and is therefore comparable to the TLM-derived SSD.

The BE-derived SSD was converted to target lipid-based SSD using equation 4. The entire distribution shifts upward and is more in line with the TLM-derived SSD (not shown). The median of the transformed critical target lipid concentrations is 290 µmol/g lipid, with a range of 120-800 µmol/g lipid. The SSD is slightly higher than the TLM-derived SSD, but it is within the observed range. The magnitude of this shift is consistent with the observed offset between lipid and PDMS measurements reported in field studies [42]. Alternatively, BE-based effect concentrations were derived using BE measurements of fresh WAFs and this may be conservatively biased

high. Actual BE exposures during static renewals may decrease during test exposures due hydrocarbon degradation particularly for more soluble monoaromatic components which can exhibit half-lives on the order of a day [47].

The TLM-derived C^*_{TL} are based on single chemical toxicity tests with a range of nonpolar organic chemicals including aliphatics, mono- and polyaromatic ring classes. The success of this comparison confirms the concept of concentration addition commonly used in hazard and risk assessments of petroleum substances [3, 4] since the measurements are based on the integrated area under the curve for all constituents representing various classes of hydrocarbons absorbed to the PDMS.

Limited chronic data are available to evaluate chronic critical BE concentrations so an analogous SSD-based analysis was not performed. However, the limited chronic critical BE data range from 4.3 to 23.8 mM (Table 2). These correlate with empirical acute to chronic ratios (ACR) of 1.6 to 4.4, which is comparable to typical ACRs for hydrocarbons and other nonpolar organics that range from 2-10 with a median around 5 [20, 35].

Predicted Partitioning in Target Lipid and PDMS

The partitioning behavior was analyzed using the linear solvation energy relationship (LSER) models for lipid-water (K_{LW}, Eqn S2) and PDMS-water (K_{FW}, Eqn S3) and lipid-PDMS (Eqn S4) partition coefficients (Figure S2). In this figure, the lines are proportional to the fractional contribution of that term in the LSER model to the overall partitioning behavior as a function of predicted TU. As expected, the aA, hydrogen bond acceptor terms, are all zero for K_{LW} and K_{FW}. The other terms that characterize polar behavior (eE, bB, sS) are all relatively small contributors (~25% together) to the predicted partitioning behavior, which is consistent with the nonpolar

nature of hydrocarbons. The largest factor is the vV terms, which indicates that larger molecules have a higher affinity for both lipid and PDMS.

The difference in these two models (Fig S2 "Target lipid-PDMS") provided insight into the chemical features that are responsible for the differential partitioning of hydrocarbons between PDMS and lipid. Similar to the K_{LW} and K_{FW} cases (Fig S2 A, B) the aA, bB and eE terms are small. The sS, polarizability, term is responsible for about half of the change in free energy at low TUs, and 75% at higher TUs, in the partitioning process and the largest reason for the observed lipid-PDMS partitioning behavior. While this is a relatively small contributor in the K_{LW} and K_{FW} systems, it is sufficient to drive most of the offset between lipid and PDMS concentrations. This dependence means that the more polar nature of biological membranes results in a slightly higher affinity for hydrocarbons compared to PDMS. This is particularly important for the aromatic constituents, which have slight polar character and are generally major contributors to toxicity. Differences in the polar character of these two phases help explain why the slope in the log BE-log TU relationship deviates from unity (Figure 1, Eqn S1-4).

The vV molecular volume term is responsible for about a 25% of the partitioning behavior, with PDMS being slightly more accommodating for hydrocarbons. The constant, *c*, is also revealed to be an important term, being responsible for about 25% partitioning behavior at low TU, but is a lower contributor at higher TU, which likely reflects the difference in the complex biological membranes relative to the PDMS polymer phase. In contrast the vV term increases slightly with increasing TU, suggesting more flexibility in the lipid membrane systems relative to the PDMS polymers to accommodate accumulation of hydrocarbons.

The partitioning behavior of a wide range of individual hydrocarbons are evaluated further in Figure 5. The predicted dissolved profiles for the pseudo-constituents in the PETROTOX calculations were used to predict the contribution of different individual hydrocarbons to BE analyses as a function of WAF loading for a medium weight crude oil using Eqn S2 (Fig S3). There are two classes of chemicals that are main contributors at high loading: C1-3 mono-aromatics, and parent and alkyl (C1-2) diaromatics. At lower loadings these more water soluble constituents are depleted from the oil and are not as abundant in the dissolved phase, and subsequently in the PDMS, based on their multi-constituent solubility behavior. Thus, these constituents contribute less to overall BE concentrations (see open blue squares in Fig S3).

Predicted Lipid-PDMS partition coefficients (Eqn S4) for the pseudoconstituents that are major contributors to the overall TU are shown in Figure 5A. The range of partition coefficients spans just an order of magnitude for a given chemical class that generally decrease by carbon number. However, the coefficients increase with increasing aromatic ring class such that the 2-ring aromatics (e.g., naphthalenes) have higher lipid-PDMS partition coefficients than the mono-aromatics for the same carbon number. At higher loadings, monoaromatic constituents are more abundant in the aqueous phase and have relatively lower lipid-PDMS partition coefficients consistent with their more polar character, which was discussed earlier in this section.

The relative change in predicted BE from low loading (0.5 mg/L) to high loadings (500 mg/L) shows that the contribution from C7-9 mono-aromatics increases more than 2-ring aromatics and other classes. This coupled with the relative lower

lipid-PDMS relationship observed in Fig 5 Panel B results in a predicted theoretical C_{PDMS}-C_{lipid} relationship that would exhibit a slope less than unity (Figure 5, Panel B) consistent with empirical relationship reported in Figure 1. However the magnitude of the intercept appears lower and may reflect compositional differences between the modeled crude oil versus substances used to derive Figure 1 as well as potential loss process that could cause empirical BE measurements to deviate from predictions that conservatively assume no losses. Nevertheless, theoretical calculations with the LFER models (Eqn S2-4) provide a plausible explanation to account for the observed slope in Eqn. 4.

Practical Considerations

BE measurement represent a substantial improvement in the ability to characterize bioavailability of hydrocarbons in WAF exposures of petroleum substances. The BE measurements can be readily related to critical effect concentrations for hazard and risk assessment. Measurements of speciated hydrocarbons (e.g., PAH, saturated hydrocarbons, volatile organics) can be useful to confirm the composition of the exposure, including the presence of droplet oil. However, these analyses represent only a subset of the total hydrocarbons that can contribute toxicity and often do not differentiate hydrocarbons in dissolved, bioavailable forms from that in oil droplet phases.

Modeled TUs derived using comprehensive analysis of petroleum substance composition as input to the PETROTOX model can be useful for determining which hydrocarbon classes are contributing to toxicity [28]. However, the analyses of aqueous exposure media needed to confirm such predictions are not widely available.

Therefore, BE fills this gap by providing a relatively simple analytical measurement that is representative of total bioavailable hydrocarbons in aqueous exposures.

Limited data are available to highlight the utility of BE measurements for evaluating toxicity of PAH contaminated sediments (Table 1) [22]. Further work is needed to extend application of BE to petroleum contaminated sediments and soils. Other considerations include exposures to substances containing heavy hydrocarbons (e.g., distillate aromatic extracts, lubricant base oils, heavy fuel oils, etc), which may not reach equilibrium within the timeframe of the analysis as indicated by the lack of equilibrium hydrocarbons with $\log K_{OW} > 6$ [5]. Thinner fibers (e.g., 10 µm) are expected to equilibrate quicker with dissolved hydrocarbons associated with such substances. However, test organisms are also unlikely to attain equilibrium with these types of substances [48] as uptake kinetics are likely much slower than PDMS fibers applied in this present study [40] . Therefore, application of BE to residual petroleum substances is likely to provide a conservative basis for hazard screening.

Summary

In summary, measurement of total hydrocarbons by the PDMS-coated SPME fibers, e.g., BE, is strongly correlated with predicted toxic units and observed toxicity of petroleum substance WAFs. Further, the BE measurements provide an exposure metric that is predictive of toxicity across a diverse range of petroleum substance categories. The BE-based SSDs are also comparable to target lipid-based SSD used to characterize acute effects and acute to chronic ratios that allow extrapolation to chronic effects. Lastly, theoretical modeling of partitioning behavior of hydrocarbons to target lipid and PDMS supports the empirical BE- C_{TL} relationship found. These

lines of evidence support the use of BE in hazard and risk assessments of petroleum substances.

The BE method serves as a convenient exposure metric for comparison of test results across substance types, but also between laboratories, and dosing methods. The BE method can be used to screen test substances to streamline study design for selection of test substances, help target selection of treatment loadings and limit animal use in subsequent toxicity testing. Future work should extend BE application to chronic and sub-lethal data as well as to soil and sediment toxicity tests. Another logical application warranting further study is environmental monitoring of effluents and field sites that are contaminated with complex hydrocarbons and/or other nonpolar organic mixtures. This would include modification of the BE method for application to weathered oils and process related wastewaters that may also include more polar as well as ionized organic contaminants.

FIGURES

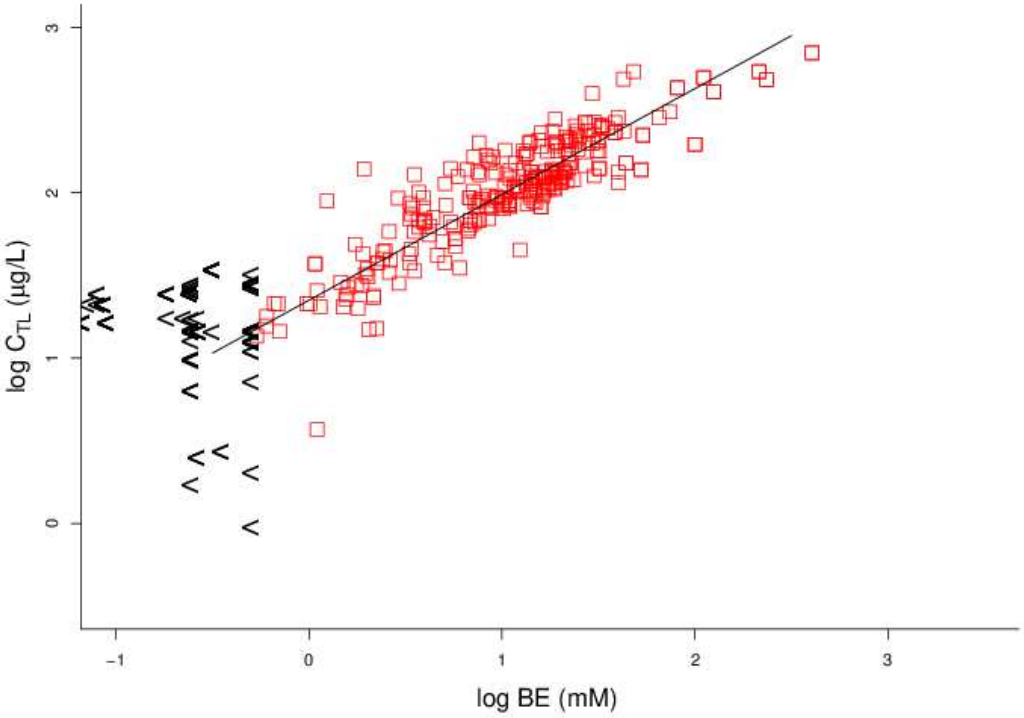

Figure 1.1 Log biomimetic extraction (BE) measurements from 30 µm fibers compared against calculated accumulation in target lipid using equations 1 and 2 as implemented in the PETROTOX model. Values plotted with '<' are measurements below the quantitation limit of the method (BE <0.5 mM PDMS). Regression line from Equation 4.

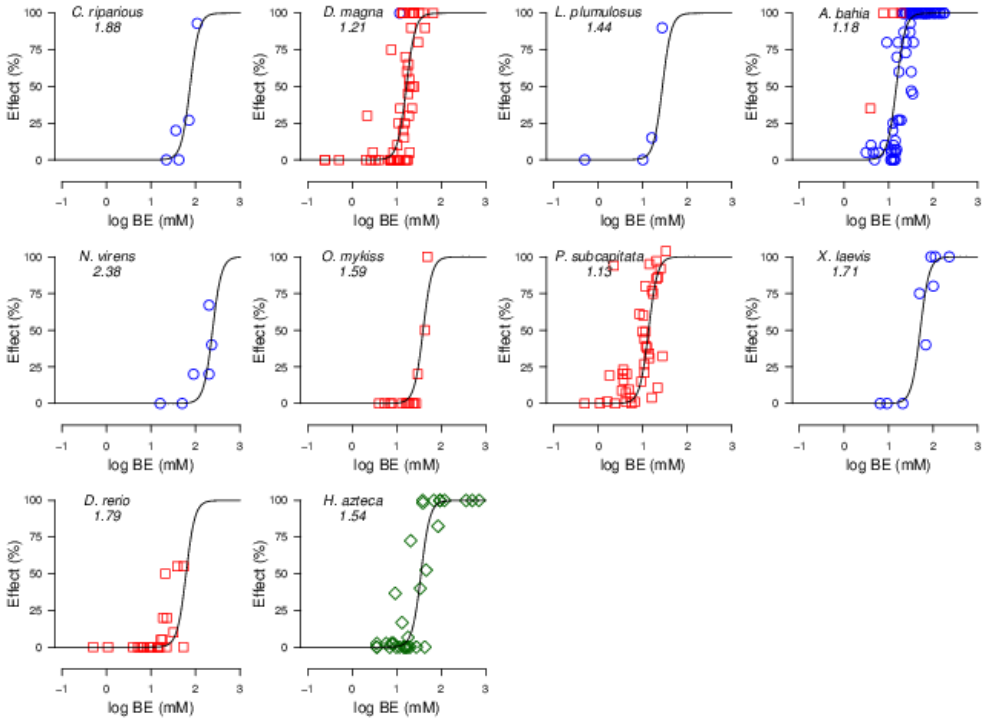

Figure 1.2 Acute dose response data using Biomimetic Extraction (BE) measurements as the exposure metric. Species and log critical BE concentrations (e.g., LC50) provided in panels. Red squares are 30 µm BE data, blue circles are 100 µm BE data, green diamonds are 10 µm BE data.

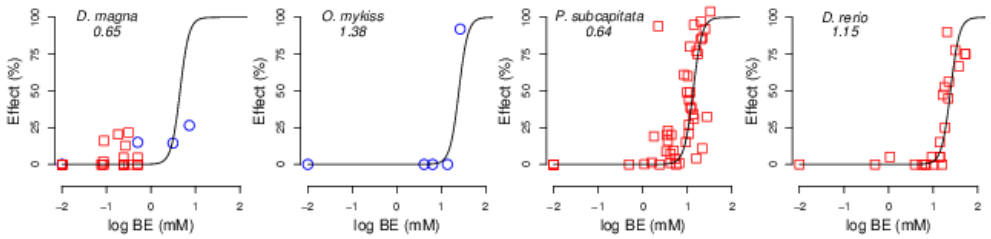

Figure 1.3 Chronic dose response data using Biomimetic Extraction (BE) measurements as the exposure metric. Species and log critical BE concentrations (e.g., EC20) provided in panels. Red squares are 30 µm BE data, blue circles are 100 µm BE data. Control data were plotted at 0.01 mM.

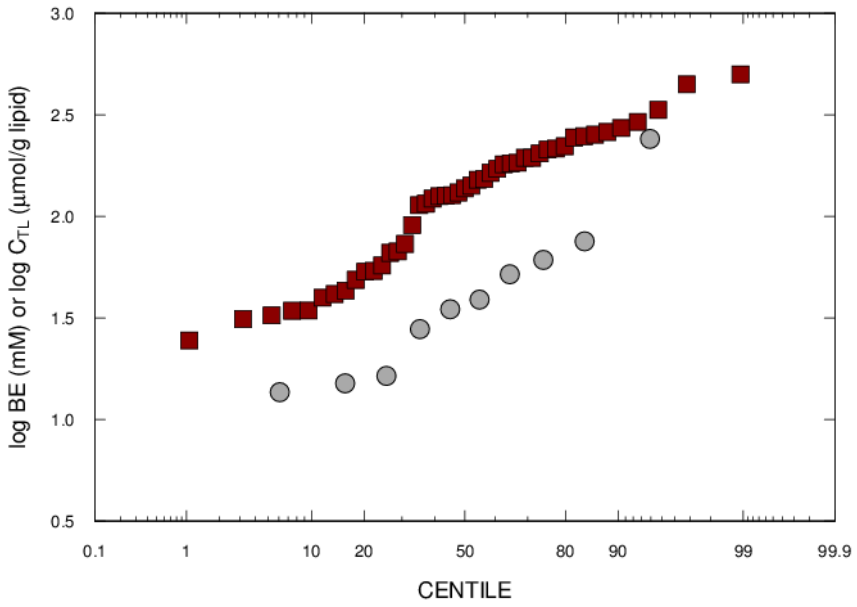

Figure 1.4 Comparing the species sensitivity distribution for critical target lipid (TL)-normalized concentrations corresponding to acute effect levels derived with TLM (red squares), and BE-based acute endpoints (circles, Fig. 2 and Table 2).

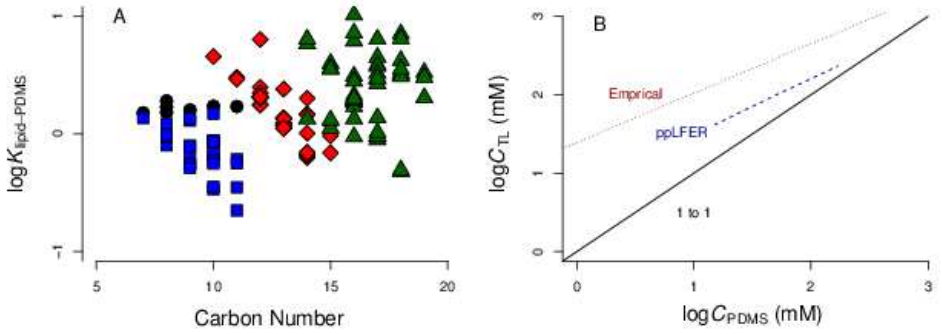

Figure 1.5 (A) The predicted lipid-fiber partition coefficients by chemical class (● aliphatic, ■ mono-aromatics, ♦ diaromatics, ▲ 3+ ring aromatics) against carbon number. (B) Predicted target lipid concentrations (C_{TL}) vs predicted BE (C_{PDMS}) based on the empirical regression (red dotted line) in Figure 1 (Eqn 5), and the predicted relationships using the predicted dissolved concentrations in panel A and $K_{PDMS\text{-}water}$ (Eqn S1) and $K_{Target\ Lipid\text{-}Water}$ (Eqn S3) partition coefficients (dashed blue line), and the 1 to 1 line (black solid line).

TABLES

Table 1.1 Summary of substances, test species, and SPME methods.

Substance type	Substances used in BE screening studies	Substances used in toxicity studies	Test species	Citations
Crude oils (fresh and weathered Kuwaiti, Forties, Endicott, Romanian, weathered Troll, Dilbit, Cold Lake , Wilmington, Timball)	2	10	*A. mysidopsis* (mortality), *D. magna* (mortality), *D. rerio* (sublethal, mortality), *O. mykiss* (growth rate)	[5, 27], Unpublished
Bitumen	1	1	*D. magna* (mortality), *P. subcapitata*, (growth rate)	[21]
Distillate aromatic extract	4	1	*D. magna* (mortality, reproduction), *P. subcapitata* (growth rate)	[21]
Solvents	1	1	*D. magna* (mortality)	[21], Unpublished
Foots oil	1	1	*D. magna* (mortality)	[21]
Gas oil	21	15	*C. tentans* (mortality), *A. mysidopsis* (mortality), *L. plumolosus* (mortality). *X. laevis* (mortality), *N. virens* (mortality), *D. magna* (mortality, reproduction), *D. rerio* (mortality, sublethal), *O. mykiss* (growth rate), *P. subcapitata* (growth rate)	[21]
Heavy fuel oil	12	4	*D. magna* (mortality, reproduction), *O. mykiss* (growth rate), *P. subcapitata* (growth rate)	[21, 28]
Lubricant base oil	1	1	*D. magna* (reproduction)	[21]
Grease	0	3	*D. magna* (mortality, reproduction)	Unpublished
Naphtha	2	0	None	[21]
Residual aromatic extract	0	1	*D. magna* (mortality), *P. subcapitata* (growth rate)	[21]
Resin	0	1	*D. magna* (mortality)	[26]
Treated distillate aromatic extract	1	1	*D. magna* (mortality), *P. subcapitata* (growth rate)	[21]
Unrefined/acid-treated oil	2	2	*D. magna* (reproduction)	[21]
PAH-contaminated sediments	0	34	*H. azteca* (mortality)	[22]

Table 1.2 Summary of regression analysis. Slopes and intercepts on individual and combined datasets

ID	Species	log BE* (mM)	SE	Endpoint	ACR	Comment
Acute endpoints						
1	*C. riparious*	1.88	0.15	2 day 50 % Mortality		
2	*D. magna*	1.21	0.06	2 day 50% Mortality		
3	*L. plumulosus*	1.44	0.13	2 day 50% Mortality		
4	*A. mysidopsis*	1.18	0.06	2 day 50% Mortality		
5	*N. virens*	2.38	0.29	2 day 50% Mortality		
6	*O. mykiss,* juvenile	1.59	0.07	4 day 50% Mortality		
7	*P. subcapitata*	1.13	0.14	3 day 50% specific growth rate inhibition		
8	*X. laevis*	1.71	0.17	2 day 50% Mortality		
9	*D. rerio,* embryo	1.79	0.28	4 day 50% Mortality		
10	*H. Azteca*	1.54	0.10	10 day 50% Mortality		
Chronic endpoints						
11	*D. magna*	0.69	1.29	21 day 20% Reproduction inhibition	3.3	ID 2 with 11
12	*O. mykiss,* juvenile	1.38	0.10	28 d 20% inhibition on growth	1.6	ID 6 with 12
13	*P. subcapitata*	0.64	0.20	3d 20% inhibition on specific growth rate	3.1	ID 7 and 13
14	*D. rerio,* embryo	1.15	0.12	4 day 20% incidence of spinal curvature	4.4	ID 9 with 14

BE* Critical BE concentrations that correlate with 50% mortality, or 20% inhibition

SE standard error of log transformed critical BE concentrations
ACR acute to chronic ratio

Chapter 2

INVESTIGATING THE ROLE OF DISSOLVED AND DROPLET OIL ON AQUATIC TOXICITY USING DISPERSED AND PASSIVE DOSING SYSTEMS

Redman, Aaron D., et al. "Investigating the role of dissolved and droplet oil in aquatic toxicity using dispersed and passive dosing systems." *Environmental toxicology and chemistry* 36.4 (2017): 1020-1028.

2.1 Abstract

Characterizing aquatic toxicity of oil is needed to support hazard assessment and inform spill response. Natural processes and mitigation strategies involving dispersant use can result in exposures to both dissolved and droplet oil that are not typically differentiated when characterizing oil exposures in toxicity tests. Thus, the impact of droplets on aquatic toxicity is largely uncharacterized. To improve understanding the role of droplets, acute toxicity tests with *Daphnia magna* and *Americamysis bahia* were performed with Endicott crude oil in low energy mixing systems with and without Corexit 9500 dispersant. Exposures were also prepared by placing crude oil in silicone tubing and passively dosing test media to provide dissolved oil exposures without droplets. A framework is described for characterizing dissolved phase exposures using both mechanistic modeling and passive sampling measurements. The approach is then illustrated by application to data from the present study. Expressing toxicity in terms of toxic units (TUs) calculated from modeled dissolved oil concentrations or passive sampling measurements showed similar dose

responses between exposure systems and organisms, despite the gradient in droplet oil. These results indicate that droplets do not appreciably contribute to toxicity for the two species investigated and further supports hazard evaluation of dispersed oil on the basis of dissolved exposure metrics.

2.2 Introduction

Reliable effects data are the foundation for hazard and risk assessments. Crude oil and refined petroleum substances are complex mixtures of hydrocarbons and other trace constituents with physicochemical properties spanning a wide range in solubility, volatility, degradability, and toxicity. The aquatic hazard of these complex substances are evaluated using a variety of dosing procedures, which complicate interpretation and comparison of toxicity test data [52-55]. Dosing procedures include leaching from oiled gravel [56-58], slow stir water accommodated fractions (WAF) [59, 60], spiked WAF exposures with continuous dilution [55, 61], mechanically dispersed oil [62, 63], chemically dispersed oil [53, 54], and passive dosing techniques [52]. These different dosing methods can result in variable dissolved and particulate oil exposures that differ not only in terms of total concentrations but also in the composition of the constituent hydrocarbons in the dissolved and droplet phases that reflect the composition and behavior of the test substance in the test system investigated.

It is generally assumed that dissolved phase hydrocarbons are the primary determinant of toxicity in exposures to crude oil and petroleum substances [64, 65]. This applies in particular when limited droplet oil is present in the exposure system [66]. Previous work has also shown that the observed toxicity is highly dependent on composition of the dissolved oil exposure [1, 67]. However, traditional exposure metrics used for in aquatic toxicity studies such as total petroleum hydrocarbons (TPH) or total polycyclic aromatic hydrocarbons (TPAH) ignore differences in dissolved and droplet phase concentration and composition. Therefore, it is important to develop improved methods to characterize dissolved exposures that can be

compared to observed effects across different oil dosing systems to discriminate if dissolved exposures dictate oil toxicity.

One practical exposure metric for expressing the toxicity of hydrocarbon mixtures involves normalization of the dissolved exposure concentrations of the hydrocarbon constituents to their corresponding effect concentrations, e.g LC50, [23, 68, 69] and then summing across constituents. This calculation is often referred to as a toxic unit (TU) approach to hazard assessment [67].

Passive samplers have become a common analytical tool to measure freely dissolved concentrations of organic chemicals that are bioavailable [5, 22, 70, 71]. These methods have been applied to measure polycyclic aromatic hydrocarbons (PAH) in water [72], soils [73], and sediments [74]. Recent applications include studies on the fate of PAHs during oil spills in the field [75] and in the laboratory [53, 76]. However, environmental exposure to petroleum substances can include many constituents from other classes (e.g., monoaromatic, linear, branched and cyclic aliphatic hydrocarbons) that can contribute to toxicity. Hydrocarbons partition to the passive sampler media in proportion to hydrophobicity [5, 22, 70, 71], much like the partitioning to biological tissues [20, 77, 78]. Therefore, passive sampler measurements of total dissolved hydrocarbons have been proposed as a promising surrogate for internal tissue concentrations that are associated with adverse effects and thus toxicity of dispersed oils [5].

The objectives of this study were to 1). develop acute toxicity data for a freshwater and marine invertebrate using crude oil with different dosing methods that provide varying droplet oil concentrations; 2) describe two methods for improved exposure characterization of dissolved phase oil exposures: modeled TUs and passive

sampler measurements; 3) illustrate the advantages of using these alternative exposure metrics for characterizing the role of droplet oil on observed toxicity. To accomplish the first objective a novel, droplet-free dosing system was developed for comparison to conventional dosing methods with and without chemical dispersant. To address the second objective, data were collected for validation of the oil-water solubility model that is the basis of the TU predictions [33]. Our hypothesis was that dissolved phase constituents are mainly responsible for observed toxicity, and that droplets would only indirectly contribute through potential replenishment of dissolved phase hydrocarbons. In support of the third study objective, this hypothesis was tested by comparing observed toxicity results to both conventional and alternative exposure metrics provided in the present study.

2.3 Methods

Organism Cultures

Cultures of the freshwater macroinvertebrate, *Daphnia magna* (daphnids) were obtained from Aquatic Research Organisms, Hampton, NH. Cultures of the saltwater macroinvertebrate, *Americamysis bahia* (mysids) were obtained from Aquatic Biosystems (Ft. Collins, CO). The *D. magna* culture contained 8 daphnids in 1 L glass bottles filled with reconstituted hard water with no headspace. The culture chambers were maintained at 20 ± 2°C under a 16 hour light: 8 hour dark photoperiod with an intensity of 550 lux, using fluorescent lamps. New cultures were started at least every five days. Neonates used for toxicity testing were less than 24 hours old and were not first brood progeny. Cultures of *D. magna* were fed every other day with *Pseudokirchneriella subcapitata ad lib* and supplemented with 25 µL/L of Vita-chem

(Boyd Enterprises, Inc., Coconut Creek, FL, USA). The organisms were transferred to fresh culture water and fed every other day.

Three day old mysids were received and acclimated in a saltwater aquaria containing artificial seawater at 20±2 ppt salinity and at approximately 25°C. Mysids were held inside a customized, circular 3L polypropylene flow-through tank inside a 132-liter aquarium with constant mechanical filtration for 2 days until they were randomly selected for testing. Mysids were fed platinum grade *Artemia nauplii ad lib* (Argent Food, Madison, WI, USA). The culture chamber was maintained at 25 ± 1°C under a 16 hour light: 8 hour dark photoperiod with an intensity of approximately 350 lux, using fluorescent lamps.

Test Substance

Endicott crude oil (API gravity 28) was obtained from SL Ross Environmental Ltd. (Ottawa ON, Canada) and used as a test substance. Comprehensive compositional analysis has been developed using two dimensional gas chromatrography (GCxGC-FID) [1, 66]. The GCxGC-FID analysis provides quantitative concentration data for a substances on the basis of carbon number and chemical class (e.g., alipahtics, alkyl and parent 1- to 3+ aromatic rings, naphthenic-aromatic species, etc). Additional characterization data that are available on this oil include: 45 specific polyaromatic hydrocarbons (PAHs): C5-C9 VOC constituents (e.g., PIONA: *n*-Paraffin, *iso*-Paraffin, Olefins, Naphthenic, Aromatic), and saturated hydrocarbons (e.g., SHC, *n*-Paraffins C9-C30). These data were used as input to the spreadsheet WAF solubility model [1] and to the droplet speciation model [12] to predict oil component speciation between dissolved and droplet phases in toxicity test exposures (See Modeling Analysis below). The common oil spill response dispersant

Corexit 9500 was obtained from Mar Inc. and used in the preparation of chemically dispersed oil treatments.

Preparation of Water Accommodated Fractions (WAFs)

Water Accommodated Fractions (WAFs) were prepared for *D. magna and A. bahia* toxicity tests. Freshwater WAFs for *D. magna* tests were prepared with hard reconstituted water at 20^{o}C with fresh crude oil. Saltwater WAFs were prepared for *A. bahia at* 25^{o}C with Instant Ocean artificial sea salts at 20 ppt in reconstituted water for all three test oils. The WAFs were prepared in 12 L aspirator bottles using Teflon stoppers to seal the containers with approximately 25% headspace. Mixing was accomplished with Teflon®-coated stir bars with a vortex 20% of the static liquid depth for 24 h. Oil loading ranged from 4 to 650 mg/L.

Chemically enhanced (CEWAF) and physically dispersed (PDWAF) treatments were prepared by adding the appropriate amount of oil and mixing with 20% vortex. During the *D. magna* tests CEWAFs were generated using a dispersant to oil ratio (DOR) of 1:10, whereas during the *A. bahia* tests CEWAFs were generated with a DOR if 1:20 based on greater dispersivity in saltwater. After adding the oil and initiating mixing, Corexit 9500 was immediately added with a syringe. Following the equilibration period, CEWAFs and PDWAFs were allowed to settle, 5 and 2 h respectively.

The passive dosing (PsvWAF) system was prepared by injecting oil into a length of silicone tubing purchased from A-M Systems, Inc. (Carlsborg, WA, USA), with a wall thickness and inside diameter of 0.0095 mm, and 1.5 mm respectively. The oil loaded tubing was then manually tied off and attached to a Teflon®-coated stir bar (see video file in S*upplementary Information* for illustration of this process). Mixing

for the PsvWAF was accomplished by vigorous stirring at ~600 rpm for 24 hours. Higher stirring rates facilitate mass transfer of hydrocarbons from the oil-filled tubing to the water phase. Equilibrium was verified by comparing measured dissolved concentrations to predicted steady-state dissolved concentrations (See Analysis of Dissolved PAH below).

The principle of the PsvWAF dosing approach is that hydrocarbons in the oil-filled tubing will equilibrate with the silicone barrier then with the water phase. Different tubing lengths were used to provide a range of oil volumes (0.16-2.5 mL, for approximately 10-30 cm lengths) for achieving different equivalent loadings that matched PDWAF and CEWAF preparations. The PsvWAF did not require any settling time and was drawn through the port on the bottom of the mixing vessel at the end of the 24 h mixing period.

Daphnia magna Toxicity Tests

Daphnid neonates (<24 h old) were used in tests that were conducted in sealed chambers with no headspace [79]. During the acute *Daphnia magna* toxicity tests four replicates per test substance concentration and a control were tested. Each replicate contained five daphnids for a total of 20 organisms per treatment level. Replicate chambers were 130 mL glass bottles with no headspace and closed with PTFE-lined screwtop caps. The light regime was 16 hours light: 8 hours dark with an intensity that ranged from approximately 137 to 204 lux, using fluorescent lamps. Water quality (temperature, pH, and dissolved oxygen) measurements were recorded per treatment at the start of the test and in a composite of the replicates at termination. The average daily temperature for all tests ranged from 19.8°C to 20.7°C. The dissolved oxygen (DO) concentrations across the exposures were typically between 8.5 and 10.5 mg/L.

The pH varied between 7.3 and 8.3 over the duration of the test. Observations for immobilization and abnormal behavior or appearance were performed at 2, 6, 24 and 48 h ± 1 h after the beginning of the test.

Americamysis bahia Toxicity Tests

Five, one-day old, mysids were randomly selected for use in toxicity tests [80]. Four replicates, each containing five mysids, for a total of 20 organisms were tested for each treatment including the control. Replicate chambers were 500 mL glass bottles with no headspace and closed with PTFE-lined screw top caps. The light regime was 16 hours light: 8 hours dark with an average intensity of 348 lux, using fluorescent lamps. Water quality measurements were recorded as previously described. In general, the water quality parameters (DO, pH) were within guideline recommendations and similar to what were observed in the daphnia tests. The average daily temperature range for all tests was 25°C to 26°C. Observations for immobilization and abnormal behavior or appearance were performed at 2, 17, 24 and 48 h ± 1 h after the beginning of the test.

Analytical characterization of WAFs

Water samples were collected from the respective WAF treatment systems for analytical characterization at the initiation of each test. Up to 1 L volumes were collected for extended suite of 45 PAHs and total petroleum hydrocarbons/saturated hydrocarbons (TPH/SHC). Additional 40 mL aliquots were collected with no headspace in volatile organic analysis (VOA) vials for analysis of volatile organics (e.g., PIONA: *n*-paraffins, *iso*-parafins, naphthenics, aromatics) . Samples were refrigerated pending shipment to Newfield's Environmental Forensics / Alpha Analytical (Mansfield, MA). Samples for PAH analysis were extracted with

dichloromethane and quantified by GC-MS using a modified version of U.S. EPA method 8270D. Volatile hydrocarbons (PIONA) were analyzed by purge and trap GC-MS. Samples for TPH/SHC were extracted with dichloromethane followed by quantitation by GC-FID against a series of n-alkane standards. Samples were stored at 4^{o} C for up to 3 weeks prior to analysis, These measurements were considered to represent the total amount of a given constituent present in the aqueous test media (e.g., droplets + dissolved) due to the exhaustive extraction procedure.

Analysis of Dissolved PAHs

A subset of dissolved PAHs were also measured using direct immersion solid phase microextraction (SPME) by ExxonMobil Biomedical Sciences, Inc. (Annandale, NJ) where the aquatic toxicity tests were performed. WAF samples were collected in ca 20 mL amber, silanized vials and capped with Teflon®-lined septa. SPME fibers coated with 30 µm polydimethylsiloxane (0.132 µL PDMS) were equilibrated with 20 mL WAF samples for 100 min at 30^{o}C with orbital agitation at 250 rpm on a CTC Analytics Combi PAL autosampler prior to injection and thermal desorption. The equilibrated SPME fibers were injected directly and thermally desorbed in an Agilent Ion Trap 240 GC-MS. The dissolved PAH analyte list included: naphthalene, acenaphthylene, acenaphthene, fluorine, methylfluorene, phenanthrene, anthracene, fluoranthene, pyrene, methylpyrene, benzo(a)anthracene, chrysene, benzo[b&k]fluoranthene, benzo(a)pyrene, indeno(1,2,3cd)pyrene, dibenzo(a,h)anthracene, and benzo(ghi)perylene. The method was calibrated by spiking a range volumes of PAH standard solutions, diluted in acetone, directly into 20 mL control test water (moderately hard reconstituted fresh water or artificial seawater) in amber, silanized vials sealed with Teflon-lined septum caps. Each standard, in

addition to each sample, was also spiked with a PAH internal standard solution diluted in acetone containing deuterated PAHs (naphthalene-$d_{8,}$ acenaphthene-$d_{10,}$ phenanthrene-$d_{10,}$ chrysene-$d_{12,}$ perylene-d_{12}). The internal standard concentration was 3 ng/mL. PAH calibration standards ranged from approximately 0.025 to 40 ng/mL, though the working range of the PAH calibration curves were generally limited by the corresponding aqueous solubility limit. The method practical quantitation limit corresponded to that of the lowest analyzed standard. The calibration standards and test water samples were extracted and analyzed using the identical direct immersion SPME followed by quantification using GC-MS .

It was observed for most of the CEWAF samples, that the response of the high K_{OW} deuterated internal standards was significantly less than that in the corresponding deuterated standards in water samples with low droplet oil in other exposure systems. It appears that the oil droplets effectively competed with the PDMS fiber coating resulting in poor recoveries of the internal standards thereby resulting in a positive bias in quantification. Therefore, reported dissolved chrysene (CHR) concentrations in CEWAF samples were instead calculated based on external standard calibration, mitigating the impact of diminished internal standard recovery due to oil droplets. More water soluble, lower K_{OW} PAHs were not impacted, nor were samples from the other treatments where droplets were at lower concentrations.

Analysis of Total Bioavailable Hydrocarbons

Biomimetic extractions (BE) were also performed in duplicate on fresh and old (24 h solutions prior to renewal) WAF preparations using a 30 µm PDMS-coated SPME fiber to provide an alternative, integrated, surrogate measurement of tissue accumulation from all dissolved phase i.e. bioavailable, hydrocarbons in the WAF test

systems [5]. This method involved equilibrating the SPME fibers with WAF samples as described for the dissolved PAH analysis except that no internal standards were added and quantification was by GC-FID. Accumulation on the fiber is due to equilibration of dissolved phase hydrocarbons. The total area under the chromatographic plot was integrated and the response was normalized to an on-fiber amount (in mmoles) based on the response of liquid, solvent-based microliter injections of 2,3-dimethylnaphthalene directly into the GC-FID. The BE results are then normalized to the volume of PDMS coating (mmol/L PDMS). The practical quantitation limit was approximately 0.5 mmol/L PDMS based on the concentration of the lowest 2,3-dimethylnaphthalene standard analyzed and the volume of PDMS.

Modeling Analysis

The modeling framework used to validate the solubility model and calibrate the PETROTOX model for calculating total TUs is outlined in Table 1. This also represents a general framework for characterizing the exposure (particulate and dissolved constituents) and for developing alternate metrics for hazard assessment based on dissolved phase exposures. The analytical data inputs to the various model applications are combined into a series of evaluation steps. The first step was to collect measurements of individual constituents (e.,g., PAHs, VOCs, SHCs) in the oil and exposure media. The speciated hydrocarbon data for the test substance are used as input to the solubility model [1] to predict dissolved concentrations for individual constituents. These model concentrations were then compared to total measurements of these compounds (reflecting dissolved plus droplet phases) to calculate the concentration of particulate, oil in each oil loading treatment and test system. The solubility model is then extended to predict total concentrations as a function of

dissolved, and particulate oil concentrations from the subset of speciated hydrocarbons that have been quantified, see Supplementary Information and Redman et al [12].

The second step is to compare the model predicted dissolved concentrations of selected individual hydrocarbon constituents to freely dissolved concentrations derived using passive sampling This step provides validation of the solubility model, which is a critical component of TU calculations in step 3. Measurements of highly soluble constituents ($\log K_{OW}$ <4) are typically not affected by particulate oil at relatively low concentrations and thus total measured concentrations of SVOCs were also used in this comparison. Calculation of TUs on this subset of analytical data likewise represent a fraction of the total TUs in a given exposure. This is discussed in more detail in Results and in Supplementary Information.

Step 3 involves calculating total TUs based on a comprehensive chemical characterization of the test substance. In this study, GCxGC-FID compositional data at the various experimental test substance loadings were used as input to the PETROTOX model [3]. This model uses the hydrocarbon block approach to apportion the test oil into pseudo-components (or blocks) of similar properties. In PETROTOX the blocks generally match the GCxGC-FID format: mass distribution of components as a function of carbon number and chemical class (branched, linear, and cyclic aliphatics, 1- to 3+ ring parent and alkylaromatics from C5-C30+). In PETROTOX, the physicochemical properties of these blocks are modeled using representative compounds, which have been mass-weighted based on the GCxGC analysis that characterizes the test oil composition. PETROTOX modeling was performed using an input headspace of 25%, consistent with WAF preparation chambers used in this study. Default critical target lipid body burden (CTLBB) inputs

for *D. magna* and *A. bahia* were assumed as well as an upper bound bioconcentration threshold corresponding to a log K_{OW} of 5.5. This upper bound is an empirically determined model input that limits the predicted bioavailability of high log K_{OW} constituents, consistent with the lack of observed acute toxicity [3, 20].

Modeled TUs, derived using the hydrocarbon block approach, were then used to analyze observed mortality responses. These TUs represent the total predicted bioavailable hydrocarbons in a given exposure since they are based on comprehensize GCxGC characterization of the crude oil investigated. TUs derived from PETROTOX are not directly comparable to TUs derived from estimated dissolved concentrations of the subset of individual speciated hydrocarbons described in Step 2, which do not represent the entire mass of the test substance. Many of the blocks simulated in the PETROTOX modeling are part of the unresolved mass using conventional GC-MS techniques but nevertheless can contribute to predicted TUs and expected toxicity.

A complementary analytical method (see discussion of BE method above) was applied in Step 4. BE measurements are considered an analytical surrogate for TUs calculated in Step 3 since this measurement reflects partitioning of total dissolved hydrocarbons to PDMS which serves as a proxy of target lipid, which is the basis for the acute toxicity model included in PETROTOX.

Application of this framework provides an understanding of the hydrocarbon speciation in test exposures, and al affords alternative exposure metrics of both modeled (e.g. TUs) and measured (e.g. BE) dissolved phase oil exposures that captures unresolved oil constituents. To illustrate application, toxicity results from the different dosing systems (CEWAF, PDWAF, PsvWAF) were compared to conventional (Loading, TPH, TPAH) and the alternative exposure metrics (e.g., TU,

BE). Deviations in the toxicity results between the different dosing systems when expressed in terms of the dissolved phase exposure metrics were then used to infer the role of droplet oil on toxicity.

2.4 Results And Discussion

Characterization of droplet oil

The first step of this study was to develop an exposure system that would preclude oil droplets that could then be compared to traditional WAF test methods that produce a range of droplet concentrations. Droplet size distribution in salt water preparations using the different dosing systems was characterized by using laser particle counting (see SI for methods). Results obtained at the highest loadings indicated high counts of small droplet sizes (1-10 µm) for the CEWAF, larger droplet sizes for the PDWAF (10-50 µm), and trace counts of small droplets (1-10 µm) in the PsvWAF system (Figure S1). Unfortunately, greater resolution of the droplet size classes could not be obtained with this method. These results confirm that the expected CEWAF treatment increased droplet concentrations and reduced the size distributions as expected following dispersant application [13, 81].

A comparison of the measured water total concentrations (droplet and dissolved phase) to the predicted dissolved concentrations was performed to estimate the hydrocarbon speciation (particulate and dissolved phase). Details of the estimation method are provided in the SI and results are shown in Figure S2a (for the freshwater exposure) and S2b (for the salt water exposure). Droplet oil is indicated by the apparent enrichment of the less water soluble 3+ ring PAH and aliphatic constituents based on measured total concentrations relative to the predicted dissolved concentrations, e.g., data points fall below the model line.

Droplet concentrations were determined by subtracting measured total concentrations from dissolved predictions obtained using the solubility model (Step 1, Table 1). Results show higher amounts of droplets in the CEWAF but trace to none in PDWAF and PsvWAF (Figure 1). This indicates a gradient of droplet across the loading regimes investigated. Estimated droplet concentrations in the CEWAF exposures ranged from 100 µg/L at low loadings to near 3000 µg/L at the highest loading. Droplet concentrations in the PDWAFs ranged from <50 to 100 µg/L, which was about a factor of two higher than the estimated droplet concentrations in the PsvWAF exposures of <10 to 100 µg/L .

Trace amounts of droplet oil (<100 µg/L) in the PsvWAF were attributed to measured concentrations of a few >C10 alkanes in the WAF, which was surprising given the silicone tubing barrier. However, concentrations were at or below quantifiable detection limits so droplet estimates are uncertain. If trace oil droplets were indeed present in the PsvWAF as also suggested by laser particle counter data presented earlier, leaking from the tied ends of the tubing could be a possible source. However, our results confirm the utility of the passive dosing method for generating oil exposures that minimize the droplet phase (diamonds, Figure 1).

As previously discussed, dispersant use had an obvious impact on the amount of entrained oil. However, less than 5 mg/L of entrained oil was estimated at loadings of >100 mg/L. This is due to the relatively low mixing energy applied to this exposure system. These droplet concentrations are consistent with levels achieved shortly after dispersant application in open ocean tests [37], where total oil concentrations would drop below 1 ppm within periods of <1 day. Droplet

concentrations are also lower in the freshwater (Figure 1 A vs B), consistent with the reduced efficacy of dispersants at lower ionic strength [82].

Dissolved phase concentrations

The Raoult's Law-based mass balance model is used to describe the dissolution behavior using the mole fraction of a constituent in the oil phase (e.g., composition) and the sub-cooled liquid solubility (a physicochemical property). See McGrath et al. [83] and *Supplemental Information* for derivation. To validate this solubility model across the experimental dosing systems and oil loadings, measurements of dissolved phase constituents were compared to predicted dissolved concentrations (Step 2, Table 1). Several 4+ ring PAHs were not measureable with this method (detection limit near 25 ng/L) consistent with low predicted dissolved concentrations (<25 ng/L). Measured data are given in *Supplementary Information* spreadsheet.

Selected 1- to 4-ring aromatic constituents with quantifiable dissolved phase concentrations are shown in Figure 2. To assess model performance, replicate analytical measurements are plotted along with model predictions denoted as lines over the range of loadings used in this study. The model correctly predicts the loading-dependent behavior as well as the onset of solubility limits for sparingly soluble constituents (e.g., the flat trends in predicted freely dissolved concentrations).

The constituents shown in the upper two rows of panels in Figure 2 include lighter, more soluble constituents (e.g., BTEX, C7 naphthenic, 2-ring aromatics), which all exhibit near-linear behavior at low loadings meaning a solubility limit has not yet been achieved. At higher loadings some of these constituents, as well as some

of the 2- and 3-ring constituents in the third row become flat at higher loadings when the respective solubility limits of these constituents are reached.

The 4+ ring aromatics on the lowest row show a generally flat response over the range of loadings reflecting the lower solubility limits of these more hydrophobic constituents. The dashed line on the figures represents the detection limit and many of the measurements and model predictions are at, or below this level, and more variability in the analytical data is expected.

Model performance was acceptable, with mean root mean square error (RMSE) of the log residuals (log predicted – log observed dissolved concentration) of 0.29 (range 0.1 to 0.5) for this subset of constituents. This is also observed across all of the different exposure systems where the different symbols overlap and show the same trends and magnitudes (Figure S3). For comparison, typical environmental fate and effects models (e.g., SPARC, EPIWIN, QSARs in general) used to estimate partitioning (e.g., logK_{OW} [84], logK_{OC} [85] or toxicity [40, 86] have RMSE of log residuals typically in the range of 0.3-0.5.

Salting out of hydrocarbons can result in lower concentrations in seawater relative to freshwater. The solubility model in the present study was applied without correction for salinity. There is a small bias in the model, evident by a slightly greater RMSE for the seawater data (0.31) than the freshwater data (0.22) mainly for the 2-ring aromatics, consistent with the minor salting out effect.

Acute toxicity

To characterize differences in the dissolved oil exposures, analytical methods and modeling were applied (Steps 3 and 4, Table 1) and compared to empirical toxicity data. Figure 3 presents mortality as a function of dissolved phase TUs

calculated using PETROTOX or total bioavailable hydrocarbon based on passive sampling measurements (i.e. BE). For comparison, mortality is shown plotted as a function of other commonly used oil toxicity exposure metrics in Figure S4 (i.e. nominal loading, TPH, TPAH).

Table S1 reports the median lethal effect level and relative standard deviation (RSD) for the different exposure metrics: TU, BE, Loading, TPAH, TPH. The RSD for TU and BE are 0.12 to 0.20, and RSD for TPAH, TPH are 0.25 to 0.52, while the RSD for loading is 0.65 to 0.93 across the different dosing systems and test organisms. Use of TU and BE provide the least degree of variability between dosing systems and test species. Dissolved phase TUs derived using PETROTOX provide an exposure metric that is comparable to the BE measurements in that both provide a holistic characterization of the unresolved oil composition of the dissolved components in the WAF. The success of the TU approach (Fig 3 A-B) is evidenced by reasonably consistent toxicity predictions that are achieved using only the chemistry of the oil and the oil loading.

A useful insight that can be obtained from the modeling analysis outlined in Table 1 is the contribution of unresolved hydrocarbon components to total TUs in the various WAF exposures. This can be inferred by calculating the total TUs that are attributed to the dissolved concentrations of speciated hydrocarbons resolved using GC-MS in Step 2 to the total TUs using GCxGC-FID in Step 3. Since the conventional analytes are only a subset of mass characterized by GCxGC, the TUs based on conventional analytical are systematically lower than TUs based on GCxGC (Figure S5). Results indicate that the resolved hydrocarbons comprise between 10-25% of the total TUs (Figure S6). At low loadings (<10 mg/L) the two approaches

can be different by almost 10-fold. However, at higher loadings (>10 mg/L) the two predictions are closer to 4-fold different. This is due to the more comprehensive characterization of mass by GCxGC. However, this relationship is considered specific to the fresh Endicott crude oil so caution should be used in extrapolating these results to test substances with different composition. This highlights the limitation of extrapolating an exposure metric that is based on a limited number of speciated hydrocarbons between different test oils since the composition of the unresolved components and their contribution to TUs will with vary depending on the substance.

The TU-based dose-responses are very steep and show little difference between exposure systems (Fig 3A-B). By definition the LC50 occurs at TU=1 so partial toxicity (e.g., 20-80% effects) should occur in this range, where model uncertainty is typically on the order of 2-3-fold [20, 67, 83]. The exposures of *D. magna* to fresh oil (Fig. 3A) shows that partial effects occur near TU 1.5, which is consistent with the expected model performance. The dose-responses of the different exposure systems overlap and do not show obvious, systematic diffences across exposure systems (e.g., droplet content), in contrast to conventional exposure metrics (Figure S4). The TU-based dose-response for the mysid exposures to fresh oil show partial to complete mortality at TUs of 2 to 4 (Fig 3B) indicating that predicted toxicity is overestimated by about a factor of three. This suggests that the CTLBB assumed as input for defining the acute sensitivity for the population of mysids tested in this study may have been too low although kinetic limitations of hydrocarbon uptake by test organisms may also help explain this observation.

Figure 3 (C-D) shows mortality plotted against BE measurements for *D. magna*, and *A. bahia*. The BE-mortality responses are steep and explain the region of

partial effects (20 to 80% mortality) to within a factor of two across the different exposure systems. The critical fiber concentrations (e.g., BE measurement at 50% effects, i.e. $LC50_{fiber}$) for *D. magna* averaged 19 mM while the mean $LC50_{fiber}$ for mysids was 5 mM (Table S1) . Prior work relating BE to 48 h mysid mortality indicated $LC50_{fiber}$ closer to 20 mM [5]. However, the prior work was based on different passive sampling protocol involving thicker fibers (100 µm vs 30 µm), and longer equilibration times (24 h vs 100 min) for BE analysis, which may account for the different mysid toxicity values reported in this study.

The modeled TUs are based on mechanistic solubility and toxicity model incorporated in PETROTOX [3] that assumes a steady state between all the constituents in the exposure system and the test organisms. The BE measurements provide an empirical measurement of dissolved (i.e. bioavailable) hydrocarbons that equilibrate with the passive sampler (i.e. PDMS-coated fiber) and represents a compromise between equilibration with the higher molecular weight constituents and potential losses of the more volatile constituents during fiber analysis.

Summary

Application of dissolved phase TUs and the BE analysis of total bioavailable hydrocarbons using passive sampling explained the observed mortality to within a factor of two across the different exposure systems and test organisms investigated. These two methods, therefore, provide complementary exposure metrics for evaluating and predicting the toxicity of passively, physically and chemically dispersed crude oil. In contrast, other metrics commonly used to describe the aquatic hazard of petroleum substances e.g., Loading, TPAH and TPH (Figure S4) can differ by 10-fold even when evaluating the toxicity of the same oil, reflecting the complexity and varying

bioavailability of oil exposures across different test systems. This analysis indicates that the alternative oil exposure metrics proposed in this study provide a more consistent basis for hazard assessment of petroleum substances consistent with conclusions from previous work [1].

Previous studies have investigated the role of droplet oil via side-by-side tests with and without filtration, or other separation strategies [87-90]. This study has used a different experimental design by varying the oil dosing method so that different droplet exposures could be generated while taking into account the changes in dissolved phase exposures that simulataneously occur at different oil loadings. Our results support the findings of a number of earlier studies indicating dissolved phase hydrocarbons dictate observed toxicity and droplet oil has no or only a minor contribution to toxicity [64, 65, 91].

While some studies have concluded droplet oil poses a toxicity concern [89, 90]. These studies, which evaluated the role of droplet oil on fish embryos, propose attachment of droplets to the chorion is a likely mechanism of toxicity. While this explanation is plausible, the dissolved phase exposures in these studies were not characterized so the role of droplet oil remains subject to debate, which may be informed using the dissolved exposure metrics described in this study.

The framework presented in this study provides a mechanistic modeling approach to characterize the speciation of hydrocarbons in oil toxicity test exposures, as well as providing a method for relating detailed oil composition to solubility and toxicity (e.g., TUs). In addition, a procedure for obtaining passive sampling measurements of bioavailable dissolved hydrocarbons (e.g., BE) is described that provides a simpler analytical surrogate for the modeled TUs. This framework was

illustrated using oil toxicity tests with freshwater and marine invertebrates using both conventional and passive oil dosing methods. This approach needs to be extended to additional species, especially early fish lifestages, and a wider range of oil types. The current work has been focused on constant, short term exposures under standard conditions. However, oil spill exposures are highly dynamic. Thus, to be relevant to field situations, the modeling and passive sampling tools described in this study need to be further extended to better characterize and interpret time-variable dissolved oil exposures.

FIGURES

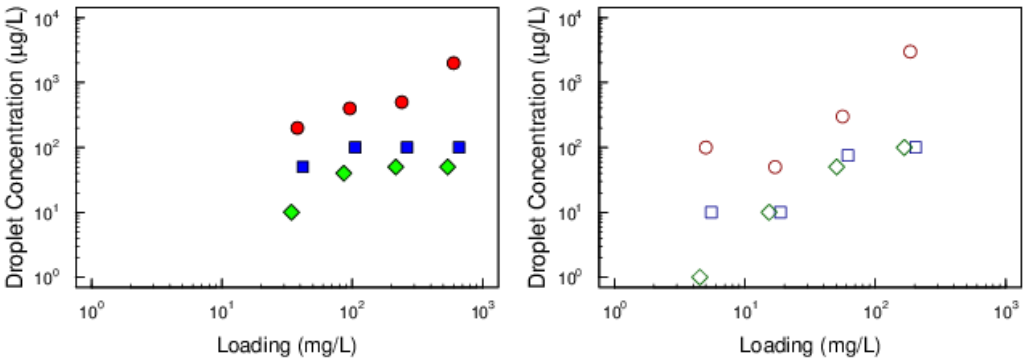

Figure 2.1 Droplet concentration plotted against measured initial fresh crude oil loading for chemically dispersed (●,○), physically dispersed (■,□), and passively dosed (♦,◊) exposure systems in freshwater (A, filled) and seawater (B, open). Droplet concentrations were determined by the difference between total measured concentrations and modeled dissolved concentrations, see text for details. Data slightly offset for visual clarity in *x*-axis.

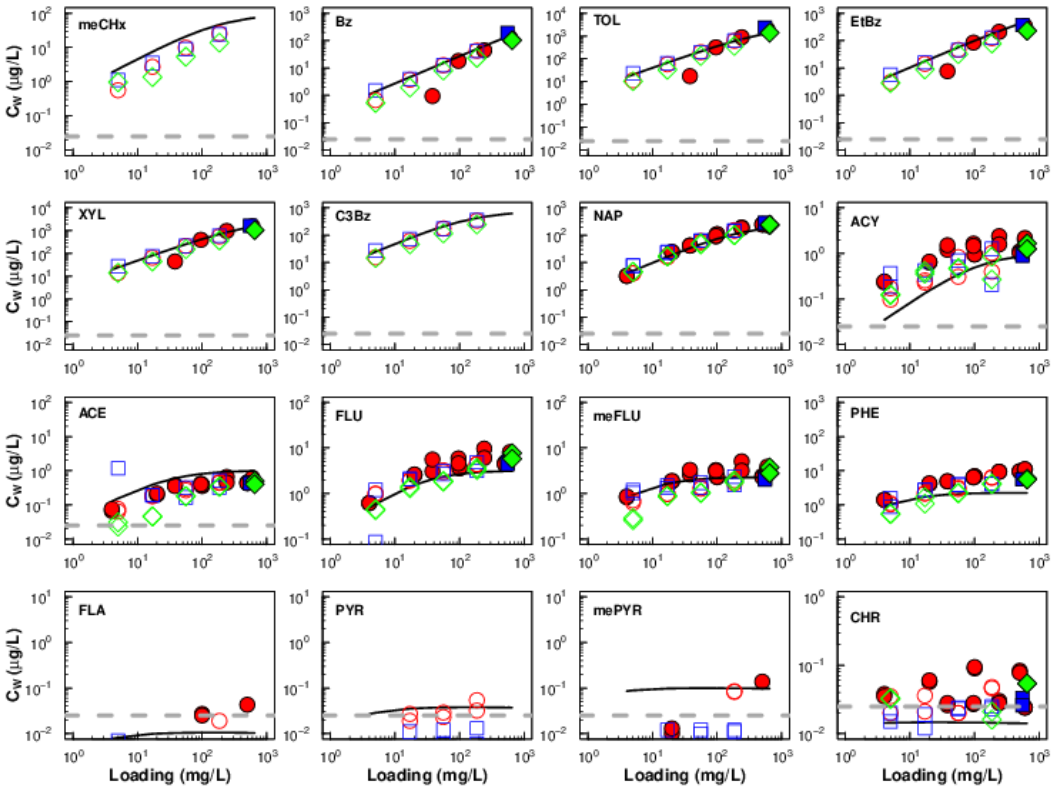

Figure 2.2 Measured, and predicted (solid line) dissolved concentrations of individual constituents shown over range of loadings in seawater (open) and freshwater (closed) for chemically dispersed (●,○), physically dispersed (■,□), and passively dosed (♦,◊) exposure systems. Dashed line represents detection limit (0.025 µg/L). Solid line represents predicted solubility determined with Raoult's Law-based solubility model. Note changing scales. meCHx methylcyclohexane, Bz benzene, TOL toluene, EtBz ethylbenzene, XYL xylenes, C3Bz trimethylbenzenes, NAP naphthalene, ACY acenaphthylene, ACE acenaphthene, FLU fluorene, meFLU methylfluorene, PHE phenanthrene, FLA fluoranthene, PYR pyrene, mePYR methylpyrene, CHR chrysene.

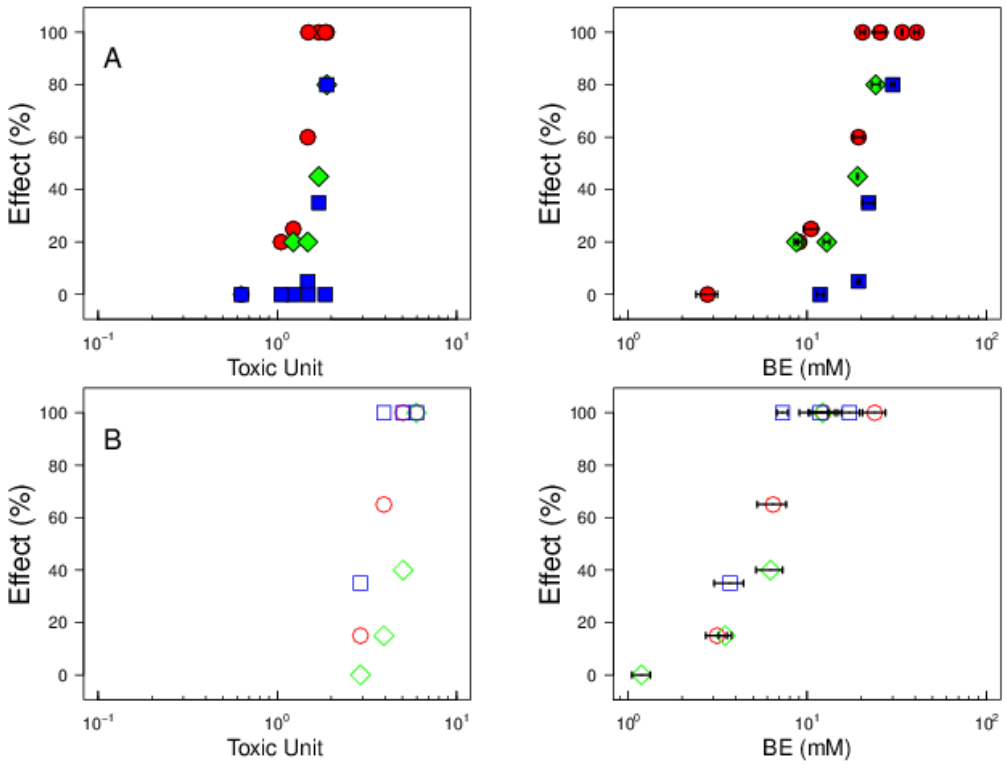

Figure 2.3 Observed 48-h effects plotted against TU (panel A-B) and BE measurements (C-D), for both daphnid (filled symbols) and mysid (open symbols) exposures to fresh Endicott oil: chemically dispersed (●,○), physically dispersed (■,□), and passively dosed (♦,◊) exposure systems. Bars indicate 1 standard deviation of replicate BE measurements.

TABLES

Table 2.1 Summary of analytical requirements to characterize dissolved phase exposures

Step	Analytical requirements	Oil	Water	Application	Data use	Output	Citation
1	Speciated PAH, VOCs including BTEX, Saturated hydrocarbons	x	x	Measure individual constituents in test substance and oil dosed water samples.	Measurements are input to solubility model for predicting dissolved and particulate concentrations. High droplet content (>10 mg/L) may buffer exposures [66].	Plot modeled dissolved and total vs measured total (Figure S2). Plot of droplet concentrations vs treatment loading (Figure 1).	[1, 12, 66]
2	Dissolved PAH, Total speciated VOCs		X	Measure <u>dissolved</u> PAHs, and total speciated VOCs.	Comparison of data to predicted dissolved concentrations (Step 1) for solubilty model validation and use in toxicity assessment (Step 3).	Plot of predicted vs measured dissolved for each treatment loading (Figures 2; S2).	This work.
3	GCxGC-FID	x		Quantitative measurements of mass distribution by C# and chemical class. See Methods.	These data, along with the test substance loading, are used to predict dissolved TU for each loading using the hydrocarbon block approach.	Plot of observed effects vs predicted total TUs (Figure 3). May also compare total TU (Step 3) to TU calculated for limited subset of individual constituents (Step 2).	[3, 28]
4	Biomimetic Extraction (BE)		x	Perform BE measurements on water samples from oil test exposures	This provides measurements of total bioavailable hydrocarbons which are, in principle, surrogates of modeled TUs (Step 3).	Plot of observed effects vs BE measurements as a surrogate for TUs (Figure 3).	[5, 28]; This work.

Chapter 3

EVALUATION OF TOXICOKINETICS OF HYDROCARBON EXPOSURES TO AQUATIC LIFE

3.1 Abstract

Hazard assessment of petroleum substances in the environment is challenging due to the variable physicochemical properties of the individual hydrocarbon constituents. Further, environmental exposures vary in space and time and are not always directly comparable to standardized toxicity data developed using constant exposure conditions. Therefore, a first order toxicokinetic model was used to estimate the dominant elimination rate constants for a range of test species and hydrocarbons. And focused experimental work was performed to understand the role of temperature and organism size on the observed toxicokinetics. The results indicated that weight and temperature had low impact on the observed toxicokinetics. Further, dependence on logK_{OW} of the test chemical was observed to be low. These results reflect the inherently variable nature of ecotoxicity data, but are likely limited by the lack of comprehensive datasets across chemicals, test organisms, and temperature conditions. Therefore, the model to generalize the toxicokinetic parameters was focused on the largest datasets on rainbow trout and fathead minnow, which resulted in logK_{OW} being the sole significant descriptor. This parameterization was compared to the toxicokinetic parameters used in existing oil spill models to support a refined hazard assessments approach.

3.2 Introduction

Exposures to chemicals in the environment are often transient in space and time, which include exposures through nonpoint source run off, permitted outfalls, and accidental releases [92]. In contrast, hazard data used to characterize the thresholds of toxicity are often based on laboratory methods using constant exposures to promote replication and to minimize potential confounding variables [93]. While constant-exposure hazard data have dramatically improved our understanding of chemical fate and toxicity they are not always representative of exposures in the environment.

Dynamic water quality modeling is one strategy used to evaluate dynamic exposure concentrations [94]. These are applied to characterize the movement of chemicals from one phase to another, e.g. volatilization, as well as to model the bioaccumulation and toxicity of chemicals in aquatic life. This is true of oil spill trajectory models as well [68, 69, 95].

Existing oil spill models use a combination of toxicokinetics and hydrocarbon blocks to estimate the hazards of complex oil substances [69, 95]. The hydrocarbon blocks, or pseudo-constituents, is a convenient method for handling the complexity of petroleum substances. They represent a discrete group of chemicals with similar properties to predict the fate of oil and the environment. The toxicokinetic models are used within the larger fate modeling to predict the dynamic uptake, elimination, and hazards of the hydrocarbon blocks.

Toxicity often occurs once the bioaccumulation of environmental contaminants exceed a threshold within the organism [18, 96]. For nonpolar organic chemicals bioconcentration factors (BCF) are often modeled as the ratio of the rate of chemical uptake (d^{-1}), k_1, to the rate of elimination, k_2 (d^{-1}) [97]. Generally, since uptake is fast, the elimination rate controls the bioaccumulation of chemicals [77, 98, 99].

$$BCF = k_1 / k_2 \quad (1)$$

Toxicokinetic modeling uses a similar approach to model the uptake, and accrual of chemicals and damage relative to the recovery and elimination processes within an organism [6, 100, 101]. In this context the overall elimination rate, k_2, is considered to be a multipurpose parameter which implicitly includes excretion, metabolism, and damage repair [6]. It is also anticipated that the lumped elimination rate will vary as a function of the organism size, exposure temperature, and physicochemical properties of the contaminants [78, 102, 103]. The primary objective of the present work was to improve the technical basis of the toxicokinetic models used in oil spill hazard assessments. The assumed form of the elimination rate (k_e) as a function of organism weight, environmental temperature, and logK_{OW} is given in Equation 2.

$$\log k_e = a_1 \log K_{OW} + a_2 \log W + a_3 (T_1\text{-}25) + b \quad (2)$$

where W is organism weight (gm), T_1 is temperature (^oC), a_1, a_2, a_3 and b are constants

These parameters are primarily based in bioaccumulation data, which are certainly related to, but not necessarily reflective of, toxicokinetics. The parameters in Equation 2 were largely based on bioaccumulation data [68, 104-106]. The log lumped elimination rate (k_e, d^{-1}) is predicted using an allometric term on weight, W (g), with a_2 as the slope factor of -0.2. The logK_{OW} represents the influence of chemical structure with a slope, a_1, of -0.41, and the constant, b, is taken as 1.47. The influence

of temperature is modeled using the Q_{10} approach [107] such that a_3 is 0.048 (note the conversion from natural log, to log-base 10 from Eqn 17 in French-McCay [68]), resulting in changes by 3-fold for every change in 10° C (T_1 = 15° C, $k_e = 10^{(0.049*(15-25))} = 10^{-0.49}$ = 0.32 – fold reduction in k_e based on lower temperature).

While it is intuitive that these parameters would influence the toxicokinetics of chemicals, there are few paired toxicokinetic data to fully calibrate these terms. Therefore, the second objective of the present work was to develop toxicokinetic data for fish and invertebrates that span a range of size and test temperature, and that were developed in the same laboratory to minimize potential confounding factors, which included evaluation of this parameterization using k_e values derived on toxicity data from literature datasets.

The focused experimental work, and resulting toxicokinetic parameters, were compared to the modeling analysis of literature data for a wide variety of test chemicals, organism sizes, and exposure temperatures. The outcome the present work will refine the hazard models used in oil spill trajectory models to provide more accurate predictions of effects in the field.

3.3 Methods

Approach

There were three datasets used to address the objective of the present work. The first data set includes internally consistent experimental work to evaluate the role of temperature and weight on a two ring aromatic hydrocarbon. The second data set was designed to evaluate the effect of temperature on one-, two-, and three-ring aromatic hydrocarbons. The third data set is a compilation of published hydrocarbon

toxicity data sets across a range of exposure conditions including size and temperature of the test organisms.

Experimental group A

This study was performed to evaluate the effect of organism size and temperature on toxicokinetics of methylnaphthalene. Three organisms were used following standardized test protocols: *Oncorhynchus mykiss* (OECD 203, rainbow trout at 0.1 and 1.0 g), *Daphnia magna* (OECD 202, daphnids, <24 h old) and *Lumbriculus variegatus* (aquatic only version of OECD 225, blackworm). Tests with *O. mykiss* were conducted with fish at approximately 0.1 g and 1.0 g. Tests were performed under flow through conditions at 10^{o} and 18^{o} C. Water chemistry (DO, pH, etc) during the tests were within guidance.

The concentration in each treatment was maintained by passive dosing silicone rubber cord. The cord was prepared by equilibration with a spiked methanol solution for 24 h at various concentrations [49]. This resulted in stable aqueous test concentrations during the test. A peristaltic pump (approximately 12.9 mL/minute) delivered fresh dilution water to each passively equilibrated test solution for each treatment group and the control group. Simultaneously, separate peristaltic pumps delivered exposure solutions to each replicate chamber from the passively dosed solution to the test chambers at approximately 5.55 mL/minute for the fish and approximately 0.88 mL/minute for the daphnia and worms.

Experimental group B

This study was performed to evaluate the acute toxicity at 5°C and 18°C to rainbow trout, *Oncorhynchus mykiss*, in a 96-hour static test (OECD 203) with 24-hour renewals. The solutions were allowed to cool to test temperature in a waterbath

for approximately one hour without stirring before removing the aqueous portions (WAFs) for testing. WAFs were prepared daily, the day preceding each renewal. All water quality parameters were within an acceptable range. Each test and control chamber was observed at time 0, 0.5, 1, 3, 5, 24, 48, 72 and 96 hours.

Exposures were conducted with o-xylene, methylnaphthalene, and phenanthrene (>96% purity, SigmaAldrich). Exposure solutions were prepared by adding the appropriate amount of test substance, via stainless steel and glass syringes, to 20 L of vehicle/dilution water in glass aspirator bottles (capacity 22 L) and stirring on magnetic stirplates for 24 hours (±1 hour).

Literature dataset

Toxicity data for hydrocarbons and aquatic species were identified in the published literature. These studies are standard testing protocols with near steady-state exposure concentrations to minimize variability introduced by variable exposure conditions. Mortality data over time and at different exposure concentrations were collected from tables in the original publications, or through digitization of figures. The studies included in this analysis are provided in Table 1. Time to death studies were not used as it is challenging to estimate both the threshold and toxicokinetic parameters.

In addition to chemical exposure and mortality data, test temperature and typical organism weights were estimated from source literature, or study protocols. Datasets were included that had survival data for multiple treatment levels over time, with reasonably consistent exposures for the duration of the exposures. This provided a basis for evaluating both the lumped elimination/damage repair rate and the slope

term of the dose response. Only toxicity data with exposure time < 4d were used for this modeling analysis to minimize bias in the parameters

Toxicokinetic modeling:

BACKGROUND

The lumped elimination rate constant, k_e, is used to describe the rate that toxicity (e.g., mortality) accrues following an exposure to a toxicant. This parameter was estimated by fitting the observed toxicity data with the general unified toxicokinetic framework (e.g. GUTS [6]). This implementation of the GUTS modeling framework is a one compartment model with first order kinetics. The exposure framework models the accumulation of chemicals in target tissues as the gradient of the external exposure to the internal concentrations.

$$\frac{\mathrm{d}C_i^*(t)}{\mathrm{d}t} = k_e(C_\mathrm{W}(t) - C_i^*(t)) \tag{3}$$

where k_e (d^{-1}) is the lumped elimination/recovery parameter, $C_W(t)$ is the external aqueous concentration and $C_i^*(t)$ is the scaled exposure concentration. The scaled exposure concentration is the hypothetical external concentration that is proportional to the internal concentration following bioaccumulation (e.g. internal concentration = $C_i^*(t)\ BCF$, For $C_\mathrm{W}(t)$ varying, Equation (3) can be solved numerically at each time step, t. For a constant $C_\mathrm{W}(0)$ the solution is

$$C_i^*(t) = C_W(0)(1 - e^{-k_e t}) \tag{4}$$

The GUTS framework provides either a stochastic death (SD) or individual tolerance (IT) approach to modeling toxicity. The SD approach implies that mortality will occur at some point once the threshold has been exceeded, whereas the IT approach predicts that effects occur in proportion to the accumulated $C_i^*(t)$ relative to a threshold [6, 101]. In practice it is difficult to distinguish between these two modeling approaches [101, 108, 109], as both approaches can be used to satisfactorily model the same datasets through various combinations of model parameters. There are few data in the literature to allow more extensive testing to enable discrimination of the IT and SD models.

Therefore, in order to simplify the analysis in the present study the IT model was chosen since it is largely compatible with the critical body burden models [18, 96] typically used in oil spill hazard assessments [68, 69]. The strategy to focus on the IT model ensures an internally consistent set of model parameters for the oil spill and Target Lipid models.

The IT model is evaluated using the cumulative log-logistic distribution of tolerances.

$$F(t) = \frac{1}{1+(\frac{\max(C_i^*(t))}{z})^{-\beta}} \tag{5}$$

where, *z*, is the toxicity threshold, and β the slope factor on the dose response. The scaled exposure concentration, $C_i^*(t)$, is compared to the threshold value (mmoles/L), *z*, which is analogous to the critical target lipid body burden (CTLBB) in the TLM [18].

The survival probability, $S(t)$, for IT is determined as a function of the hazard rate and background mortality, h_b

$$S(t) = (1 - F(t))e^{-h_b} \quad (6)$$

where $F(t)$ is the result of the Eqn 5, and h_b is the background mortality rate.

This GUTS_IT approach for the present study utilizes the implementation developed for R [110]. This package provided features to optimize parameters and to estimate confidence intervals for those parameters. There are three main optimizable parameters in the GUTS_IT model: k_e, β, and z.

The main parameter of interest is the lumped elimination rate, k_e. The slope term, β, and the threshold, z, were constrained in order to focus on k_e. The threshold, z, was determined empirically as the 4-d LC50 for each dataset (or 2-d in the case of *D. magna* exposures). The rationale is that in practice the thresholds for effects would be selected from existing compilations of critical tissue residue concentrations, e.g., TLM [20], for which the range and variability are relatively well known [111]. The slope parameter is generally steep for acute hydrocarbon toxicity data consistent with prior applications to nonpolar organics (range 1-8 [7]) The slope parameter, β, was therefore set at the median value of 5.09 (95% confidence intervals 2.59-7.21) based on the average fit for the entire dataset of 4d mortality and exposure concentrations. The background hazard rate, h_b, is typically low (h_b<0.001 d^{-1}) in standard tests <5 d and was fit empirically to control data

A second fitting analysis was performed to estimate k_e directly by rearranging equations 4, 5 and 6 to solve for k_e assuming a negligible background hazard rate.

$$S(t) = \left(1 - \frac{1}{1 + (\frac{(C_{W,i}(1 - e^{-k_e t}))}{z})^{-\beta}}\right) \quad (7)$$

The ratio of the exposure concentration, C_W to z is referred to as a toxic unit (TU), which is a useful concept for evaluating relative potency of multiple chemicals and mixtures.

$$S(t) = \left(1 - \frac{1}{1 + ((TU(1 - e^{-k_e t})))^{-\beta}}\right) \quad (8)$$

Solving Eq.(8) for k_e directly from the observed survival data yields.

$$k_e = -\ln(\frac{(\left(1 - \frac{1}{1 - S}\right)^{\frac{1}{-\beta}})}{TU} - 1)\frac{1}{t} \quad (9)$$

In this formulation there are two limiting cases for which k_e cannot be determined: when the fraction surviving *S* is unity (e.g., the controls, or low exposures, or early time points) a divide-by-zero occurs, and again when *S* is zero (e.g., high exposures, longer time points) the top term is zero. Therefore, this direct analysis of *k*e is based only on the partial survival data.

Regression Analysis

The objective of this work is to investigate the dependence of k_e on various organism and chemical properties. This was accomplished by comparing the fitted k_e values using either the whole dataset, or by the direct calculation method, to the major controlling factors: log K_{OW}, tested species, organism weight, and test temperature.

The estimated k_e was further analyzed using multiple linear regressions using the GLM package in R [34].

3.4 Results

Experimental Set A – role of weight and temperature

This first set of experiments was designed to evaluate the role of organism weight, and exposure temperature on k_e. This dataset is unique in that passive dosing was employed to maintain constant exposures. In addition to testing organisms of different sizes, at different temperatures, all the tests were performed in the same laboratory using the same batch of test organisms. This design was intended to limit inter-lab variability and to improve the ability to evaluate the role of the major testing variable: weight, temperature.

Utilization of the passive dosing and flow through design resulted in stable exposure concentrations of methylnaphthalene in the large and small exposure vessels. The coefficient of variation of exposure concentrations among the different exposure levels is 7.6% consistent with prior applications of passive dosing to maintain exposure concentrations [49, 50, 112]. The exposure levels were widely spaced around the LC50 to promote effects in the short term (< 1d).

For fish and daphnids the onset of toxicity at the higher treatment levels occurred within the first few hours of exposure (Figure 1). The highest treatment levels are approximately 10-fold greater than the threshold, *z*. This resulted in rapid onset of toxicity at the highest levels. The lowest treatment level was approximately 10-fold lower than the threshold and resulted in no effects through the study. The middle treatment level resulted in near complete mortality at 4 days. These curves result in estimated k_e values of approximately 0.5-1.0 d^{-1}.

The tests with blackworm had notably slower kinetics (0.3 d^{-1}, Figure 1) than the fish and daphnids (0.76-1.5 d^{-1}, Table 1). Similar to the fish, complete mortality was observed at 4 days in the high and middle treatment levels with no effects at the low treatment level. The slower kinetics is likely due to the physiology of worms that respire via diffusive exchange through the skin. In contrast fish and daphnids respire via gills that employ active movement of water across the gills to facilitate gas exchange. Another likely explanation is the lower metabolic capability of the blackworms compared to daphnids and fish.

The role of temperature remains unclear in this dataset despite the well-controlled experimental conditions. Results from the Experimental dataset A are given in Figure 2 showing the estimated k_e from the fit of the nonlinear solution (Eqn 2,3) against the organism weight during testing. The different temperatures of *O. mykiss* testing are given as different symbols. The k_e values estimated at 10^o C were comparable to those observed at 18^o C (Figure 2), with all estimated values of k_e being within a factor of 2 of each other. The variation in test temperature only varied by 8^o C, which is within the expected variation in biological processes, which typically increase by factors of 2-3 over rise by 10-20^o C [113]. It is possible that this variation in temperature is not wide enough to observe a measureable response in k_e.

The role of weight was evaluated by performing side-by-side testing with organisms of dramatically different weights. For example, in the present study the adult daphnids weight approximately 500 µg wet weight, the blackworms 8 mg, and the fish were tested as recent swim up (~0.11 g) and as juveniles (~1.1 g). This dataset spans three orders of magnitude in body weight.

The observed variation in k_e for these organisms is also unclear (Figure 2). There are no clear trends in k_e since the blackworm data, which are in the middle of the weight series, is less than the daphnid and fish results. As noted above, this is likely a reflection of the different physiology of these organisms. However, the daphnid and fish data, despite having very different body sizes show essentially the same k_e.

The model (Eqn 2) predicts larger variation in k_e than is observed. The modeled temperature shift (dashed vs solid line, Fig 2) is wider than the observed data (blue vs grey points, Fig 2). Application of the original parameterization of Equation 2 provided model predictions that are in reasonable agreement with the estimated k_e to an order of magnitude. Regression modeling of these individual k_e estimates return regression coefficients that are not statistically significant (a=0.05).

Experimental Set B – role of logK_{OW} and temperature

This set of experiments was performed to evaluate the role of log K_{OW} and temperature on the toxicity of xylene, methylnaphthalene, and phenanthrene to juveline *O. mykiss*. There were five treatment levels in these exposures. The higher two treatment levels resulted in entire mortality at 4 days for all exposures, with partial effects often observed at the middle treatment level. Control and lower treatments did not produce toxicity in 4 days.

Similar to the results from experimental set A, toxicity at the higher treatment levels occurred within the first few hours (<4h). The estimated k_e values range from approximately 6 d^{-1} to 0.5 d^{-1} for the tests at 18^o C, and approximately 1.5 d^{-1} to 0.5 d^{-1} for the tests at 5^o C (Table 1). The k_e values at 18^0 C generally decline in a log-linear

manner with log K_{OW}, whereas the results from 5° C tests are equivocal with respect to log K_{OW}.

The model predictions from Eq.(2) are in general agreement in that it confirms the inverse log-linear relationship. The magnitude of the k_e for the juvenile rainbow trout (~1 g) in this experimental set B are higher than for the comparable larger fish in Figure 2. It is assumed that the differences are due to individual tolerances of different groups of fish as these tests were performed several years apart.

These tests were performed at 5° and 18° C, and the resulting k_e are different by a factor of three. The model predictions are different by approximately 4.2-fold (lines, Figure 3) showing general agreement with the k_e estimated from the experimental data against log K_{OW} of the test chemical. The general outcome from the analysis of data from experimental set B are that k_e has some dependence on log K_{OW} and that temperature effects are slight.

Modeling analysis of combined Set A and B

Datasets A and B discussed above are unique in that they report toxicity data developed at different temperatures, organism weights, and a range of hydrocarbon classes (1-, 2- and 3-ring aromatics). These data, therefore, provide a strong technical basis to test the k_e framework in Eqn 2. These data were, therefore, analyzed using multiple linear regression.

Using the GLM package in R, Eq. (2) was fit to the combined experimental datasets A and B. The results are show that the coefficients for weight and temperature are small in magnitude and non-significant at the 95% confidence level. Visual inspection of Figure 2 confirms the low impact of weight on the derived k_e, and the temperature dependence is inconsistent across the entire dataset. The only

parameter that appears significant is the dependence on log K_{OW}. The slope of -0.42 (standard error, SE, 0.19) and intercept 1.66 (SE 0.76) are very similar to the slope and intercept used in French-McCay model [68] (-0.41, 1.47, respectively) in Eqn 2. While the coefficients are found to be significant, the standard errors are large, which highlights the low impact of log K_{OW} on the observed k_e.

Application to compiled dataset

Individual datasets were analyzed with the GUTS toxicokinetic framework using scaled internal concentrations and the IT hazard model [6]. The compiled dataset included studies on 16 species including freshwater and marine fish and invertebrates (Table 1) and 23 chemicals including a few aliphatic molecules (C6-7), and 1-, to 4-ring aromatic hydrocarbons. Five+ ring aromatic toxicokinetic data were available [49] but showed no toxicity so were not used in the present work.

The individual fitted k_e are given in Table 1. This broader datasets was evaluated for trends with respect to log K_{OW}, organism weight, and temperature during the exposures (Figure 4). Visual inspection of k_e derived for fish shows slight trend with log K_{OW}, but no discernable trend with weight or temperature (Figure 4, A, C, E). Analysis of the invertebrate dataset (Figure 4, B, D, F) show that the magnitude of the k_e are similar to those found in the fish dataset but no statistically significant parameters were identified with log K_{OW}, weight or test temperature.

A multiple linear regression analysis was performed to evaluate the role of log K_{OW}, organism weight, test temperature, and species on the observed toxicokinetics, k_e. This was performed by allowing a species-specific intercept to account for species-specific traits (e.g., tolerance, metabolism). There were no statistically significant parameters (probability < 0.05). The magnitude of the log K_{OW}, temperature and log

weight coefficients are small indicating low impact of these variables on the final results. This result indicates that the best fit is species specific constant k_e.

Analysis of composite dataset

Equation 7 shows that survival (S) is proportional to the inverse of the time-weighted TU. This also demonstrates that the survival is proportional to the inverse of the TU and exponential terms, which is useful for comparing data across multiple species, chemicals, k_e, and exposures. The composite exposure term, *F'*, is used to evaluate the performance of the entire dataset.

$$S \propto F' = \frac{1}{((TU(1 - e^{-k_e t})))^{-\beta}} \quad (10)$$

The first analysis of the model performance was evaluated with *F'* (Eq 10) using k_e estimated on the individual datasets using the nonlinear fit (Eq 2,3, Table 1, Fig 4). Evaluation of the entire dataset was analyzed with hex bin plot that uses shaded hexagons that are scaled by the number of observations in that plotting space. This allows evaluation of datasets with multiple entries that over-plot each other.

Application of Eqn 10 to the observed mortality datasets resulted in characteristic logistic shape where high survival rates (S>0.9) correlated with low *F'* values (Figure 5 A, e.g., low TUs, low t) which are found for low concentration exposures and short time points. Low survival rates (S<0.1) are correlated with high TUs and at longer time points. The logistic model (line Fig 5 A) using the empirically derived slope factor, β=-5.09, indicates general agreement of the model (Eq 10) with

the predicted time variable mortality. The root mean square error (RMSE) on the log values of *F'* is 0.22, indicated good agreement between the model and observations.

A second analysis of the dataset using F' was performed by using k_e which had been calculated directly from the partial survival data (Eqn 9). The magnitude of the parameters is similar to those found in the analysis of the whole datasets but are small. Further, implementation of this model resulted in a less accurate model based on the RMSE (0.28 using direct calculations, Eqn 9, vs 0.22 using k_e fitted to individual datasets).

Two separate analyses of the toxicokinetic data indicated that the influence of log K_{OW}, temperature and organism weight were small. More complete datasets in terms of temperature variation, and different chemicals may help refine the observed variability in k_e in the larger dataset.

3.5 Discussion

Variation in k_e

Across the entire dataset (fish and invertebrates, Table 1) the range is 7.0 to 0.04 d^{-1}, with a median of 0.50 d^{-1} and an inner quartile of 0.36 to 1.03 d^{-1}. Therefore, variation between species is hard to discern.

The lack of dependence on temperature and weight is different than what is commonly observed in bioaccumulation kinetics [78, 114, 115]. The magnitude of the allometric scaling terms used in bioaccumulation kinetics is modest, scaling factors range over 2- to 3-fold over 6+ orders of magnitude in weight (Fig 4). It is likely that the dataset compiled in the present study is not sufficiently comprehensive in terms of organism types, size, and chemical classes to fully evaluate the role of temperature or weight. However, the magnitude of those variations is small and is, therefore,

generally consistent with our observation that these parameters are not significant contributors to k_e.

One possible explanation for the lack of temperature dependence is that the test organisms were tested at optimum, or tolerable, temperatures. This is consistent with the observed comparable sensitivity of arctic and temperate species as well as between fish and invertebrate species [20, 116, 117]. The findings of the present study are consistent with prior applications of GUTS to oil exposures, where k_e is found to be relatively constant between age classes of arctic copepods [9]

Further, the lack of dependence by k_e on W and T could also be explained by differences in the mechanisms of toxicodynamics (TD). For example, the metabolism of chemicals is a major, and often one of the fastest, elimination process in organisms [77, 97, 118, 119]. The k_e values derived in this study are compared to compilations of measured fish *in-vivo* metabolism rates from published literature [118, 119] against $\log K_{OW}$ of the test chemicals in Figure 6. The magnitude of k_m are comparable to the magnitude of k_e derived in the present study for the fathead minnow and rainbow trout datasets, which represent the largest datasets of juvenile fish in the present study.

Many of the subsets in the compilation of literature datasets are small, having only a few chemicals, or treatments. This is particularly true of the invertebrate datasets. The fish datasets include three species that have exposures to multiple (n > 3) treatments or chemicals: *D. rerio, O. mykiss, P. promelas*. Therefore, the final formulation of the k_e parameter was performed separately on the Fish and Invertebrate datasets.

The invertebrate dataset has data for 11 species, but nine were evaluated on only one chemical (Table 1). The other two species had data for three (*C. dubia*) and

five chemicals (*A.bahia*). The linear regression analysis indicated that no variables were statistically significant (a=0.05). Therefore, the median k_e for the species-specific dataset is provided (Table 2). The species median k_e values spanned approximately an order of magnitude (Figure 7A). For risk assessment, it is recommended that either data for a representative species be used, or that a conservatively large k_e be used. Further, additional focused data for a range of chemicals on model test organisms could refine this recommendation.

The fish dataset includes five species, with data for *O. mykiss* (n = 10) and *P. promelas* (n = 16) being the most abundant. Multiple linear regression indicated that log K_{OW} was the only statistically significant (a = 0.05) variable (slope = -0.21, SE = 0.10) in addition to the species-specific intercepts (b_i, Table 3).

$$\log k_e = -0.21\, logK_{OW} + b_i \quad (11)$$

Variation in the intercept terms vary approximately 5-fold for fish (Figure 7B), and nearly 30-fold for invertebrates (Figure 7A), which is similar is magnitude to the range of organism sensitivity observed for species exposure to hydrocarbons [120]. However, sensitivity of the test organism was already accounted for during the empirical determination of the threshold term, *z* (see Methods). Therefore, the range of intercept likely reflect the ability of test species to recover from damages accrued from the exposures either through elimination, repair, or metabolism.

The primary objective of this work was to improve the technical basis of the toxicokinetic parameters, namely k_e, used in oil spill hazard assessment models. Therefore, predicted LC50s at different time points are compared in Figure 8 for the

different models for fish (Table 3, Eqn 11), invertebrates (Table 2), and the previous work by French-McCay model 2002. In general the shapes and magnitudes of the different models are similar. The impact of the different slope terms (Eqn 2 vs 11) is apparent when comparing the red and black lines for benzene (Fig 7A) and pyrene (Fig 7D).

What is notable about the dynamics is the comparison between the predicted LC50s at short time periods to the water solubility for these chemicals. At short time points, e.g., exposures < 0.5 days, the predicted LC50s are above the solublity limits. Meaning these constituents would not invoke toxicity at under short time periods. Only low MW aromatics 1- and 2-ring aromatics, would contribute to short term effect with higher MW chemicals contributing only fractionally.

Future work:

The present work established the technical basis for estimating the first order lumped elimination/damage repair rate, k_e. for hydrocarbons. The training set included focused testing to evaluate the role of organism weight, test temperature, and log K_{OW}. A larger dataset compiled from literature was also investigated. There are large species specific differences. However for fish, k_e is slightly dependent on log K_{OW} and for invertebrates k_e is invariant with W, T, or log K_{OW}.

Future work should include additional validation of this toxicokinetic framework on well characterized oil substances. Further, time variable exposures will allow for refinement of damage-repair parameters. The present work can be extended to estimating time-weighted effect levels (e.g., LC50s) to support hazard assessments during oil spill, or other transient exposure scenarios.

FIGURES

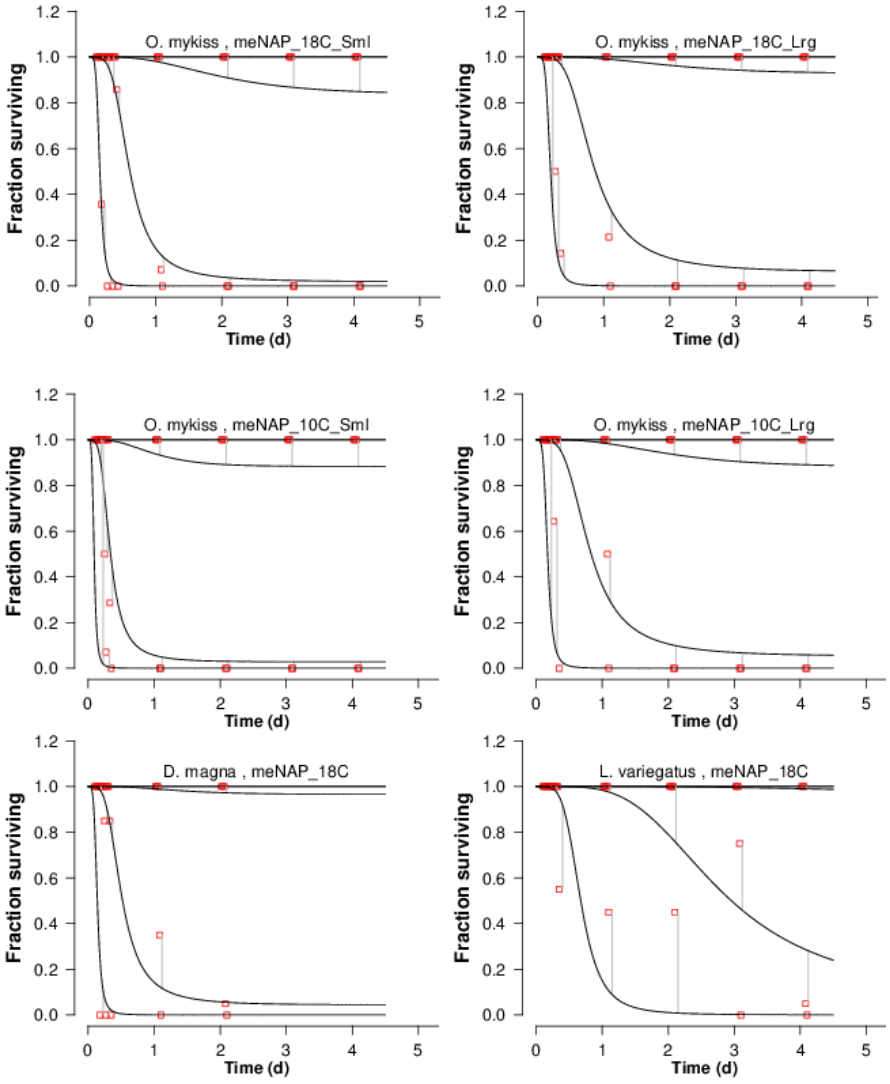

Figure 3.1 Time series for Experimental dataset A, temperature controlled exposures to *O. mykiss*, *D. magna*, and *L.* variegatus. Each line represents a different treatment level: control, low, mid, high, with periodic observations over 24 to 48 h. See SI table for details.

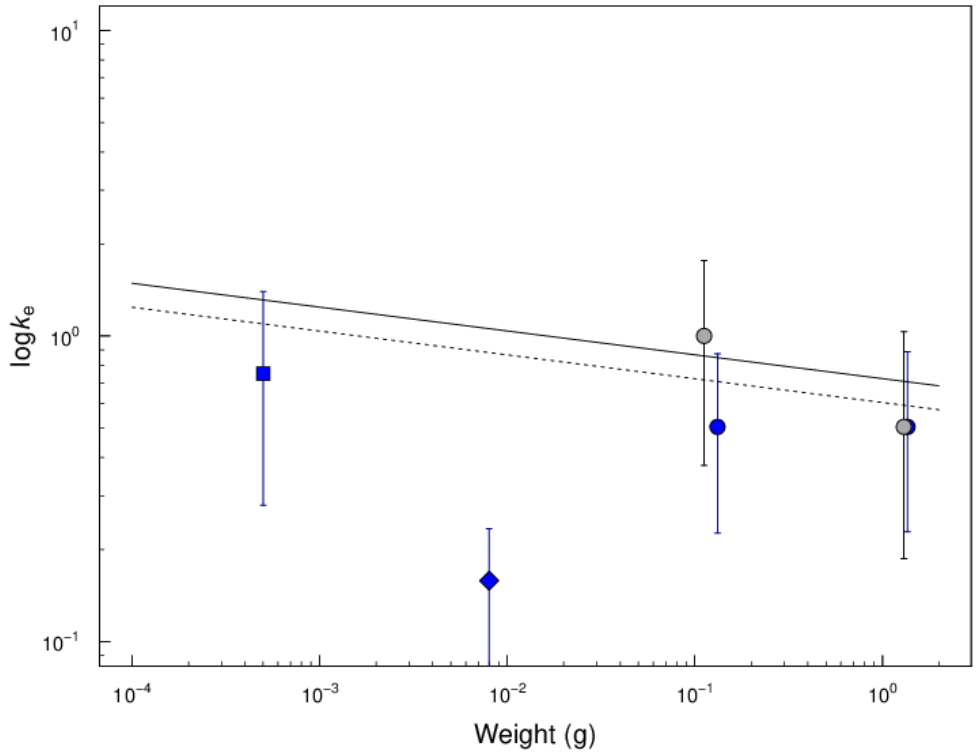

Figure 3.2 Comparing the lumped elimination rate from experimental group A against the wet weight of the test organisms. Blue symbols tested at 18° C, Grey shaded symbols tested at 10° C. Square represent the *D. magna* test, diamond represent the *L. variegatus* test, circles represent the *O. mykiss* tests. The line represents Eqn 2 at 18° C (solid), and at 10° C (dashed) with variable organism weight. Points are median estimates, and bars are 95% confidence intervals.

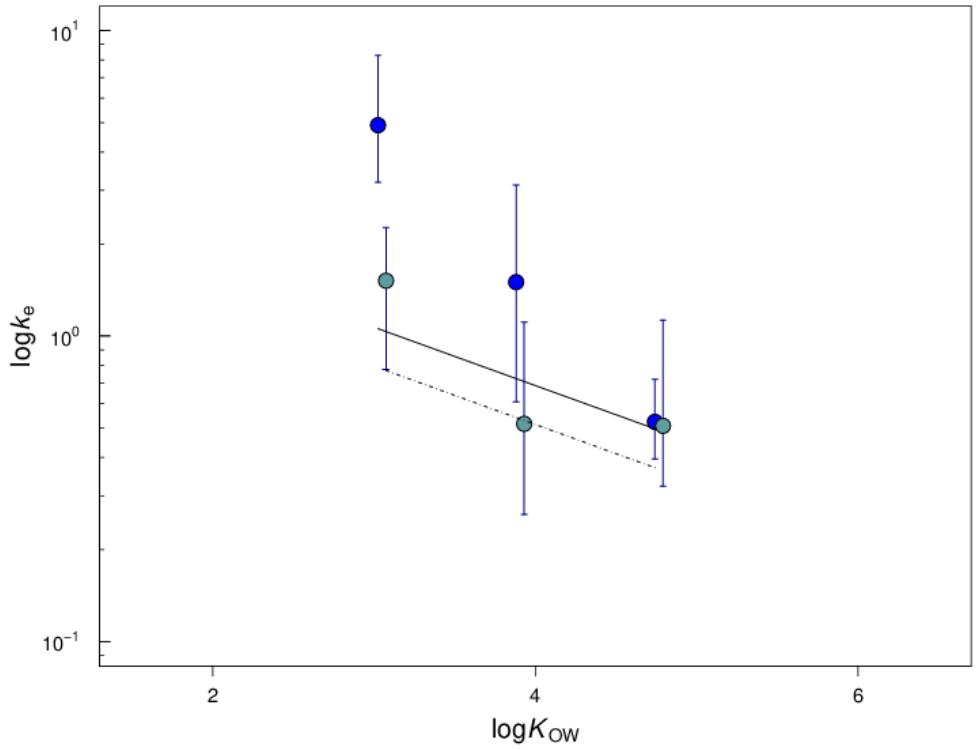

Figure 3.3 Comparing the lumped elimination rate from experimental group B against the logK_{OW} of the test chemicals at 18° C (blue) and 5° C (grey shaded) for *O. mykiss* juvelines. Lines represent Eqn 2 at 18° C (solid), and 5° C (dashed) for fish with weight of 1 g. Points are median estimates, and bars are 95% confidence intervals.

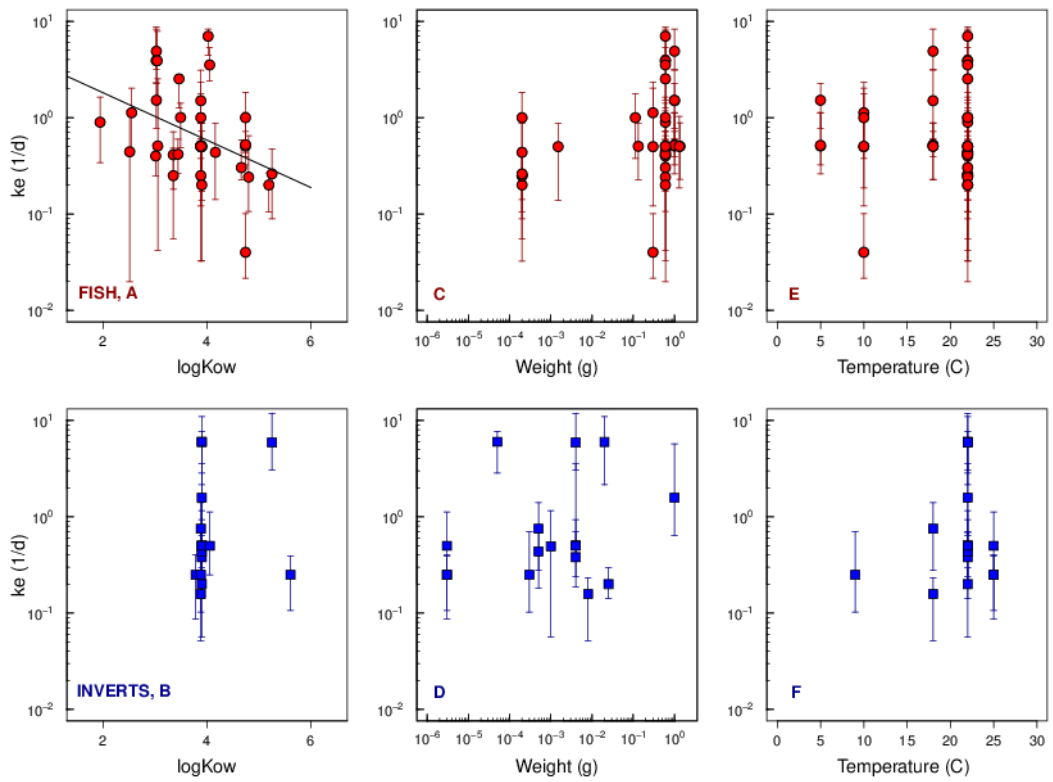

Figure 3.4 Lumped elimination rates derived from literature datasets of hydrocarbon exposures (Table 1) for fish (upper panels), and invertebrates (lower panels) compared to the log K_{OW} for the test chemicals (Panels A, B), approximate wet weight of the test organisms (C, D), and approximate temeprature of the exposure system (E, F). Line in panel A is from Eqn 11. Points are median estimates, and bars are 95% confidence intervals.

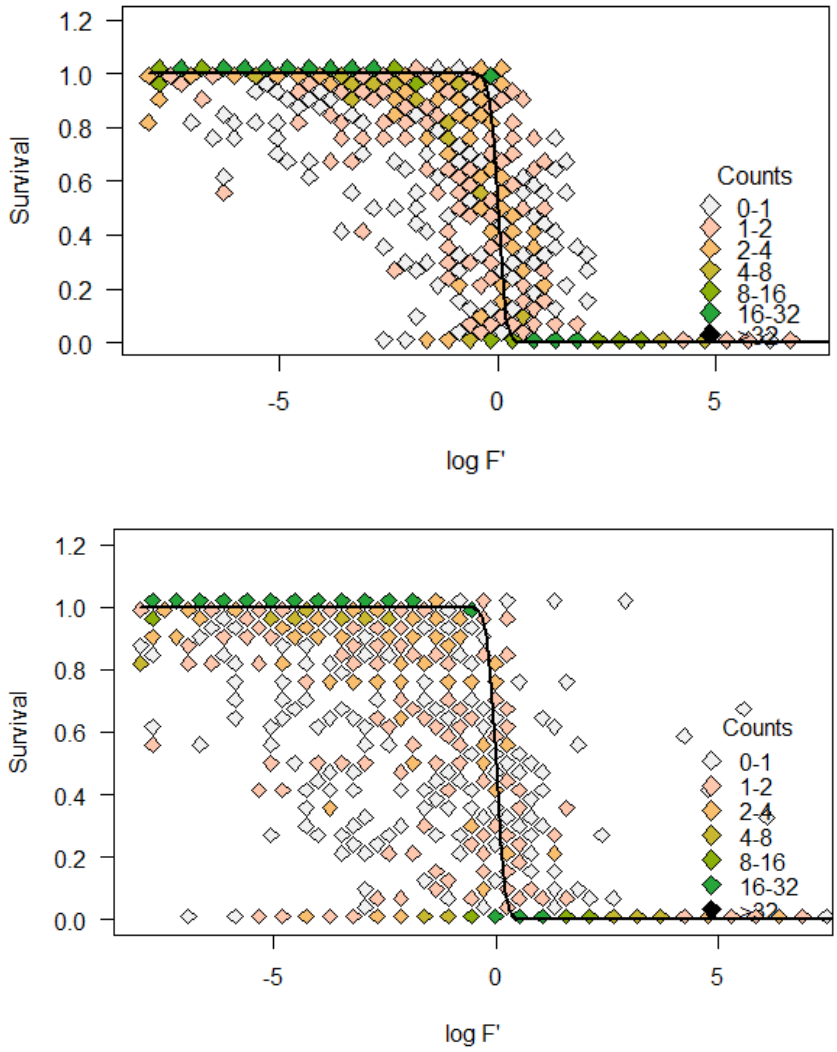

Figure 3.5 Fraction surviving S for all datasets (Table 1) to the composite exposure metric, *F*' (Eqn 9). The diamond symbols are color coded to indicate the number of observations within the plotting symbol. The line represents the log logistic (RMSE 0.22), and lower panel is data fit using k_e calcualted directly with Eq 9 (RMSE 0.28).

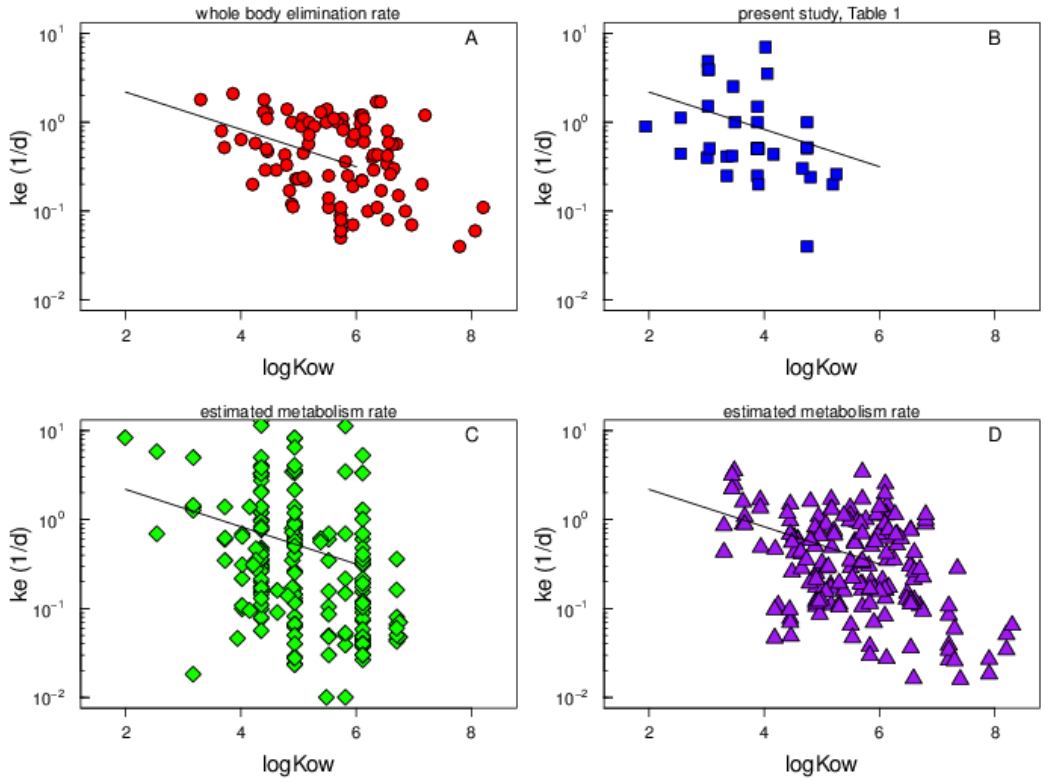

Figure 3.6 Comparing whole body elimination rates, k_b (Panel A) [121], to the lumped elimination/damage repair rate, k_e (♦), from the present study (Table 1, panel B), with estimated whole body metabolism rates, k_m [118, 119] (Panels C, D) for various fish species from literature.

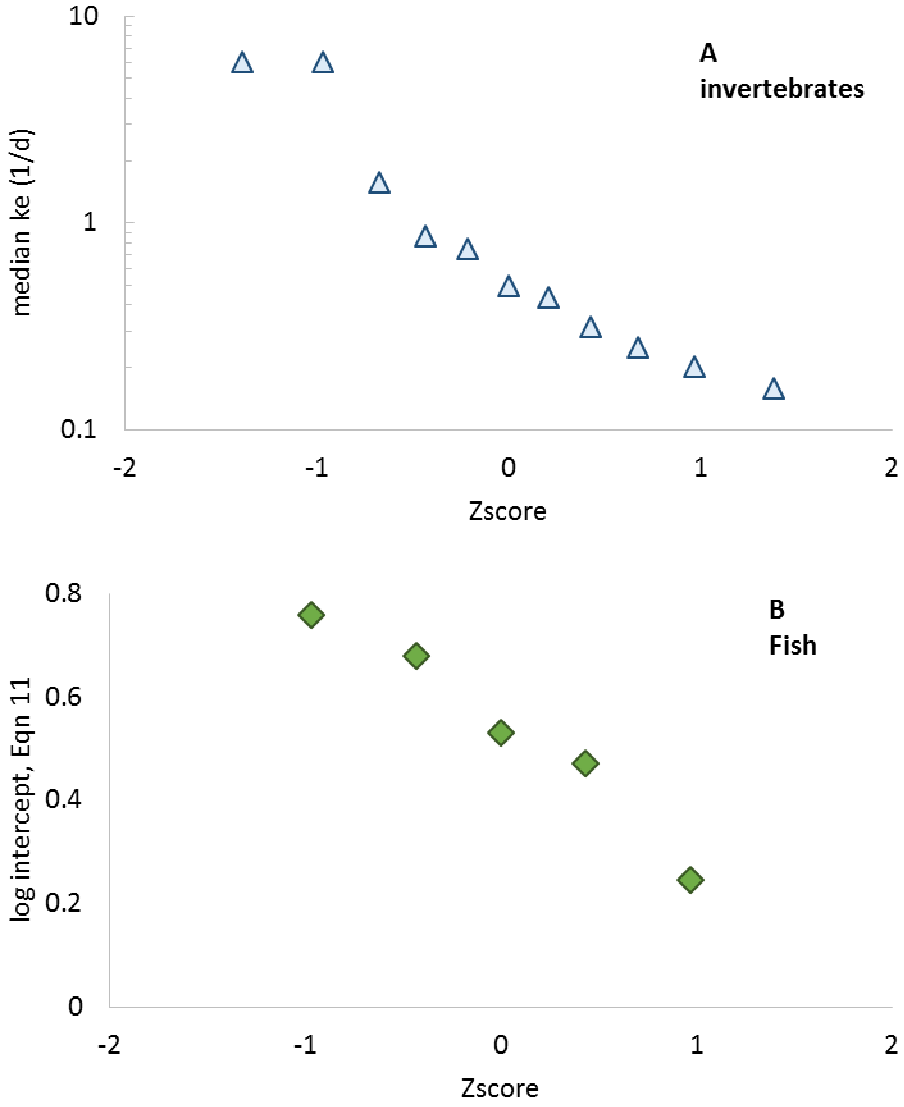

Figure 3.7 Comparing distribution of median k_e for invertebrates (Table 2, upper panel), and the species specific intercept (Eqn 11) for fish (Table 3, lower panel).

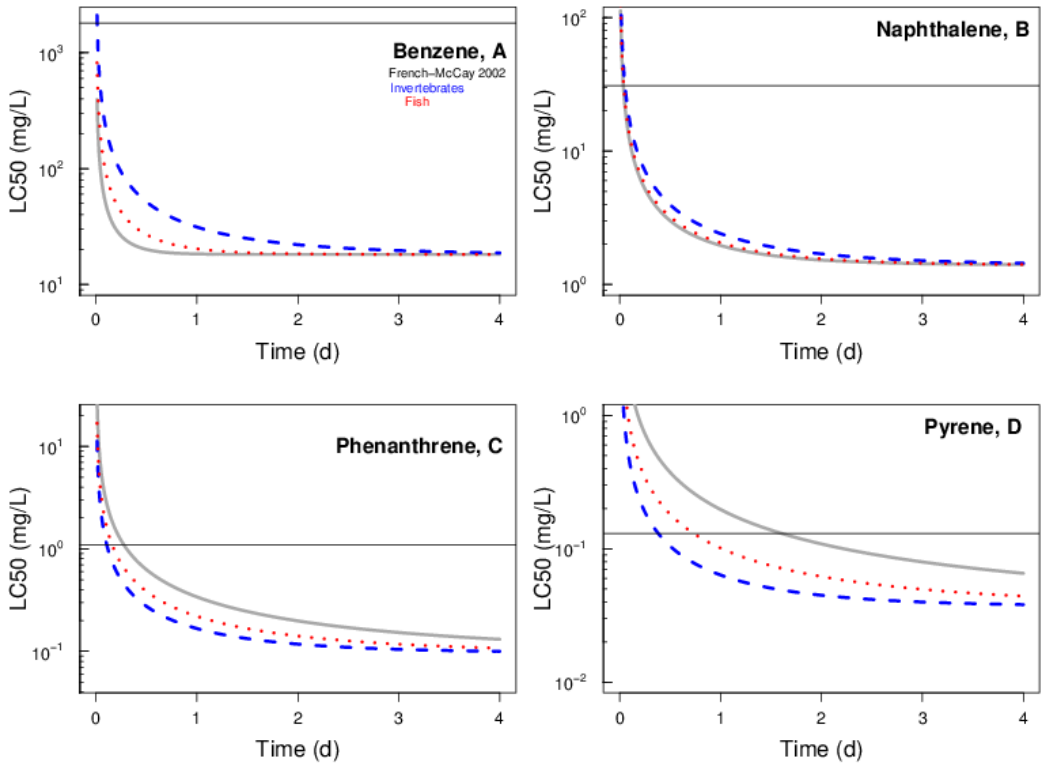

Figure 3.8 LC50s predicted for the French-McCay [68] model (solid black line, Eqn 2, assuming 1 g fish at 25 °C), the invertebrate data for *A. bahia* (dashed blue line, Table 3), and the model for *O. mykiss* (dotted red line, Eqn 11, Table 2). The horizontal line represents the water solubility limit for these chemicals. The threshold is the 5 percentile acute value on the acute species sensitivity distribution [20].

TABLES

Table 3.1 Datasets for calibrating toxicokinetic models

Species	Chemical	logK_{OW}	T (C)	W (g)	ke (1/d)	Study
D. rerio	Octahydrophenanthrene	5.19	22	2.0E-04	3.75	Butler2016
D. rerio	Phenanthrene	4.74	22	2.0E-04	4.00	Butler2016
D. rerio	Methylnaphthalene	3.88	22	2.0E-04	0.12	Butler2016
D. rerio	Naphthalene	3.35	22	2.0E-04	0.30	Butler2016
D. rerio	Biphenyl	4.16	22	2.0E-04	0.36	Butler2016
D. rerio	Pyrene	5.25	22	2.0E-04	0.14	Butler2016
O. mykiss	Phenanthrene	4.74	5	1.0E+00	0.34	Present study
O. mykiss	Phenanthrene	4.74	18	1.0E+00	0.28	Present study
O. mykiss	Methylnaphthalene	3.88	5	1.0E+00	0.25	Present study
O. mykiss	Methylnaphthalene	3.88	18	1.0E+00	0.33	Present study
O. mykiss	o-xylene	3.02	5	1.0E+00	0.77	Present study
O. mykiss	o-xylene	3.02	18	1.0E+00	0.35	Present study
A fimbria	Toluene	2.55	10	3.0E-01	0.29	Branders et al 2018
A fimbria	Phenanthrene	4.74	10	3.0E-01	0.10	Branders et al 2018
A fimbria	methylnaphthalene	3.88	10	3.0E-01	0.09	Branders et al 2018
P. promelas	t-butylstyrene	4.80	22	6.0E-01	0.44	EPA
P. promelas	Acenaphthene	3.90	22	6.0E-01	1.01	EPA
P. promelas	Naphthalene	3.35	22	6.0E-01	1.50	EPA
P. promelas	Toluene	2.55	22	6.0E-01	0.85	EPA
P. promelas	ethylbenzene	3.01	22	6.0E-01	0.97	EPA
P. promelas	p-xylene	3.05	22	6.0E-01	2.42	EPA
P. promelas	isopropylbenzene	3.44	22	6.0E-01	1.18	EPA
P. promelas	1,2,4-trimethylbenzene	3.46	22	6.0E-01	3.85	EPA
P. promelas	1,3-diethylbenzene	4.02	22	6.0E-01	1.50	EPA
P. promelas	n-amylbenzene	4.66	22	6.0E-01	0.65	EPA
P. promelas	Benzene	1.94	22	6.0E-01	2.50	EPA
P. promelas	cyclohexane	3.49	22	6.0E-01	1.88	EPA
P. promelas	o-xylene	3.02	22	6.0E-01	9.00	EPA
P. promelas	m-xylene	3.04	22	6.0E-01	9.00	EPA
P. promelas	Hexane	4.05	22	6.0E-01	5.12	EPA
A. bahia	acenaphthene	3.90	22	4.0E-03	0.50	Horne1983
A. bahia	acenaphthene	3.90	22	4.0E-03	0.35	Horne1983
M. beryllina	acenaphthene	3.90	22	1.5E-03	0.45	Horne1983

Table 3.1 continued						
N. arenaceodentata	acenaphthene	3.90	22	1.0E-03	0.59	Horne1983
C. septemspinosus	acenaphthene	3.90	22	1.0E+00	1.01	Horne1983
G. annulatus	acenaphthene	3.90	22	2.0E-02	7.00	Horne1983
A. tonsa	acenaphthene	3.90	22	5.0E-05	8.75	Horne1983
P. maria	acenaphthene	3.90	22	2.5E-02	0.97	Horne1983
G. minus	acenaphthene	3.90	22	5.0E-04	0.51	Horne1983
A. bahia	Flouranthene	5.25	22	4.0E-03	0.28	Turner1982
A. bahia	Acenaphthene	3.90	22	4.0E-03	0.31	Turner1982
P. promelas	acenaphthene	3.90	22	6.0E-01	0.20	Turner1982
C. dubia	Fluorine	4.05	25	3.0E-06	0.61	Bragin et al 2016
C. dubia	Methylpyrene	5.61	25	3.0E-06	0.34	Bragin et al 2016
C. dubia	Methylhexene	3.78	25	3.0E-06	0.47	Bragin et al 2016
C. finmarchicus	methylnaphthalene	3.88	9	3.0E-04	0.28	Jager et al 2017
O. mykiss	methylnaphthalene	3.88	18	1.3E-01	0.67	Present study
O. mykiss	methylnaphthalene	3.88	18	1.4E+00	0.67	EMBSI 2017
O. mykiss	methylnaphthalene	3.88	10	1.1E-01	1.33	EMBSI 2017
O. mykiss	methylnaphthalene	3.88	10	1.3E+00	0.67	EMBSI 2017
D. magna	methylnaphthalene	3.88	18	5.0E-04	1.50	EMBSI 2017
L. variegatus	methylnaphthalene	3.88	18	8.0E-03	0.30	EMBSI 2017

T – Temperature
W – approximate organism weight
k_e – lumped elimination rate

Table 3.2 Species-median k_e for invertebrates

Species	**k_e (1/d)**	**SE**	***n***
A. bahia	0.87	0.32	4
C. finmarchicus	0.25	NA	1
N. arenaceodentata	0.49	NA	1
C. septemspinosus	1.58	NA	1
G. annulatus	5.97	NA	1
A. tonsa	6.00	NA	1
P. maria	0.20	NA	1
G. minor	0.44	NA	1
D. magna	0.75	NA	1
C. dubia	0.31	0.12	3
L variegatus	0.16	NA	1

SE Standard Error

3.3 Regression analysis of k_e for fish

Variable	**Value**	**SE**	***N***
logK_{OW}	-0.21	0.10	36
Species	**Intercept**	**SE**	***n***
P. promelas	0.68	0.38	16
D. rerio	0.47	0.50	6
O. mykiss	0.76	0.43	10
Sablefish	0.25	0.46	3
M. beryllina	0.53	0.59	1

SE standard error

REFERENCES

1. Redman, A.D. and T.F. Parkerton, *Guidance for improving comparability and relevance of oil toxicity tests.* Marine pollution bulletin, 2015. **98**(1): p. 156-170.

2. King, D., et al., *Environmental risk assessment of petroleum substances: The hydrocarbon block method*. 1996: CONCAWE.

3. Redman, A.D., et al., *PETROTOX: An aquatic toxicity model for petroleum substances.* Environmental Toxicology and Chemistry, 2012. **31**(11): p. 2498-2506.

4. Redman, A.D., et al., *PETRORISK: A risk assessment framework for petroleum substances.* Integrated environmental assessment and management, 2014. **10**(3): p. 437-448.

5. Letinski, D., et al., *Use of passive samplers for improving oil toxicity and spill effects assessment.* Marine pollution bulletin, 2014. **86**(1): p. 274-282.

6. Jager, T., et al., *General unified threshold model of survival-a toxicokinetic-toxicodynamic framework for ecotoxicology.* Environmental Science & Technology, 2011. **45**(7): p. 2529-2540.

7. Ashauer, R., et al., *Death dilemma and organism recovery in ecotoxicology.* Environmental science & technology, 2015. **49**(16): p. 10136-10146.

8. Klok, C., M. Hjorth, and I. Dahllöf, *Qualitative use of Dynamic Energy Budget theory in ecotoxicology: Case study on oil contamination and Arctic copepods.* Journal of sea research, 2012. **73**: p. 24-31.

9. Jager, T., et al., *Stage-dependent and sex-dependent sensitivity to water-soluble fractions of fresh and weathered oil in the marine copepod Calanus finmarchicus.* Environmental Toxicology and Chemistry, 2016. **35**(3): p. 728-735.

10. Redman, A., et al., *Technical basis for using passive sampling as a biomimetic extraction procedure to assess bioavailability and predict toxicity of petroleum substances.* Chemosphere, 2018.

11. Redman, A.D., et al., *Investigating the role of dissolved and droplet oil on aquatic toxicity using dispersed and passive dosing systems.* Environmental Toxicology and Chemistry, 2016.

12. Redman, A.D., et al., *Quantifying the concentration of crude oil microdroplets in oil–water preparations.* Environmental Toxicology and Chemistry, 2012. **31**(8): p. 1814-1822.

13. Board, O.S., *Oil Spill Dispersants:: Efficacy and Effects*. 2005: National Academies Press.

14. Kvenvolden, K. and C. Cooper, *Natural seepage of crude oil into the marine environment.* Geo-Marine Letters, 2003. **23**(3-4): p. 140-146.

15. Arey, J.S., et al., *Using comprehensive two-dimensional gas chromatography retention indices to estimate environmental partitioning properties for a complete set of diesel fuel hydrocarbons.* Analytical chemistry, 2005. **77**(22): p. 7172-7182.

16. Mackay, D., W.Y. Shiu, and K.-C. Ma, *Illustrated handbook of physical-chemical properties of environmental fate for organic chemicals*. Vol. 5. 1997: CRC press.

17. Prausnitz, J.M., R.N. Lichtenthaler, and E.G. de Azevedo, *Molecular thermodynamics of fluid-phase equilibria*. 1998: Pearson Education.

18. Di Toro, D.M., J.A. McGrath, and D.J. Hansen, *Technical basis for narcotic chemicals and polycyclic aromatic hydrocarbon criteria. I. Water and tissue.* Environmental Toxicology and Chemistry, 2000. **19**(8): p. 1951-1970.

19. Di Toro, D.M. and J.A. McGrath, *Technical basis for narcotic chemicals and polycyclic aromatic hydrocarbon criteria. II. Mixtures and sediments.* Environmental Toxicology and Chemistry, 2000. **19**(8): p. 1971-1982.

20. McGrath, J.A. and D.M. Di Toro, *Validation of the target lipid model for toxicity assessment of residual petroleum constituents: monocyclic and polycyclic aromatic hydrocarbons.* Environmental Toxicology and Chemistry, 2009. **28**(6): p. 1130-1148.

21. Redman, A.D., et al., *A re-evaluation of PETROTOX for predicting acute and chronic toxicity of petroleum substances.* Environmental Toxicology and Chemistry, 2017.

22. Mayer, P., et al., *Passive sampling methods for contaminated sediments: Scientific rationale supporting use of freely dissolved concentrations.* Integrated environmental assessment and management, 2014. **10**(2): p. 197-209.

23. Hawthorne, S.B., D.J. Miller, and J.P. Kreitinger, *Measurement of total polycyclic aromatic hydrocarbon concentrations in sediments and toxic units used for estimating risk to benthic invertebrates at manufactured gas plant sites.* Environmental toxicology and chemistry, 2006. **25**(1): p. 287-296.

24. Scarlett, A., T.S. Galloway, and S.J. Rowland, *Chronic toxicity of unresolved complex mixtures (UCM) of hydrocarbons in marine sediments.* Journal of Soils and Sediments, 2007. **7**(4): p. 200-206.

25. Leonards, P.E., et al., *Impact of biodegradation on the potential bioaccumulation and toxicity of refinery effluents.* Environmental toxicology and chemistry, 2011. **30**(10): p. 2175-2183.

26. Parkerton, T., M. Stone, and D. Letinski, *Assessing the aquatic toxicity of complex hydrocarbon mixtures using solid phase microextraction.* Toxicology letters, 2000. **112**: p. 273-282.

27. Redman, A.D., et al., *Investigating the role of dissolved and droplet oil in aquatic toxicity using dispersed and passive dosing systems.* Environmental Toxicology and Chemistry, 2016.

28. Redman, A.D., et al., *Evaluating toxicity of heavy fuel oil fractions using complementary modeling and biomimetic extraction methods.* Environmental Toxicology and Chemistry, 2014. **33**(9): p. 2094-2104.

29. Woods, R., et al., *Assessing the aquatic hazard of commercial hydrocarbon resins.* Ecotoxicology and environmental safety, 2007. **66**(2): p. 159-168.

30. Girling, A., R. Markarian, and D. Bennett, *Aquatic toxicity testing of oil products-some recommendations.* Chemosphere, 1992. **24**(10): p. 1469-1472.

31. Adams, W.J. and C.D. Rowland, *Aquatic toxicology test methods.* Handbook of ecotoxicology, 2003: p. 19-38.

32. OECD., *Good Laboratory Practice*. OECD Publishing.

33. Deming, W.E., *Statistical adjustment of data.* 1943.

34. Team, R.C., *R: A language and environment for statistical computing.* 2013.

35. McGrath, J.A., T.F. Parkerton, and D.M. Di Toro, *Application of the narcosis target lipid model to algal toxicity and deriving predicted-no-effect concentrations.* Environmental toxicology and chemistry, 2004. **23**(10): p. 2503-2517.

36. Abraham, M.H., *Application of solvation equations to chemical and biochemical processes.* Pure and applied chemistry, 1993. **65**(12): p. 2503-2512.

37. Endo, S., T.N. Brown, and K.-U. Goss, *General model for estimating partition coefficients to organisms and their tissues using the biological compositions and polyparameter linear free energy relationships.* Environmental science & technology, 2013. **47**(12): p. 6630-6639.

38. Endo, S. and K.-U. Goss, *Applications of polyparameter linear free energy relationships in environmental chemistry.* Environmental science & technology, 2014. **48**(21): p. 12477-12491.

39. Sprunger, L., et al., *Characterization of the sorption of gaseous and organic solutes onto polydimethyl siloxane solid-phase microextraction surfaces using the Abraham model.* Journal of chromatography A, 2007. **1175**(2): p. 162-173.

40. Kipka, U. and D.M. Di Toro, *Technical basis for polar and nonpolar narcotic chemicals and polycyclic aromatic hydrocarbon criteria. III. A polyparameter model for target lipid partitioning.* Environmental Toxicology and Chemistry, 2009. **28**(7): p. 1429-1438.

41. Smit, M.G.D., et al., *The Variation in Slope of Concentration–Effect Relationships.* Ecotoxicology and Environmental Safety, 2001. **48**(1): p. 43-50.

42. Joyce, A.S., et al., *Evaluating the Relationship between Equilibrium Passive Sampler Uptake and Aquatic Organism Bioaccumulation.* Environmental Science & Technology, 2016. **50**(21): p. 11437-11451.

43. DiFilippo, E.L. and R.P. Eganhouse, *Assessment of PDMS-water partition coefficients: implications for passive environmental sampling of hydrophobic organic compounds.* Environmental science & technology, 2010. **44**(18): p. 6917-6925.

44. Reible, D. and G. Lotufo, *Demonstration and evaluation of solid phase microextraction for the assessment of bioavailability and contaminant mobility*. 2012, DTIC Document.

45. Mayer, P., W.H. Vaes, and J.L. Hermens, *Absorption of hydrophobic compounds into the poly (dimethylsiloxane) coating of solid-phase microextraction fibers: High partition coefficients and fluorescence microscopy images.* Analytical Chemistry, 2000. **72**(3): p. 459-464.

46. Paschke, A. and P. Popp, *Solid-phase microextraction fibre–water distribution constants of more hydrophobic organic compounds and their correlations with octanol–water partition coefficients.* Journal of Chromatography A, 2003. **999**(1): p. 35-42.

47. Prosser, C.M., et al., *Evaluating persistence of petroleum hydrocarbons in aerobic aqueous media.* Chemosphere, 2016. **155**: p. 542-549.

48. Mackay, D., D.E. Powell, and K.B. Woodburn, *Bioconcentration and Aquatic Toxicity of Superhydrophobic Chemicals: A Modeling Case Study of Cyclic Volatile Methyl Siloxanes.* Environmental science & technology, 2015. **49**(19): p. 11913-11922.

49. Butler, J.D., et al., *Assessing Aromatic Hydrocarbon Toxicity to Fish Early Life Stages Using Passive Dosing Methods and Target Lipid/Chemical Activity Models.* Environmental Science & Technology, 2016.

50. Bragin, G.E., et al., *Chronic toxicity of selected polycyclic aromatic hydrocarbons to algae and crustaceans using passive dosing.* Environmental toxicology and chemistry, 2016. **35**(12): p. 2948-2957.

51. ACD/Labs, *Absolv data sheet.* *http://www.acdlabs.com/products/percepta/predictors/absolv/.*

52. Kang, H.-J., et al., *Prediction of ecotoxicity of heavy crude oil: contribution of measured components.* Environmental science & technology, 2014. **48**(5): p. 2962-2970.

53. Van Scoy, A.R., et al., *Use of semipermeable membrane devices (SPMDs) to characterize dissolved hydrocarbon fractions of both dispersed and undispersed oil.* Environmental Science: Processes & Impacts, 2013. **15**(11): p. 2016-2022.

54. Ramachandran, S.D., et al., *Oil dispersant increases PAH uptake by fish exposed to crude oil.* Ecotoxicology and environmental safety, 2004. **59**(3): p. 300-308.

55. Gardiner, W.W., et al., *The acute toxicity of chemically and physically dispersed crude oil to key arctic species under arctic conditions during the open water season.* Environmental Toxicology and Chemistry, 2013. **32**(10): p. 2284-2300.

56. Carls, M.G., S.D. Rice, and J.E. Hose, *Sensitivity of fish embryos to weathered crude oil: Part I. Low-level exposure during incubation causes malformations, genetic damage, and mortality in larval pacific herring (Clupea pallasi).* Environmental Toxicology and Chemistry, 1999. **18**(3): p. 481-493.

57. Heintz, R.A., J.W. Short, and S.D. Rice, *Sensitivity of fish embryos to weathered crude oil: Part II. Increased mortality of pink salmon (Oncorhynchus gorbuscha) embryos incubating downstream from weathered Exxon Valdez crude oil.* Environmental Toxicology and Chemistry, 1999. **18**(3): p. 494-503.

58. Brannon, E.L., et al., *Toxicity of weathered Exxon Valdez crude oil to pink salmon embryos.* Environmental toxicology and chemistry, 2006. **25**(4): p. 962-972.

59. Singer, M., et al., *Standardization of the preparation and quantitation of water-accommodated fractions of petroleum for toxicity testing.* Marine Pollution Bulletin, 2000. **40**(11): p. 1007-1016.

60. Barron, M.G. and L. Ka'aihue, *Critical evaluation of CROSERF test methods for oil dispersant toxicity testing under subarctic conditions.* Marine pollution bulletin, 2003. **46**(9): p. 1191-1199.

61. Singer, M.M., et al., *Effects of spiked exposure to an oil dispersant on the early life stages of four marine species.* Environmental toxicology and chemistry, 1991. **10**(10): p. 1367-1374.

62. Incardona, J.P., et al., *Exxon Valdez to Deepwater Horizon: Comparable toxicity of both crude oils to fish early life stages.* Aquatic toxicology, 2013. **142**: p. 303-316.

63. Nordtug, T., et al., *Oil droplets do not affect assimilation and survival probability of first feeding larvae of North-East Arctic cod.* Science of the Total Environment, 2011. **412**: p. 148-153.

64. Carls, M.G., et al., *Fish embryos are damaged by dissolved PAHs, not oil particles.* Aquatic toxicology, 2008. **88**(2): p. 121-127.

65. Adams, J., M. Sweezey, and P.V. Hodson, *Oil and oil dispersant do not cause synergistic toxicity to fish embryos.* Environmental toxicology and chemistry, 2014. **33**(1): p. 107-114.

66. Redman, A., *Role of entrained droplet oil on the bioavailability of petroleum substances in aqueous exposures.* Marine pollution bulletin, 2015. **97**(1): p. 342-348.

67. Di Toro, D.M., J.A. McGrath, and W.A. Stubblefield, *Predicting the toxicity of neat and weathered crude oil: toxic potential and the toxicity of saturated mixtures.* Environmental Toxicology and Chemistry, 2007. **26**(1): p. 24-36.

68. French-McCay, D.P., *Development and application of an oil toxicity and exposure model, OilToxEx.* Environmental Toxicology and Chemistry, 2002. **21**(10): p. 2080-2094.

69. Reed, M., et al., *Oil spill modeling towards the close of the 20th century: overview of the state of the art.* Spill Science & Technology Bulletin, 1999. **5**(1): p. 3-16.

70. Ghosh, U., et al., *Passive sampling methods for contaminated sediments: Practical guidance for selection, calibration, and implementation.* Integrated environmental assessment and management, 2014. **10**(2): p. 210-223.

71. Lydy, M.J., et al., *Passive sampling methods for contaminated sediments: State of the science for organic contaminants.* Integrated environmental assessment and management, 2014. **10**(2): p. 167-178.

72. Claessens, M., et al., *Modelling the fate of micropollutants in the marine environment using passive sampling.* Marine pollution bulletin, 2015. **96**(1): p. 103-109.

73. Marchal, G., et al., *Impact of soil amendments and the plant rhizosphere on PAH behaviour in soil.* Environmental Pollution, 2014. **188**: p. 124-131.

74. Fernandez, L.A. and P.M. Gschwend, *Predicting bioaccumulation of polycyclic aromatic hydrocarbons in soft-shelled clams (Mya arenaria) using field deployments of polyethylene passive samplers.* Environmental Toxicology and Chemistry, 2015. **34**(5): p. 993-1000.

75. Tidwell, L.G., et al., *Polycyclic Aromatic Hydrocarbon (PAH) and Oxygenated PAH (OPAH) Air–Water Exchange during the Deepwater Horizon Oil Spill.* Environmental science & technology, 2014. **49**(1): p. 141-149.

76. Reitsma, P.J., D. Adelman, and R. Lohmann, *Challenges of using polyethylene passive samplers to determine dissolved concentrations of parent and alkylated PAHs under cold and saline conditions.* Environmental science & technology, 2013. **47**(18): p. 10429-10437.

77. Arnot, J.A. and F.A. Gobas, *A review of bioconcentration factor (BCF) and bioaccumulation factor (BAF) assessments for organic chemicals in aquatic organisms.* Environmental Reviews, 2006. **14**(4): p. 257-297.

78. Hendriks, A.J., et al., *The power of size. 1. Rate constants and equilibrium ratios for accumulation of organic substances related to octanol-water partition ratio and species weight.* Environmental toxicology and chemistry, 2001. **20**(7): p. 1399-1420.

79. OECD., *Test No. 202: Daphnia sp. Acute Immobilisation Test*. OECD Publishing.

80. Weber, C.I., *Methods for measuring the acute toxicity of effluents and receiving waters to freshwater and marine organisms*. 1991: Environmental Monitoring Systems Laboratory, Office of Research and Development, US Environmental Protection Agency.

81. Lee, K., et al., *Lab tests on the biodegradation of chemically dispersed oil should consider the rapid dilution that occurs at sea.* Marine pollution bulletin, 2013. **73**(1): p. 314-318.

82. Blondina, G., et al., *Influence of salinity on petroleum accommodation by dispersants.* Spill Science & Technology Bulletin, 1999. **5**(2): p. 127-134.

83. McGrath, J.A., et al., *Validation of the narcosis target lipid model for petroleum products: Gasoline as a case study.* Environmental toxicology and chemistry, 2005. **24**(9): p. 2382-2394.

84. Hilal, S., S. Karickhoff, and L. Carreira, *Verification and validation of the SPARC model.* US Environmental Protection Agency, 2003.

85. Kipka, U. and D.M. Di Toro, *A linear solvation energy relationship model of organic chemical partitioning to particulate organic carbon in soils and sediments.* Environmental Toxicology and Chemistry, 2011. **30**(9): p. 2013-2022.

86. Redman, A.D., et al., *Extension and validation of the target lipid model for deriving predicted no-effect concentrations for soils and sediments.* Environmental Toxicology and Chemistry, 2014. **33**(12): p. 2679-2687.

87. Olsvik, P.A., et al., *Transcriptional evidence for low contribution of oil droplets to acute toxicity from dispersed oil in first feeding Atlantic cod (Gadus morhua) larvae.* Comparative Biochemistry and Physiology Part C: Toxicology & Pharmacology, 2011. **154**(4): p. 333-345.

88. Olsvik, P.A., et al., *Is chemically dispersed oil more toxic to Atlantic cod (Gadus morhua) larvae than mechanically dispersed oil? A transcriptional evaluation.* BMC genomics, 2012. **13**(1): p. 1.

89. Sørhus, E., et al., *Unexpected interaction with dispersed crude oil droplets drives severe toxicity in Atlantic haddock embryos.* PloS one, 2015. **10**(4): p. e0124376.

90. González-Doncel, M., et al., *Toxic effects of an oil spill on fish early life stages may not be exclusively associated to PAHs: studies with Prestige oil and medaka (Oryzias latipes).* Aquatic Toxicology, 2008. **87**(4): p. 280-288.

91. Dussauze, M., et al., *Acute toxicity of chemically and mechanically dispersed crude oil to juvenile sea bass (Dicentrarchus labrax): Absence of synergistic effects between oil and dispersants.* Environmental Toxicology and Chemistry, 2015. **34**(7): p. 1543-1551.

92. van Leeuwen, C.J. and T.G. Vermeire, *Risk assessment of chemicals: an introduction*. 2007: Springer Science & Business Media.

93. Rand, G.M., *Fundamentals of aquatic toxicology: effects, environmental fate and risk assessment*. 1995: CRC Press.

94. Chapra, S.C., *Surface water-quality modeling*. 2008: Waveland press.

95. French-McCay, D.P., *Oil spill impact modeling: Development and validation.* Environmental Toxicology and Chemistry, 2004. **23**(10): p. 2441-2456.

96. Veith, G.D., D.J. Call, and L. Brooke, *Structure–toxicity relationships for the fathead minnow, Pimephales promelas: Narcotic industrial chemicals.* Canadian Journal of Fisheries and Aquatic Sciences, 1983. **40**(6): p. 743-748.

97. Thomann, R.V., *Bioaccumulation model of organic chemical distribution in aquatic food chains.* Environmental science & technology, 1989. **23**(6): p. 699-707.

98. Mackay, D. and A. Fraser, *Bioaccumulation of persistent organic chemicals: mechanisms and models.* Environmental pollution, 2000. **110**(3): p. 375-391.

99. Goss, K.U., T.N. Brown, and S. Endo, *Elimination half-life as a metric for the bioaccumulation potential of chemicals in aquatic and terrestrial food chains.* Environmental toxicology and chemistry, 2013. **32**(7): p. 1663-1671.

100. Lee, J.-H., P.F. Landrum, and C.-H. Koh, *Toxicokinetics and time-dependent PAH toxicity in the amphipod Hyalella azteca.* Environmental science & technology, 2002. **36**(14): p. 3124-3130.

101. Ashauer, R., et al., *Modelling survival: exposure pattern, species sensitivity and uncertainty.* Scientific Reports, 2016. **6**: p. 29178.

102. Gergs, A., D. Kulkarni, and T.G. Preuss, *Body size-dependent toxicokinetics and toxicodynamics could explain intra-and interspecies variability in sensitivity.* Environmental Pollution, 2015. **206**: p. 449-455.

103. McCarty, L., et al., *Residue-based interpretation of toxicity and bioconcentration QSARs from aquatic bioassays: Neutral narcotic organics.* Environmental Toxicology and Chemistry, 1992. **11**(7): p. 917-930.

104. Baussant, T., et al., *Bioaccumulation of polycyclic aromatic compounds: 2. Modeling bioaccumulation in marine organisms chronically exposed to dispersed oil.* Environmental Toxicology and Chemistry, 2001. **20**(6): p. 1185-1195.

105. Feijtel, T., et al., *Integration of bioaccumulation in an environmental risk assessment.* Chemosphere, 1997. **34**(11): p. 2337-2350.

106. Spacie, A. and J.L. Hamelink, *Alternative models for describing the bioconcentration of organics in fish.* Environmental Toxicology and Chemistry, 1982. **1**(4): p. 309-320.

107. Downs, C., J. Hayes, and C. Tracy, *Scaling metabolic rate with body mass and inverse body temperature: a test of the Arrhenius fractal supply model.* Functional Ecology, 2008. **22**(2): p. 239-244.

108. Newman, M.C. and J.T. McCloskey, *The individual tolerance concept is not the sole explanation for the probit dose-effect model.* Environmental Toxicology and Chemistry, 2000. **19**(2): p. 520-526.

109. Baudrot, V., et al., *New insights to compare and choose TKTD models for survival based on an inter-laboratory study for Lymnaea stagnalis exposed to Cd.* Environmental science & technology, 2018.

110. Albert, C., S. Vogel, and R. Ashauer, *Computationally Efficient Implementation of a Novel Algorithm for the General Unified Threshold Model of Survival (GUTS).* PLoS Comput Biol, 2016. **12**(6): p. e1004978.

111. HDR, *Refinement and Validation of TLM-Derived HC5 Values.* CONCAWE, 2016.

112. Gilbert, D., et al., *Polymers as reference partitioning phase: polymer calibration for an analytically operational approach to quantify multimedia phase partitioning.* Analytical chemistry, 2016. **88**(11): p. 5818-5826.

113. Tattersall, G.J., et al., *Coping with thermal challenges: physiological adaptations to environmental temperatures.* Comprehensive Physiology, 2012.

114. Barber, M.C., *A review and comparison of models for predicting dynamic chemical bioconcentration in fish.* Environmental Toxicology and Chemistry, 2003. **22**(9): p. 1963-1992.

115. Hendriks, A.J., *The power of size: A meta-analysis reveals consistency of allometric regressions.* Ecological Modelling, 2007. **205**(1): p. 196-208.

116. Bejarano, A.C., et al., *Relative sensitivity of Arctic species to physically and chemically dispersed oil determined from three hydrocarbon measures of aquatic toxicity.* Marine Pollution Bulletin, 2017. **122**(1-2): p. 316-322.

117. de Hoop, L., et al., *Sensitivity of polar and temperate marine organisms to oil components.* Environmental science & technology, 2011. **45**(20): p. 9017-9023.

118. Arnot, J.A., D. Mackay, and M. Bonnell, *Estimating metabolic biotransformation rates in fish from laboratory data.* Environmental Toxicology and Chemistry, 2008. **27**(2): p. 341-351.

119. De Hoop, L., et al., *Modelling bioaccumulation of oil constituents in aquatic species.* Marine pollution bulletin, 2013. **76**(1): p. 178-186.

120. McGrath, J.A., et al., *Re-evaluation of Target Lipid Model-Derived HC5 Predictions for Hydrocarbons.* Environmental toxicology and chemistry, 2018.

121. Lo, J.C., et al., *Somatic and gastrointestinal in vivo biotransformation rates of hydrophobic chemicals in fish.* Environmental Toxicology and Chemistry, 2015. **34**(10): p. 2282-2294.

Appendix A

CHAPTER 1 SUPPLEMENTAL INFORMATION

Links to article and SI material
https://www.sciencedirect.com/science/article/pii/S0045653518302248
https://ars.els-cdn.com/content/image/1-s2.0-S0045653518302248-mmc1.docx

Comparison of PDMS- and Target Lipid-based SSD using ppLFER

Empirical lipid-fiber partition coefficients were characterized through analysis of paired field samples of PAH in biota or water [42]. The average offset between lipid- and PDMS-based concentrations of PAH was 0.5 log units. Meaning lipid-based concentrations were about a factor of three higher than PDMS-based concentrations This offset is consistent with ratio of fiber-water [11, 39, 43-46, 49, 50] and lipid-water [20] relationships in the literature.

The mechanistic basis of this offset was evaluated using polyparameter linear solvation relationships (LSER) of lipid-water (e.g., LSER-based TLM) [40] and fiber-water [39] systems. The general form of the polyparameter LSER model is given here

$$\log K = eE + sS + aA + bB + vV + c \qquad \text{(S1)}$$

where the lower case parameters (esabv) correspond to the solvent system (e.g., target lipid-water), and the upper case parameters (ESABV) are chemical interaction terms for the solutes. The parameter E is excess molar refractivity, S is polarizability, A is the ability to donate a hydrogen bond, B is the ability to accept a hydrogen bond, and

V is the molar volume. The term, *c*, is a constant whose physical meaning may reflect non-deal conditions, inherent properties of the solvent system, or a scalar (e.g., similar to a unit conversion) to provide a common basis for comparison between solvent systems. This general LSER modeling approach is widely applied to partitioning data and is described in more detail elsewhere [36-38].

The ratio of the lipid-water and PDMS-water partition coefficients will provide the effective lipid-PDMS partition coefficient. This is calculated as the difference of the log lipid-water partition coefficient ($\log K_{LW}$) from the LSER-based TLM [40]

$$\log K_{LW} = 0.51\,E + 0.71\,S + 0.92\,A - 4.40\,B + 3.14\,V - 0.44 \qquad \text{(S2)}$$

and the log of the PDMS-water ($\log K_{FW}$) LSER [39]. While it is not clear that this model is directly applicable to the BE system used to characterize hydrocarbon exposures, it is used to illustrate order of magnitude behaviors and processes that control partitioning or organics to PDMS.

$$\log K_{FW} = 0.60\,E - 1.41\,S - 2.52\,A - 4.11\,B + 3.64\,V + 0.27 \qquad \text{(S3)}$$

The resulting lipid-PDMS ($\log K_{LF}$) model is (e.g., Eqn 4 minus Eqn 5)

$$\log K_{LF} = -0.09\,E + 2.12\,S + 3.44\,A - 0.29\,B - 0.50\,V - 0.71 \qquad \text{(S4)}$$

The solute parameters (ESABV) were computed using Absolv [51] for all the structures in the PETROTOX library (n=1512) [3] for application to the model in Eqn

6. The values for E range from 0 to 4 for most hydrocarbon constituents in the library, 0 to 2 for S, essentially all zero for A, 0 to 0.5 for B, and 0 to 4 for V. This means that hydrocarbons have little ability to accept or donate hydrogen bonds and that partitioning in the environment is mainly driven by the balance between polarity (E, S) and molecular volume (V).

To be consistent with the goals of this paper (e.g., compare BE to TU), the overall contribution from each process (e.g., eE, sS, bB, aA, vV, c) was determined by computing the magnitude for each term, and then summing those terms across all the constituents. In order to focus on the most relevant constituents the target lipid (Eqn 5), and PDMS (Eqn 6) concentrations were calculated using predicted dissolved concentrations for constituents based on PETROTOX calculations for a medium crude oil (Endicott) across a range of loadings (0.5 – 500 mg/L). This eliminated constituents that were not abundant, not present, or not toxic from the analysis and provided a range of exposure conditions. For example, at higher loadings (>10 mg/L) lighter constituents are major contributors to toxicity, whereas at lower loadings 2+ ring PAH are the primary contributors [1].

Figures

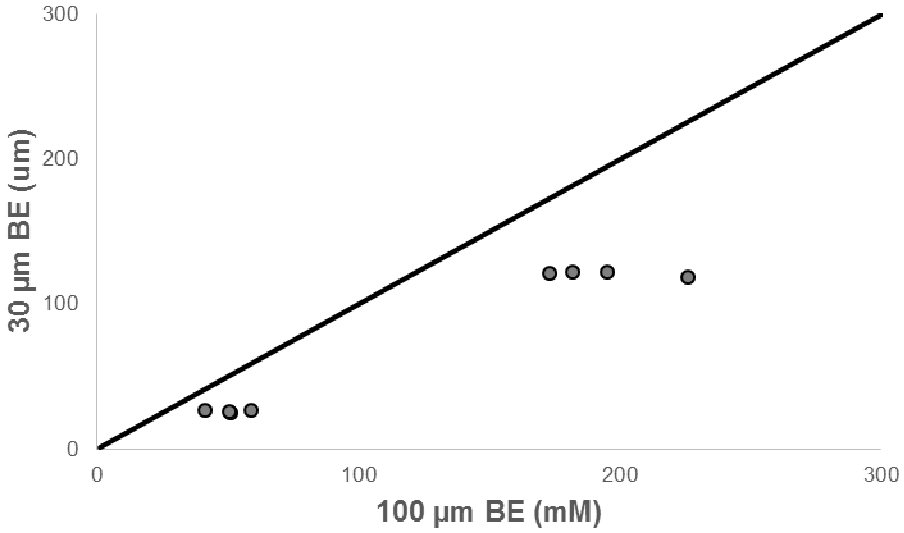

Figure A.1. Comparing biomimetic extraction (BE) measurements for exposures to No. 2 Fuel Oil characterized by 100 µm and 30 µm fibers at 100 and 1 mg/L loadings. The 30 µm measurements are a factor of 1.8 lower than the 100 µm fiber measurements (Table S1).

Table A.1. Measured BE concentrations for No. 2 Fuel oil preparations comparing the automated (30 µm) and manual (100 µm) BE methods

	1 mg/L	100 mg/L
100 µm manual	50.6 (7.0)	194 (50.6)
30 µm automated	26.5 (1.1)	121 (26.5)

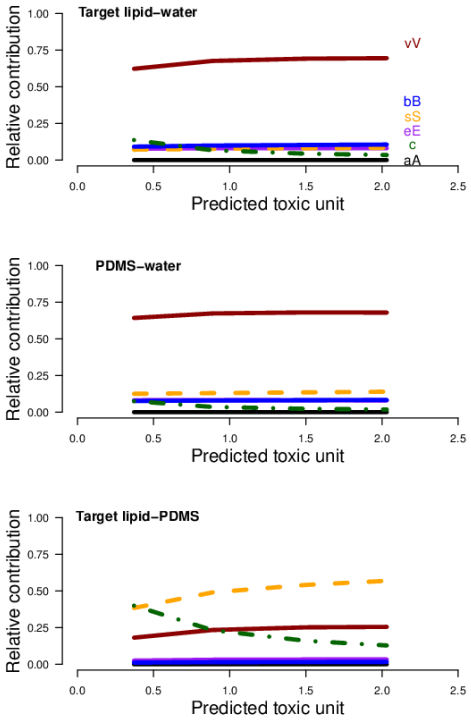

Figure A.2. Fractional contribution of major chemical processes in the polyparameter models (Eqn 4-7) for partition coefficients for target lipid-water ("Target lipid-water"), PDMS-water ("PDMS-water"), and the difference for those models ("Target lipid-PDMS"), which is the target lipid-PDMS partition coefficient. Model terms: "vV" contribution from molecular volume on partitioning, "bB" contribution from hydrogen bond acceptance, "sS" contribution from polarity, "eE" contribution from excess polarity, "c" contribution from intercept terms, and "aA" contribution from hydrogen bond donation – these values are all zero. Legend in top panel.

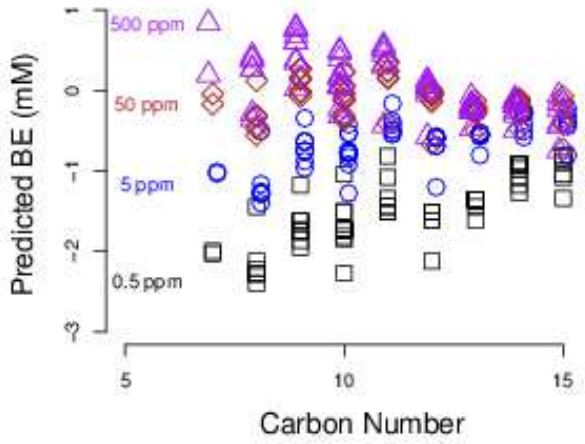

Figure A.3. Predicted BE profiles for library constituents in PETROTOX based on a medium crude oil and the fiber-water partition coefficient (Eqn S2) vs carbon number for selected loadings of a medium weight crude oil, see *Methods* and *Supplementary Information*.

Table A.2. BE and effects data used in plotting

Category	Organism	endpoint	loading (mg/L)	SPME thickness (um)	BE (mM)	Effect (%)	TU
UATO	D.magna	reproduction	1.1	30	0.309	0	0.30
LBO	D.magna	reproduction	1	30	0.08775	0	0.14
UATO	D.magna	reproduction	0.1	30	0.26375	12.8	0.12
DAE	D.magna	reproduction	1	30	bdl	4.51128	0.02
foots oil	D.magna	reproduction	1.1	30	bdl	0	0.00
UATO	D.magna	reproduction	1	30	bdl	0	0.00
HFO	*p.subcapitata*	growth rate	0	30	1.00E-02	0	0.00
HFO	*p.subcapitata*	growth rate	1	30	6.6	1	0.70
HFO	*p.subcapitata*	growth rate	4	30	15.9	4	1.09
HFO	*p.subcapitata*	growth rate	10.8	30	21.7	10.8	1.32
HFO	*p.subcapitata*	growth rate	32.3	30	27.8	32.3	1.51
HFO	*p.subcapitata*	growth rate	103.8	30	33.3	103.8	1.63
HFO	D.magna	Mortality	0	30	1.00E-02	0	0.00
HFO	D.magna	Mortality	1	30	3.91	0	**0.48**
HFO	D.magna	Mortality	2.8	30	10.5	0	**0.74**
HFO	D.magna	Mortality	7.5	30	24.8	50	**1.05**
HFO	D.magna	Mortality	19	30	42.9	90	**1.39**
HFO	D.magna	Mortality	52	30	65.1	100	**1.74**
Gas oil	D.magna	Mortality	0	30	1.00E-02	0	0.00
Gas oil	D.magna	Mortality	0.05	30	1.00E-20	0	**0.26**
Gas oil	D.magna	Mortality	0.15	30	1.00E-20	30	**0.59**
Gas oil	D.magna	Mortality	0.45	30	1.00E-20	85	**1.17**
Gas oil	D.magna	Mortality	1.35	30	1.00E-20	100	**1.94**
Gas oil	D.magna	Mortality	4.05	30	1.00E-20	100	**2.70**
Gas oil	D.magna	Mortality	0	30	1.00E-02	0	0.00
Gas oil	D.magna	Mortality	0.32	30	1.00E-20	0	**0.42**
Gas oil	D.magna	Mortality	1.6	30	1.00E-20	0	**0.83**
Gas oil	D.magna	Mortality	0.05	30	1.00E-20	0	**0.13**
Gas oil	D.magna	Mortality	0.15	30	1.00E-20	0	**0.32**
Gas oil	D.magna	Mortality	0.45	30	1.00E-20	10	**0.75**
Gas oil	D.magna	Mortality	1.35	30	1.00E-20	100	**1.55**

Table continued

Gas oil	D.magna	Mortality	4.05	30	1.00E-20	100	**2.78**
Gas oil	D.magna	Mortality	0	30	1.00E-02	0	0.00
Gas oil	D.magna	Mortality	0.05	30	1.00E-20	0	**0.17**
Gas oil	D.magna	Mortality	0.15	30	1.00E-20	0	**0.40**
Gas oil	D.magna	Mortality	0.45	30	1.00E-20	80	**0.84**
Gas oil	D.magna	Mortality	1.35	30	1.00E-20	100	**1.53**
Gas oil	D.magna	Mortality	4.05	30	1.00E-20	100	**2.43**
Gas oil	*p.subcapitata*	growth	0	30	1.00E-02	0	0.00
Gas oil	*p.subcapitata*	growth	0.1	30	1.00E-20	0	0.22
Gas oil	*p.subcapitata*	growth	1	30	1.00E-20	27	1.13
Gas oil	*p.subcapitata*	growth	10	30	1.00E-20	100	2.48
Gas oil	*p.subcapitata*	growth	100	30	1.00E-20	100	3.21
Gas oil	*p.subcapitata*	growth	1000	30	1.00E-20	100	3.43
Gas oil	*p.subcapitata*	growth	0	30	1.00E-02	0	0.00
Gas oil	*p.subcapitata*	growth	0.32	30	1.00E-20	0	0.21
Gas oil	*p.subcapitata*	growth	1.6	30	1.00E-20	13	0.51
Gas oil	*p.subcapitata*	growth	8	30	1.00E-20	34	0.92
Gas oil	*p.subcapitata*	growth	40	30	1.00E-20	98	1.29
Gas oil	*p.subcapitata*	growth	200	30	1.00E-20	98	1.56
Gas oil	*p.subcapitata*	growth	0	30	1.00E-02	0	0.00
Gas oil	*p.subcapitata*	growth	0.05	30	1.00E-20	5	0.06
Gas oil	*p.subcapitata*	growth	0.23	30	1.00E-20	17	0.28
Gas oil	*p.subcapitata*	growth	1.01	30	1.00E-20	77	0.95
Gas oil	*p.subcapitata*	growth	4.56	30	1.00E-20	100	2.48
Gas oil	*p.subcapitata*	growth	20.5	30	1.00E-20	100	4.38
Gas oil	*p.subcapitata*	growth	0	30	1.00E-02	0	0.00
Gas oil	*p.subcapitata*	growth	0.05	30	1.00E-20	2	0.09
Gas oil	*p.subcapitata*	growth	0.23	30	1.00E-20	10	0.32
Gas oil	*p.subcapitata*	growth	1.01	30	1.00E-20	50	0.93
Gas oil	*p.subcapitata*	growth	4.56	30	1.00E-20	95	2.04
Gas oil	*p.subcapitata*	growth	20.5	30	1.00E-20	100	3.24
UATO	D.magna	reproduction	1.1	30	0.309	21.6	0.30
LBO	D.magna	reproduction	1	30	0.08775	16	0.14
UATO	D.magna	reproduction	0.1	30	bdl	0	0.12
LBO	D.magna	reproduction	0	30	1.00E-02	0	0.00
LBO	D.magna	reproduction	0.1	30	bdl	0	0.05

Table continued

LBO	D.magna	reproduction	1	30	0.0664	3.8835	0.14
LBO	D.magna	reproduction	3	30	0.08483	1.94175	0.18
LBO	D.magna	reproduction	10	30	0.239	20.3883	0.22
fluid	D.magna	reproduction	0	30	1.00E-02		0.00
fluid	D.magna	reproduction	0.1	30	bdl		0.04
fluid	D.magna	reproduction	1	30	bdl		0.13
DAE	D.magna	reproduction	0	30	1.00E-02	0	0.00
DAE	D.magna	reproduction	1	30	bdl	4.51128	0.02
foots oil	D.magna	reproduction	1.1	30	bdl	0	0.00
UATO	D.magna	reproduction	1	30	bdl	0	0.00
HFO	D.magna	reproduction	0	30	1.00E-02	0	0.00
HFO	D.magna	reproduction	1.2	30	bdl	0	0.00
DAE	D.magna	Mortality	100	30	bdl	0	0.37
TDAE	D.magna	Mortality	100	30	bdl	0	0.21
HFO	D.magna	Mortality	0	30	1.00E-02	0	0.00
HFO	D.magna	Mortality	0.8	30	2.9	5	**0.66**
HFO	D.magna	Mortality	2.5	30	7.5	75	**0.95**
HFO	D.magna	Mortality	9.8	30	13.3	100	**1.25**
HFO	D.magna	Mortality	30	30	18.9	100	**1.43**
HFO	D.magna	Mortality	101	30	24.2	100	**1.56**
HFO	D.magna	Mortality	0	30	1.00E-02	0	0.00
HFO	D.magna	Mortality	1.3	30	8.28	5	**1.38**
HFO	D.magna	Mortality	3.8	30	15.5	70	**1.75**
HFO	D.magna	Mortality	11.5	30	24.7	100	**2.04**
HFO	D.magna	Mortality	33	30	31.9	100	**2.22**
HFO	D.magna	Mortality	95	30	38.5	100	**2.34**
HFO	D.magna	Mortality	0	30	1.00E-02	0	0.00
HFO	O. mykiss, juveline	Mortality	0.7	30	5.4	0	1.13
HFO	O. mykiss, juveline	Mortality	3	30	7.6	0	1.67
HFO	O. mykiss, juveline	Mortality	8.3	30	16	0	1.96
HFO	O. mykiss, juveline	Mortality	28	30	24	0	2.20
HFO	O. mykiss, juveline	Mortality	94	30	27	0	2.33
HFO	D.magna	reproduction	0	30	1.00E-02	0	0.00
HFO	D.magna	reproduction	1.2	30	bdl	0	0.10
crude	D.magna	survival	38	30	11.8	0	1.23
crude	D.magna	survival	96	30	19.35	5	1.48

Table continued

crude	D.magna	survival	240	30		22.0	35	1.71
crude	D.magna	survival	600	30		30.1	80	1.89
Gas oil	*p.subcapitata*	growth rate	0		999	1.00E-20	0	0.00
Gas oil	*p.subcapitata*	growth rate	0.1		999	1.00E-20	0	0.22
Gas oil	*p.subcapitata*	growth rate	0.32		999	1.00E-20	5.40541	0.65
Gas oil	*p.subcapitata*	growth rate	1.02		999	1.00E-20	7.20721	1.76
Gas oil	*p.subcapitata*	growth rate	3.28		999	1.00E-20	18.018	3.87
Gas oil	*p.subcapitata*	growth rate	10.5		999	1.00E-20	106.306	6.10
Gas oil	*p.subcapitata*	growth rate	0		999	1.00E-20	0	0.00
Gas oil	*p.subcapitata*	growth rate	0.1		999	1.00E-20	0.90909	0.08
Gas oil	*p.subcapitata*	growth rate	0.32		999	1.00E-20	16.3636	0.21
Gas oil	*p.subcapitata*	growth rate	1.02		999	1.00E-20	65.4545	0.45
Gas oil	*p.subcapitata*	growth rate	3.28		999	1.00E-20	115.455	0.80
Gas oil	*p.subcapitata*	growth rate	10.5		999	1.00E-20	115.455	1.16
Gas oil	D.magna	growth rate	0		999	1.00E-20	0	0.00
Gas oil	D.magna	growth rate	0.102		999	1.00E-20	0	**0.34**
Gas oil	D.magna	growth rate	0.256		999	1.00E-20	0	**0.76**
Gas oil	D.magna	growth rate	0.64		999	1.00E-20	0	**1.60**
Gas oil	D.magna	growth rate	1.6		999	1.00E-20	20	**3.05**
Gas oil	D.magna	growth rate	4		999	1.00E-20	90	**4.96**
Gas oil	D.magna	growth rate	0		999	1.00E-20	0	0.00
Gas oil	D.magna	growth rate	0.1		999	1.00E-20	0	**0.17**
Gas oil	D.magna	growth rate	0.26		999	1.00E-20	0	**0.34**
Gas oil	D.magna	growth rate	0.64		999	1.00E-20	0	**0.58**
Gas oil	D.magna	growth rate	1.6		999	1.00E-20	20	**0.88**
Gas oil	D.magna	growth rate	4		999	1.00E-20	90	**1.19**
Gas oil	D.magna	reproduction	0		999	1.00E-20	0	0.00
Gas oil	D.magna	reproduction	0.04		999	1.00E-20	0	0.08
Gas oil	D.magna	reproduction	0.08		999	1.00E-20	3.59712	0.14
Gas oil	D.magna	reproduction	0.16		999	1.00E-20	0	0.24
Gas oil	D.magna	reproduction	0.32		999	1.00E-20	0	0.39
Gas oil	D.magna	reproduction	0.64		999	1.00E-20	4.31655	0.58
Gas oil	D.magna	reproduction	0		999	1.00E-20	0	0.00
Gas oil	D.magna	reproduction	0.08		999	1.00E-20	2.75229	0.28
Gas oil	D.magna	reproduction	0.19		999	1.00E-20	3.66972	0.59
Gas oil	D.magna	reproduction	0.48		999	1.00E-20	17.4312	1.28

Table continued

Gas oil	D.magna	reproduction	1.2		999	1.00E-20	37.6147	2.53
Gas oil	D.magna	reproduction	3		999	1.00E-20	100	4.35
Gas oil	O. mykiss, juveline	mortality	0		999	1.00E-20	0	0.00
Gas oil	O. mykiss, juveline	mortality	0.3		999	1.00E-20	0	**0.87**
Gas oil	O. mykiss, juveline	mortality	0		999	1.00E-20	0	0.00
Gas oil	O. mykiss, juveline	mortality	2.6		999	1.00E-20	0	**1.04**
Kerosene	D.magna	reproduction	0		999	1.00E-20	0	0.00
Kerosene	D.magna	reproduction	0.08		999	1.00E-20	2.75229	0.15
Kerosene	D.magna	reproduction	0.19		999	1.00E-20	3.66972	0.30
Kerosene	D.magna	reproduction	0.48		999	1.00E-20	17.4312	0.54
Kerosene	D.magna	reproduction	1.2		999	1.00E-20	94.4954	0.79
Kerosene	D.magna	reproduction	3		999	1.00E-20	100	1.05
crude	mysid	survival	5.9	30		3.91	35	0.40
crude	mysid	survival	18.8	30		7.67	100	0.59
crude	mysid	survival	58.3	30		13	100	0.79
crude	mysid	survival	197	30		19.3	100	0.97
Gas oil	*p.subcapitata*	growth rate	0.6	30		1.6	1.3	0.26
Gas oil	*p.subcapitata*	growth rate	1.3	30		1.00E-20	1.2	0.38
Gas oil	*p.subcapitata*	growth rate	3.2	30		4.2	1	0.53
Gas oil	*p.subcapitata*	growth rate	8	30		1.00E-20	8.8	0.68
Gas oil	*p.subcapitata*	growth rate	20	30		11	21	0.82
Gas oil	*p.subcapitata*	growth rate	0.6	30		1.1	0.1	0.25
Gas oil	*p.subcapitata*	growth rate	2.2	30		1.00E-20	0.2	0.45
Gas oil	*p.subcapitata*	growth rate	5.9	30		5.4	3.9	0.62
Gas oil	*p.subcapitata*	growth rate	17	30		1.00E-20	16	0.79
Gas oil	*p.subcapitata*	growth rate	47	30		12	39	0.92
Gas oil	*p.subcapitata*	growth rate	1.6	30		2.4	0	0.38
Gas oil	*p.subcapitata*	growth rate	4.4	30		1.00E-20	3.5	0.58
Gas oil	*p.subcapitata*	growth rate	13	30		9.3	15	0.83
Gas oil	*p.subcapitata*	growth rate	35	30		1.00E-20	40	1.05
Gas oil	*p.subcapitata*	growth rate	100	30		22	86	1.26
Gas oil	*p.subcapitata*	growth rate	0.6	30		3.5	20	0.56
Gas oil	*p.subcapitata*	growth rate	1.6	30		1.00E-20	31	0.89
Gas oil	*p.subcapitata*	growth rate	4.3	30		11	44	1.26
Gas oil	*p.subcapitata*	growth rate	12	30		1.00E-20	83	1.62
Gas oil	*p.subcapitata*	growth rate	36	30		25	92	1.93

Table continued

Gas oil	*p.subcapitata*	growth rate	4.4	30	5.63	0	0.58
Gas oil	*p.subcapitata*	growth rate	16	30	1.00E-20	18	0.79
Gas oil	*p.subcapitata*	growth rate	48	30	14.2	31	0.92
Gas oil	*p.subcapitata*	growth rate	157	30	1.00E-20	50	1.02
Gas oil	*p.subcapitata*	growth rate	513	30	20.5	85	1.07
Gas oil	*p.subcapitata*	growth rate	4.8	30	4.23E+00	7.2	0.58
Gas oil	*p.subcapitata*	growth rate	16	30	1.00E-20	19	0.78
Gas oil	*p.subcapitata*	growth rate	54	30	1.24E+01	38	0.94
Gas oil	*p.subcapitata*	growth rate	196	30	1.00E-20	89	1.05
Gas oil	*p.subcapitata*	growth rate	614	30	2.03E+01	97	1.10
Gas oil	*p.subcapitata*	growth rate	3.2	30	3.40E+00	8.8	0.44
Gas oil	*p.subcapitata*	growth rate	12	30	1.00E-20	15	0.62
Gas oil	*p.subcapitata*	growth rate	37	30	9.98E+00	49	0.77
Gas oil	*p.subcapitata*	growth rate	141	30	1.00E-20	75	0.91
Gas oil	*p.subcapitata*	growth rate	439	30	1.71E+01	75	0.99
Gas oil	*p.subcapitata*	growth rate	3.5	30	3.70E+00	16	0.59
Gas oil	*p.subcapitata*	growth rate	12	30	1.00E-20	34	0.77
Gas oil	*p.subcapitata*	growth rate	38	30	8.52E+00	61	0.89
Gas oil	*p.subcapitata*	growth rate	125	30	1.00E-20	70	0.95
Gas oil	*p.subcapitata*	growth rate	414	30	1.15E+01	80	0.98
Gas oil	*p.subcapitata*	growth rate	3.9	30	3.68E+00	23	0.64
Gas oil	*p.subcapitata*	growth rate	13	30	1.00E-20	41	0.85
Gas oil	*p.subcapitata*	growth rate	42	30	1.03E+01	60	1.00
Gas oil	*p.subcapitata*	growth rate	140	30	1.00E-20	80	1.09
Gas oil	*p.subcapitata*	growth rate	464	30	1.43E+01	95	1.14
Gas oil	*p.subcapitata*	growth rate	4.7	30	4.40E+00	20	0.66
Gas oil	*p.subcapitata*	growth rate	14	30	1.00E-20	30	0.84
Gas oil	*p.subcapitata*	growth rate	46	30	1.15E+01	49	0.99
Gas oil	*p.subcapitata*	growth rate	158	30	1.00E-20	60	1.08
Gas oil	*p.subcapitata*	growth rate	512	30	1.64E+01	77	1.13
Gas oil	*p.subcapitata*	growth rate	7.9	30	4.92E+00	9.4	0.47
Gas oil	*p.subcapitata*	growth rate	27	30	1.00E-20	15	0.63
Gas oil	*p.subcapitata*	growth rate	90	30	1.10E+01	27	0.76
Gas oil	*p.subcapitata*	growth rate	305	30	1.00E-20	30	0.84
Gas oil	*p.subcapitata*	growth rate	1026	30	1.40E+01	34	0.89
Gas oil	D.magna	survival	8.6	30	10.2	10	0.69

Table continued

Gas oil	D.magna	survival	19	30	1.00E-20	15	0.81
Gas oil	D.magna	survival	40	30	18.8	50	0.90
Gas oil	D.magna	survival	86	30	1.00E-20	100	0.98
Gas oil	D.magna	survival	194	30	23.5	100	1.03
Gas oil	D.magna	survival	3.9	30	6.9	0	0.55
Gas oil	D.magna	survival	11	30	1.00E-20	0	0.72
Gas oil	D.magna	survival	35	30	15	0	0.89
Gas oil	D.magna	survival	91	30	1.00E-20	45	0.99
Gas oil	D.magna	survival	258	30	19	55	1.07
Gas oil	D.magna	survival	1.5	30	3.3	0	0.37
Gas oil	D.magna	survival	4	30	1.00E-20	0	0.56
Gas oil	D.magna	survival	9.1	30	10	0	0.74
Gas oil	D.magna	survival	24	30	1.00E-20	35	0.97
Gas oil	D.magna	survival	63	30	21	90	1.18
Gas oil	D.magna	survival	0.5	30	2.6	0	0.50
Gas oil	D.magna	survival	1.1	30	1.00E-20	0	0.75
Gas oil	D.magna	survival	2.5	30	11	25	1.05
Gas oil	D.magna	survival	5.7	30	1.00E-20	75	1.36
Gas oil	D.magna	survival	14	30	23	100	1.67
Gas oil	D.magna	survival	8.1	30	7.2	0	0.57
Gas oil	D.magna	survival	21	30	1.00E-20	0	0.70
Gas oil	D.magna	survival	50	30	14	20	0.81
Gas oil	D.magna	survival	124	30	1.00E-20	35	0.90
Gas oil	D.magna	survival	327	30	18	45	0.97
Gas oil	D.magna	survival	28	30	1.08E+01	0	0.74
Gas oil	D.magna	survival	72	30	1.00E-20	0	0.85
Gas oil	D.magna	survival	168	30	1.85E+01	30	0.93
Gas oil	D.magna	survival	409	30	1.00E-20	35	0.99
Gas oil	D.magna	survival	1146	30	2.19E+01	50	1.03
Gas oil	D.magna	survival	20.7	30	8.55E+00	0	0.60
Gas oil	D.magna	survival	69	30	1.00E-20	0	0.74
Gas oil	D.magna	survival	224	30	1.63E+01	0	0.83
Gas oil	D.magna	survival	801	30	1.00E-20	0	0.88
Gas oil	D.magna	survival	2636	30	1.74E+01	0	0.90
Gas oil	D.magna	survival	7.6	30	7.60E+00	0	0.76
Gas oil	D.magna	survival	24	30	1.00E-20	0	0.94

Table continued

Gas oil	D.magna	survival	86	30		1.44E+01	15	1.06
Gas oil	D.magna	survival	281	30		1.00E-20	55	1.13
Gas oil	D.magna	survival	1026	30		1.68E+01	60	1.16
Gas oil	D.magna	survival	8.3	30		7.20E+00	0	0.76
Gas oil	D.magna	survival	35	30		1.00E-20	0	0.97
Gas oil	D.magna	survival	82	30		1.49E+01	25	1.04
Gas oil	D.magna	survival	327	30		1.00E-20	30	1.12
Gas oil	D.magna	survival	1171	30		1.81E+01	65	1.15
Gas oil	D.magna	survival	8.6	30		7.44E+00	0	0.72
Gas oil	D.magna	survival	29	30		1.00E-20	15	0.86
Gas oil	D.magna	survival	102	30		1.19E+01	35	0.94
Gas oil	D.magna	survival	314	30		1.00E-20	70	0.97
Gas oil	D.magna	survival	1113	30		1.33E+01	100	0.98
RAE	*p.subcapitata*	survival	1018	30		0.5	0	0.24
BIT	*p.subcapitata*	survival	1035	30		2.25	94	0.13
Gas oil	*p.subcapitata*	survival	1013	30		1.79	19	0.20
RAE	D.magna	survival	1000	30		0.5	0	0.24
BIT	D.magna	survival	1000	30		2.035	0	0.13
Gas oil	D.magna	survival	1000	30		2.155	30	0.20
crude	D.rerio	survival	2.5		30	0.5	0	0.23
crude	D.rerio	survival	8		30	1.075	0	0.32
crude	D.rerio	survival	27		30	5.7	0	0.45
crude	D.rerio	survival	90		30	15.9	0	0.70
crude	D.rerio	survival	300		30	52.7	0	1.19
crude	D.rerio	survival	1000		30	53.8	55	1.92
crude	D.rerio	survival	4.1		30	3.955	0	0.56
crude	D.rerio	survival	14		30	6.785	0	0.79
crude	D.rerio	survival	45		30	14.25	0	1.00
crude	D.rerio	survival	150		30	18.15	5	1.18
crude	D.rerio	survival	500		30	22.7	20	1.30
Gas oil	D.rerio	survival	1.3		30	9.4	0	0.75
Gas oil	D.rerio	survival	3.2		30	14.15	0	1.08
Gas oil	D.rerio	survival	8		30	22.15	0	1.42
Gas oil	D.rerio	survival	20		30	31.55	10	1.73
Gas oil	D.rerio	survival	50		30	38.4	55	1.96
crude	D.rerio	survival	30		30	5.08	1E-20	1.02

Table continued

crude	D.rerio	survival	162	30	9.015	1E-20	1.44
Gas oil	D.rerio	survival	3.2	30	6.87	0	0.56
Gas oil	D.rerio	survival	11	30	10.3	0	0.78
Gas oil	D.rerio	survival	36	30	14.15	0	0.95
Gas oil	D.rerio	survival	120	30	16.6	5	1.06
Gas oil	D.rerio	survival	400	30	18.65	20	1.12
Gas oil	D.rerio	survival	1000	30	20.8	50	1.14
crude	control	survival	0.1	7	0.5	0	0.01
crude	D.rerio	survival	2.5	7	0.7565	0	0.23
crude	D.rerio	survival	8	7	3.035	0	0.32
crude	D.rerio	survival	27	7	8.765	0	0.45
crude	D.rerio	survival	90	7	23.55	0	0.70
crude	D.rerio	survival	300	7	87.5	0	1.19
crude	D.rerio	survival	1000	7	82.2	55	1.92
crude	D.rerio	survival	4.1	7	5.635	0	0.56
crude	D.rerio	survival	14	7	13.05	0	0.79
crude	D.rerio	survival	45	7	19.2	0	1.00
crude	D.rerio	survival	150	7	27.95	5	1.18
crude	D.rerio	survival	500	7	28.35	20	1.30
Gas oil	D.rerio	survival	1.3	7	15.1	0	0.75
Gas oil	D.rerio	survival	3.2	7	26.4	0	1.08
Gas oil	D.rerio	survival	8	7	38.4	0	1.42
Gas oil	D.rerio	survival	20	7	47.3	10	1.73
Gas oil	D.rerio	survival	50	7	61.65	55	1.96
crude	D.rerio	survival	3	7	1.00E-20	1E-20	0.45
crude	D.rerio	survival	30	7	1.00E-20	1E-20	1.02
crude	D.rerio	survival	162	7	1.00E-20	1E-20	1.44
Gas oil	D.rerio	survival	3.2	7	12.3	0	0.56
Gas oil	D.rerio	survival	11	7	21.5	0	0.78
Gas oil	D.rerio	survival	36	7	22	0	0.95
Gas oil	D.rerio	survival	120	7	23.95	5	1.06
Gas oil	D.rerio	survival	400	7	24.3	20	1.12
Gas oil	D.rerio	survival	1000	7	28.15	50	1.14
crude	Control	deformity	0.1	30	0.5	0	0.01
crude	D.rerio	deformity	2.5	30	0.5	0	0.23
crude	D.rerio	deformity	8	30	1.075	5	0.32

Table continued

crude	D.rerio	deformity	27	30	5.7	0	0.45
crude	D.rerio	deformity	90	30	15.9	0	0.70
crude	D.rerio	deformity	300	30	52.7	75	1.19
crude	D.rerio	deformity	1000	30	53.8	75	1.92
crude	D.rerio	deformity	4.1	30	3.955	0	0.56
crude	D.rerio	deformity	14	30	6.785	0	0.79
crude	D.rerio	deformity	45	30	14.25	15	1.00
crude	D.rerio	deformity	150	30	18.15	52.6316	1.18
crude	D.rerio	deformity	500	30	22.7	56.25	1.30
Gas oil	D.rerio	deformity	1.3	30	9.4	5	0.75
Gas oil	D.rerio	deformity	3.2	30	14.15	5	1.08
Gas oil	D.rerio	deformity	8	30	22.15	45	1.42
Gas oil	D.rerio	deformity	20	30	31.55	77.7778	1.73
Gas oil	D.rerio	deformity	50	30	38.4	66.6667	1.96
Gas oil	D.rerio	deformity	3.2	30	6.87	0	0.56
Gas oil	D.rerio	deformity	11	30	10.3	0	0.78
Gas oil	D.rerio	deformity	36	30	14.15	5	0.95
Gas oil	D.rerio	deformity	120	30	16.6	47.3684	1.06
Gas oil	D.rerio	deformity	400	30	18.65	25	1.12
Gas oil	D.rerio	deformity	1000	30	20.8	90	1.14
Gas oil	O. mykiss, juveline	mortality	2.7	30	18.9	0	2.40
Gas oil	O. mykiss, juveline	mortality	9	30	29.3	20	3.43
Gas oil	O. mykiss, juveline	mortality	30	30	42.6	50	4.20
Gas oil	O. mykiss, juveline	mortality	100	30	48.2	100	4.66
crude	O. mykiss, juveline	mortality	2.5	30	4	0	0.59
crude	O. mykiss, juveline	mortality	8.1	30	7.1	0	0.88
crude	O. mykiss, juveline	mortality	27	30	13	0	1.21
crude	O. mykiss, juveline	mortality	90	30	17.2	0	1.53
crude	O. mykiss, juveline	mortality	300	30	22.6	0	1.81

Appendix B

CHAPTER 2 SUPPLEMENTAL INFORMATION\

Supplementary information is found with the published version of this work.

Spreadsheet that contains GCxGC-FID compositional data; PAH, PIONA, SHC compositional data; BE measurements; mortality data, which were used in the present study

Word document that contains supporing figures and text.

Video file that demonstrates preparation of the passive dosing system.

Links to publication and SI material

https://setac.onlinelibrary.wiley.com/doi/full/10.1002/etc.3624

https://setac.onlinelibrary.wiley.com/action/downloadSupplement?doi=10.1002%2Fetc.3624&attachmentId=152153637

https://setac.onlinelibrary.wiley.com/action/downloadSupplement?doi=10.1002%2Fetc.3624&attachmentId=152153638

https://setac.onlinelibrary.wiley.com/action/downloadSupplement?doi=10.1002%2Fetc.3624&attachmentId=152153639

Supporting Information.

- Methods for Image and Particle Size Analysis
- Description of Raoult's Law-based water solubility model
- Chemical profiles for each exposure
- Chart of RMSE of solubility model performance

- Charts and table of effects data using common exposure metrics
- Comparing TUs calculating using conventional analytical to those from GCxGC
- Additional chemical characterization (PIONA, PAH, SHC, BE) and biological effects data provided in *Supplementary Information* spreadsheet.

Particle counts

Laser particle counting was performed using Mettler Toledo OptiMax 1001 particle analyzer coupled with a Mettler Toledo Focused Beam Reflectance Measurement G400 probe while stirring at 200 RPM taking continuous readings over a 10 minute period. Particle sizes of droplets were characterized by binning counts in 10-50, 50-150, and 150-300 µm diameter size classes.

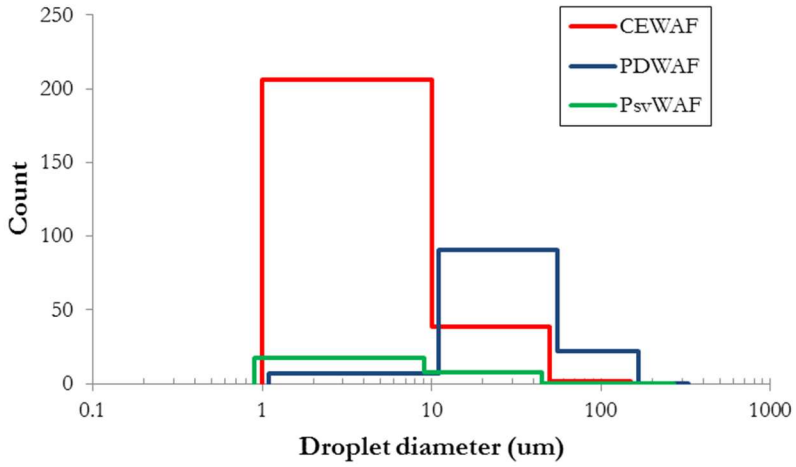

Figure B.1. Size class distribution of droplets in 185 mg/L loading of Endicott oil in salt water.

Modeling analysis

Toxicity Model Framework

The Target Lipid Model (TLM) extends the critical body burden (CBB) hypothesis (McCarty 1991) by assuming that lipid is the target tissue, e.g., critical target lipid body burden (BTLBB), on the organism. The target lipid-water partition coefficient (K_{LW}) is used to estimate the critical body burden on a lipid basis (McGrath and Di Toro 2009). The K_{LW} (L/kg lipid) is defined as the ratio of the chemical concentration on the target lipid, C_L (mmol/kg lipid), to the chemical concentration in the water, C_W (mmol/L).

$$K_{LW} = \frac{C_L}{C_W} \tag{1}$$

The organism target lipid (C_L) computed at the LC50 (C_W) yields the CTLBB. This is the definition of the critical target lipid body burden and, from Equation 1,

$$\log(LC50) = \log(C_L^*) - \log(K_{LW}) \tag{2}$$

Using Equation 2, the critical target lipid body burden can be calculated for any chemical using the LC50 and the K_{LW}. It is assumed that the K_{LW} can be related to K_{OW} using a linear free energy relationship.

$$\log(K_{LW}) = a_0 + a_1 \log(K_{ow}) \tag{3}$$

Equations 2 and 3 are combined to produce a single linear relationship between log(LC50) and log(K_{OW})

$$\log(LC50) = \log(C_L^*) - a_0 - a_1 \log(K_{ow}) \quad (4)$$

Where a_1 is the slope of LC50-K_{OW} log linear regression (Eqn. 4), which is constant across the training and validation datasets at -0.936. The a_0 term becomes a correction factor for certain chemical classes that were observed to be systematically offset from the larger dataset. This correction factor amounts for a factor of 2-3 from the baseline calculation and is applied to 1- and 2+ ring aromatics: -0.109, -0.352, respectively. The CTLBB is species specific, and can be used to compare relative sensitivity between species: 116 (*D.magna*) and 34 (*A.bahia*) µmol/g lipid.

Mixture toxicity is determined by first computing the solubility of the constituents (C_{Wi}) and then normalizing those concentrations to the TLM-predicted effect levels (e.g., $LC50_i$). This results in a Toxic Unit (TU) for each constituent and represents the relative contribution from a given constituent to the overall effect.

$$\mathrm{TU} = \sum_{i=1}^{n} \frac{C_{W,i}}{\mathrm{LC50}_i} \quad (5)$$

The TUs reflect the bioavailability of the hydrocarbons in the exposure water. The TUs scale linearly between organisms since the CTLBB acts as a scalar quantity (Eqn. 4) in the TLM.

Solubility Model Framework

The solubility model is a Raoult's Law based mass balance model predicts the distribution of hydrocarbon constituents between the oil, air (headspace), and water phases. The model is sensitive to the abundance of a constituent in the oil, as well as the solubility of that constituent. The only optimizable parameter is the volume of the oil phase in the preparation system. See McGrath et al 2005 for derivation, and Redman et al 2012; Redman and Parkerton 2015 for additional applications.

$$x_i = \frac{m_{i,system}}{(V_{oil}\, p_{oil} + V_{Air} S_{L,i} H_i + V_W S_{L,i})} \quad (6)$$

$m_{i,\text{system}} = m_{i,\text{dissolved\_step1}} + m_{i,\text{droplet}}$.
m_i = mass of constituent i in system:
$m_i = C_{\text{oil},i}$ (µg/g) * Loading (g/L system) * system Volume (L, $V_{\text{air}} + V_{\text{w}}$)
rho_{oil} = density of oil substance (g/L)
x_i = mole fraction of constituent i
V_{oil} = volume of undissolved oil phase, sole fitting parameter, L
P_{oil} = molar density of oil (moles constituent i / L oil)
V_{air} = headspace volume (L air), assumed 25% for all calculations
$S_{\text{L}i}$ = sub-cooled liquid solubility (moles constituent i / L water) * MW (g/mol)
H_i = unitless Henry's Law constant for constituent i
V_{w} = = water volume (L water)

Once the computed dissolved profile is determined the speciation model is compared to the measured total concentrations (C_{T}, µg/L). It is assumed that the measurements represent both dissolved (C_{W}, µg/L) and particulate (C_{P}, µg/L) concentrations of each constituent, i.

$$C_{\text{T,i}} = C_{\text{W,i}} + C_{\text{P,i}} \quad (7)$$

The concentration of particulate oil in the exposures can be determined as the product of the concentration of a consistuent, *i*, in the oil phase (C_O, µg/g oil) and the droplet concentration (C_D, g/L as entrained oil) in the exposure system.

$$C_{T,i} = C_{W,i} + C_{O,I} * C_D \quad (8)$$

The droplet oil (C_D) concentration is determined by least-squares fitting of the model predicted total to the measurements. See Redman et al [2012] for more detail.

Figures

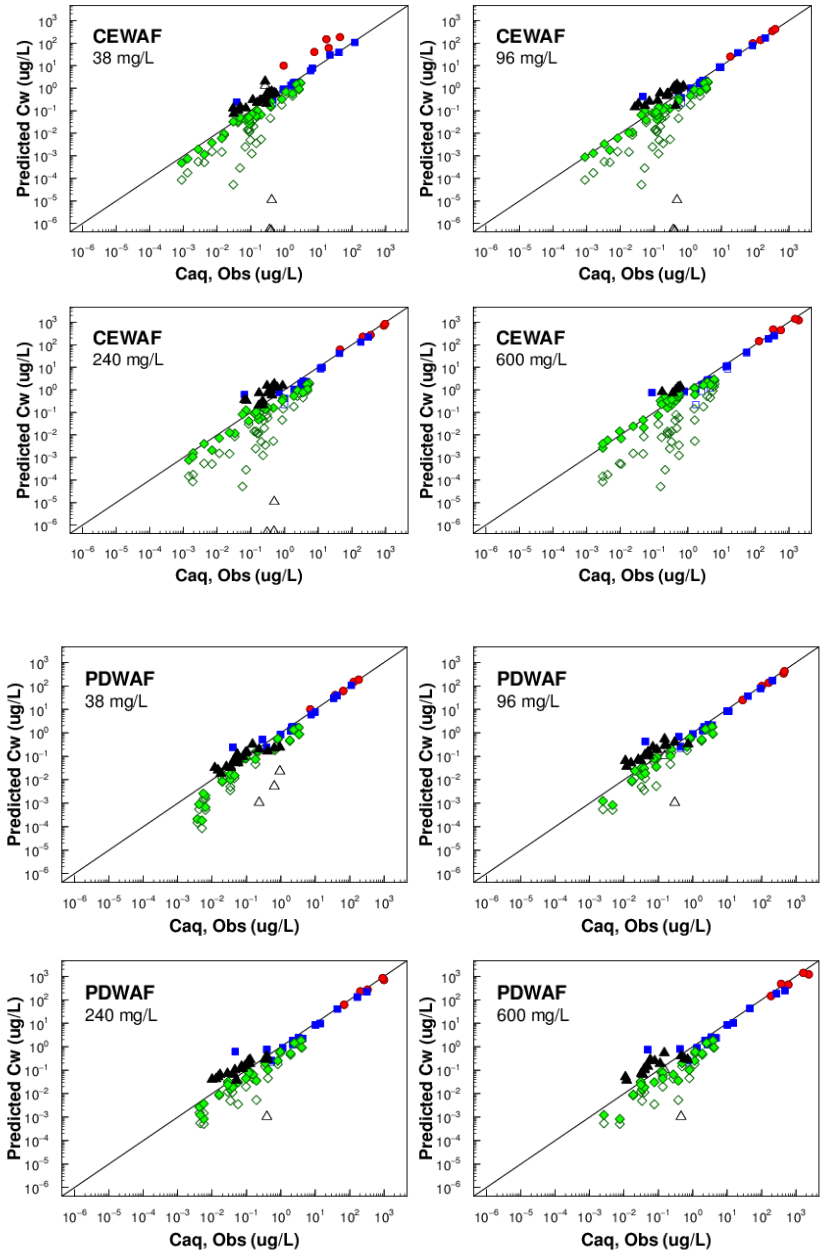
CEWAF
38 mg/L
CEWAF
96 mg/L
CEWAF
240 mg/L
CEWAF
600 mg/L
PDWAF
38 mg/L
PDWAF
96 mg/L
PDWAF
240 mg/L
PDWAF
600 mg/L
Predicted Cw (ug/L)
Caq, Obs (ug/L)

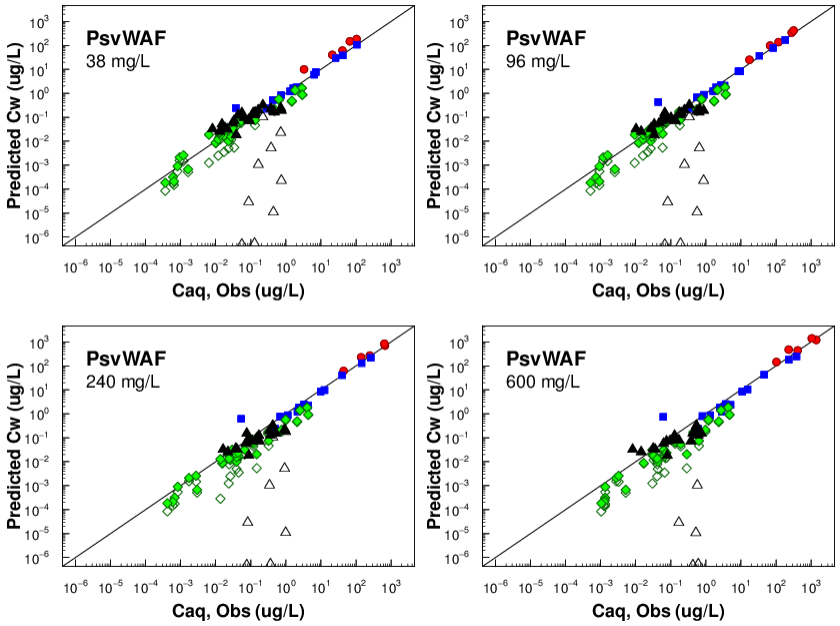

Figure B.2a. Predicted dissolved (open) or Predicted Total (filled) concentrations vs measured concentrations for each loading from the freshwater exposures. Data presented for 1-ring (**RED**), 2-ring (**BLUE**), and 3+ ring aromatics (**GREEN**) and C9-C30 saturates (**BLACK**).

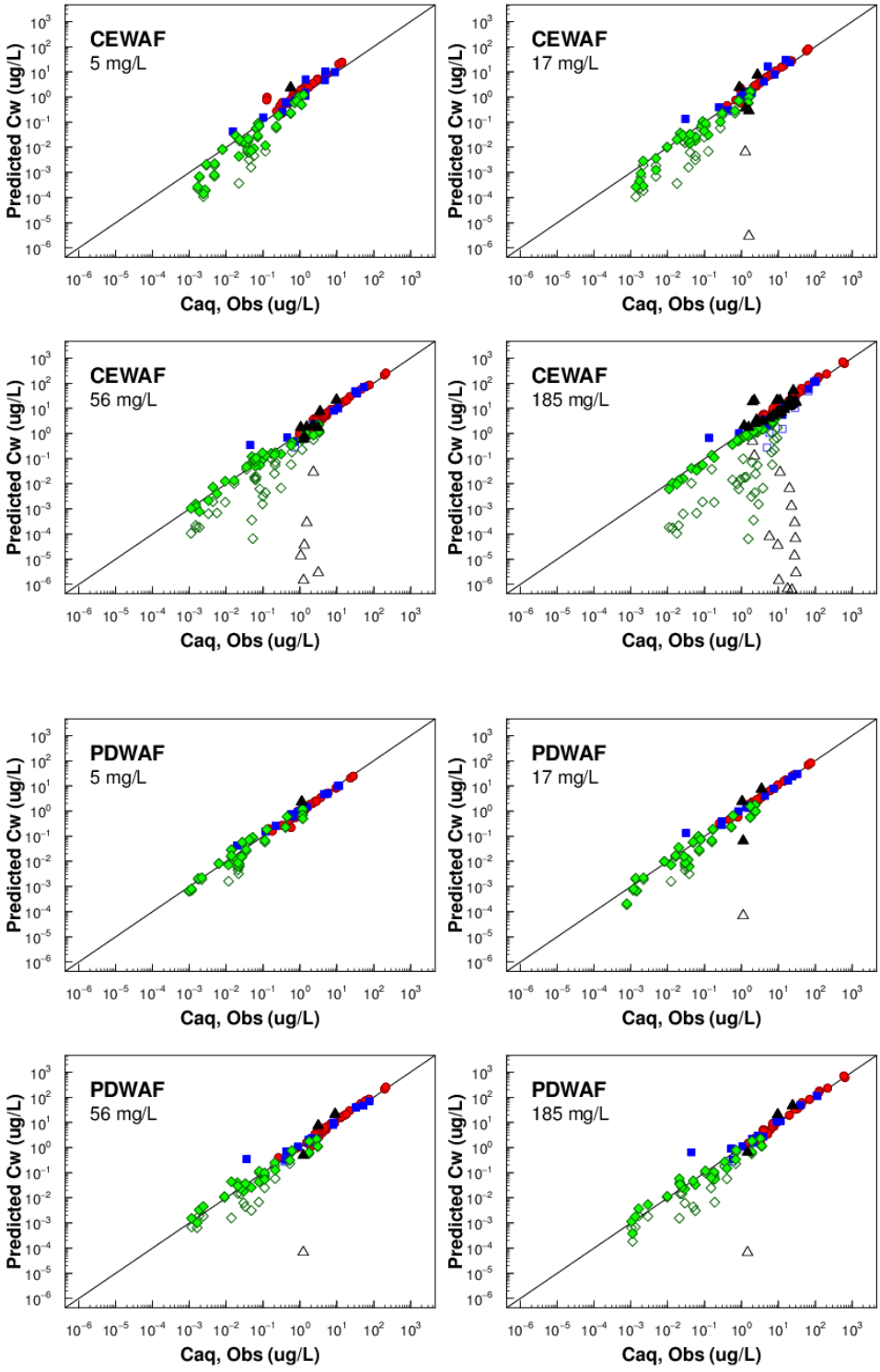
CEWAF
5 mg/L
CEWAF
17 mg/L
CEWAF
56 mg/L
CEWAF
185 mg/L
PDWAF
5 mg/L
PDWAF
17 mg/L
PDWAF
56 mg/L
PDWAF
185 mg/L
Predicted Cw (ug/L)
Caq, Obs (ug/L)

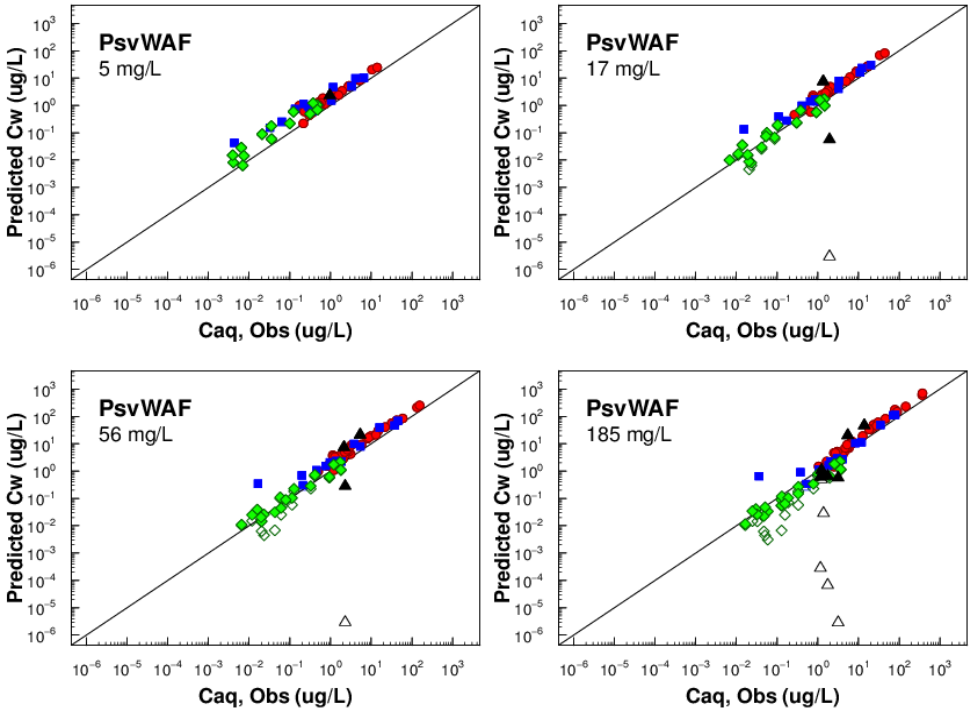

Figure B.2b**.** Predicted dissolved (open) or Predicted Total (filled) concentrations vs measured concentrations for each loading from the salt water exposures. Data presented for 1-ring (**RED**), 2-ring (**BLUE**), and 3+ ring aromatics (**GREEN**) and C5-C30 saturates (**BLACK**).

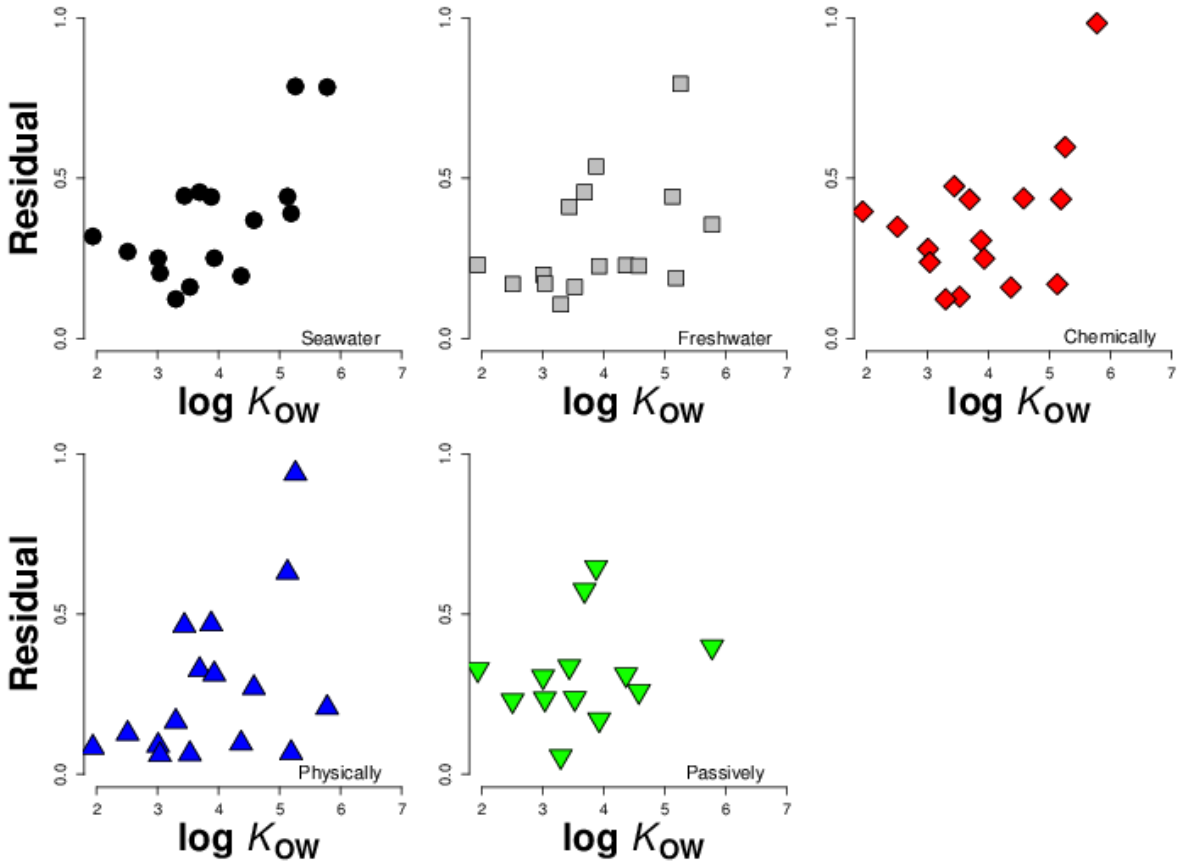

Figure B.3. Log of root mean square error of solubility model vs logK_{OW} for constituentsin Figure 2. Model performance was essentially equivalent over the range of chemicals evaluated, with possible outlier of Chrysene in CEWAF, which appears to be impacted by depletive extraction of the droplet onto the SPME fibers. In the Physically Dosed system, mePYR is the main outlier, which is a result of measurements at or below the detection limit. There are no consistent trends in residuals with logK_{OW} suggesting adequate model performance across the range of interest in physicochemical properties.

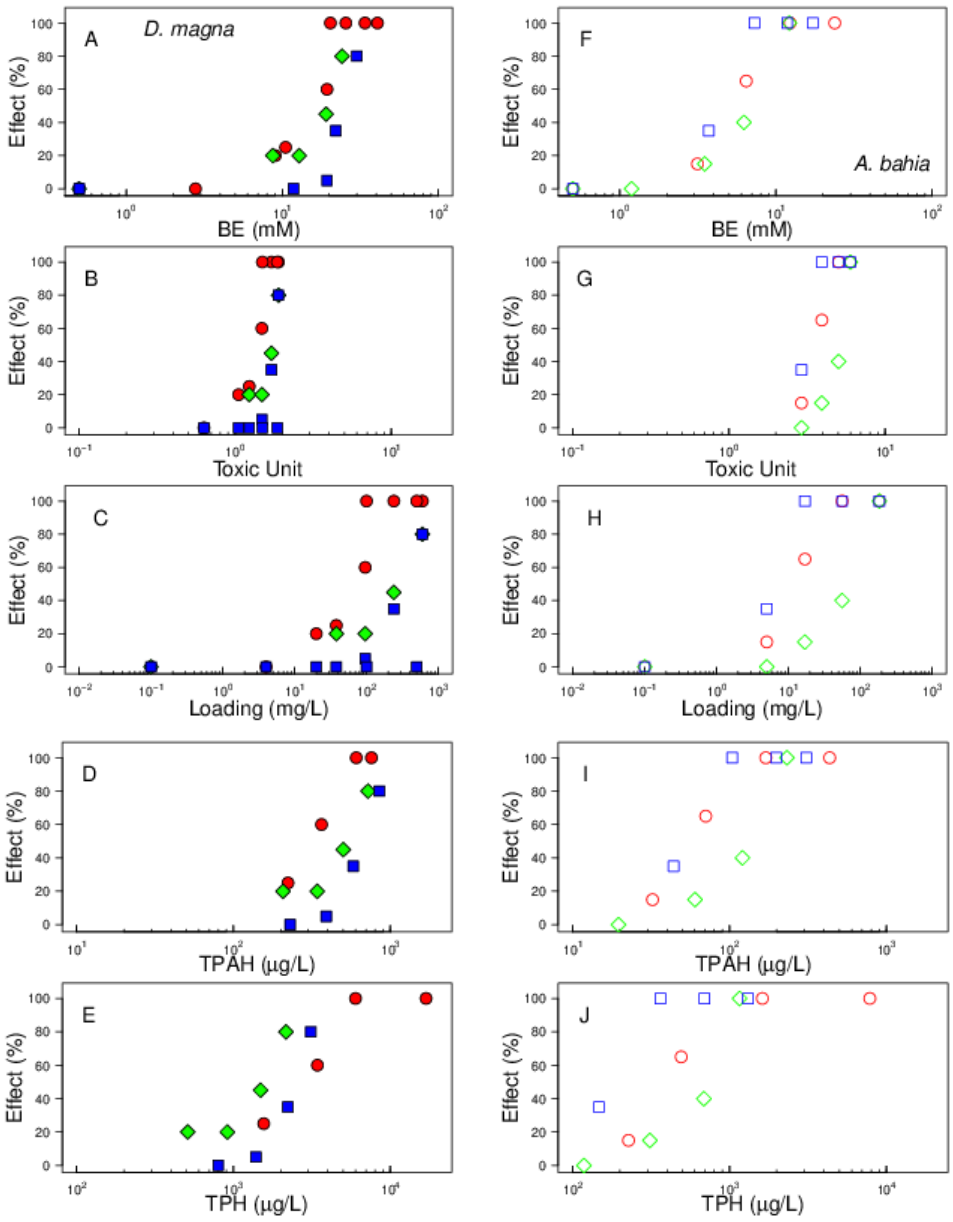

Figure B.4. Observed 48 h effects data plotted against common effect metrics. Comparing observed 48-h mortality vs BE (panel A,F), Toxic Units (B,G), Loading (C,H), Total PAH (D,I), and TPH (E,J) for both daphnid (filled, left column) and mysid (open, right column) exposures. Chemically dispersed (**RED circles**), physically dispersed (**BLUE squares**), and passively dosed (**GREEN diamonds**)

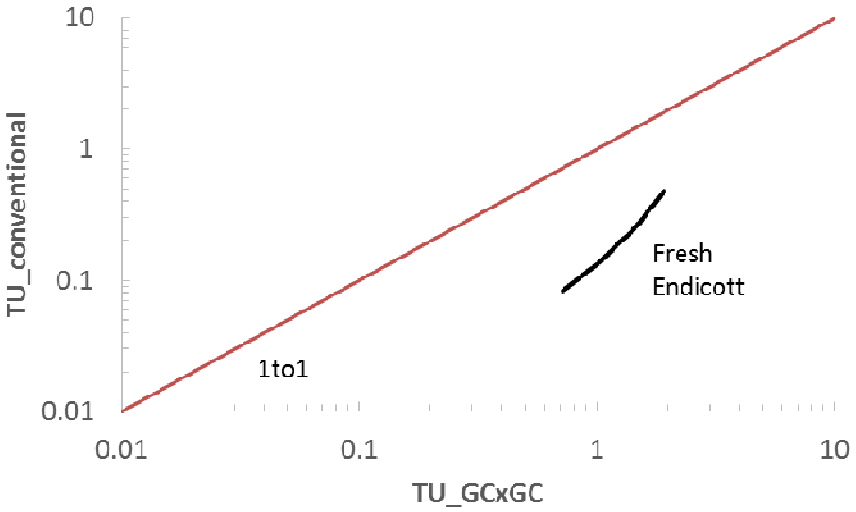

Figure B.5. Comparing TUs based on conventional (TU_conventional) analytical measurements (e.g., VOC, PAH, SHC) to TUs based on comprehensive (TU_GCxGC) analytical characterization (GCxGC). See Methods and Supplementary Information spreadsheet for data. The red line is the 1-to-1 for reference indicating perfect agreement. The black line represents the TU predictions for the loadings of fresh Endicott oil used in the present study. The TUs based on conventional analytical systematically under-predicts TUs based on comprehensive analytical. All TUs are normalzed to *D. magna.*

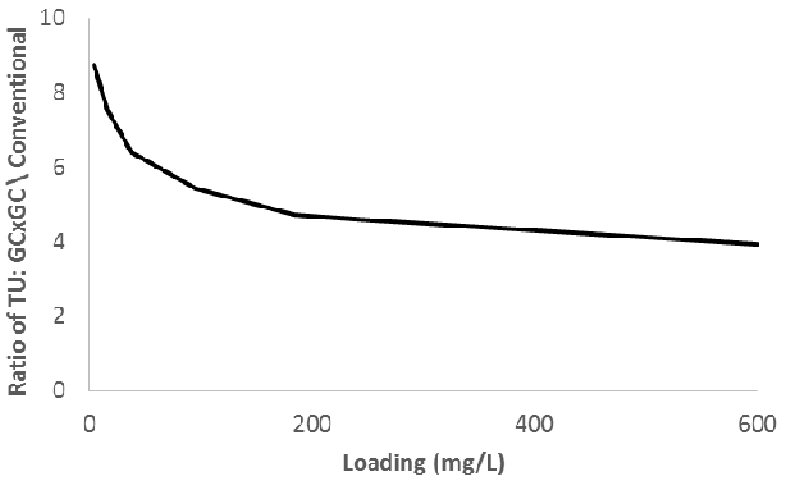

Figure B.6. Plot of the ratio of TU_GCxGC to TU_Conventional vs substance loading. This indicates that TUs based on conventional analytical are under-predicted by approximately 10-fold at loadings < 10 mg/L. At higher loadings (>10 mg/L), the ratio is closer to 5-fold. This is presented only for the range of loadings of fresh Endicott used in the present study. All TUs are normalized to *D. magna.*

Table B.1. Critical effect levels for selected dose metrics

		Daphnid LC50	Mysid LC50
TU_GCxGC	CEWAF	1.4	3.6
	PDWAF	1.9	2.9
	PsvWAF	1.7	4.7
	Average	**1.7**	**3.8**
	Relative std. dev.(RSD)	**0.12**	**0.20**
TU_Conventional	CEWAF	0.26	0.42
	PDWAF	0.20	0.96
	PsvWAF	0.37	0.42
	Average	**0.3**	**0.6**
	RSD	**0.25**	**0.4**
BE (mmol/L PDMS)	CEWAF	14	5.5
	PDWAF	25	3.8
	PsvWAF	19	6.5
	Average	**19**	**5.3**
	RSD	**0.23**	**0.21**
Loading (mg/L)	CEWAF	62	14
	PDWAF	560	5.2
	PsvWAF	320	63
	Average	**310**	**27**
	RSD	**0.65**	**0.93**
TPAH (µg/L)	CEWAF	320	61
	PDWAF	680	45
	PsvWAF	520	120
	Average	**510**	**75**
	RSD	**0.29**	**0.43**
TPH (µg/L)	CEWAF	2800	420
	PDWAF	2520	150
	PsvWAF	1500	690
	Average	**2300**	**420**
	RSD	**0.25**	**0.52**

Table B.2. GCxGC on Endicott

C No.	nP	isoP	N	2N	pN	mo-A	nMoa	di-A	nDia	PAH
6	0.00%	0.00%	0.00%	0.00%	0.00%	0.00%	0.00%	0.00%	0.00%	0.00%
7	0.27%	0.09%	0.07%	0.00%	0.00%	0.76%	0.00%	0.00%	0.00%	0.00%
8	0.47%	0.29%	0.13%	0.00%	0.00%	0.49%	0.00%	0.00%	0.00%	0.00%
9	0.50%	0.67%	0.63%	0.00%	0.00%	1.26%	0.05%	0.00%	0.00%	0.00%
10	0.57%	0.64%	1.00%	0.17%	0.00%	0.56%	0.22%	0.20%	0.00%	0.00%
11	0.55%	0.62%	0.74%	0.31%	0.00%	0.46%	0.29%	0.64%	0.00%	0.00%
12	0.54%	0.58%	0.69%	0.46%	0.00%	0.44%	0.35%	0.94%	0.02%	0.00%
13	0.54%	0.71%	0.81%	0.53%	0.00%	0.50%	0.46%	0.72%	0.12%	0.00%
14	0.54%	0.68%	0.84%	0.48%	0.00%	0.62%	0.53%	0.67%	0.35%	0.11%
15	0.50%	0.62%	0.88%	0.40%	0.00%	0.60%	0.48%	0.55%	0.44%	0.39%
16	0.44%	0.55%	0.80%	0.34%	0.00%	0.46%	0.44%	0.47%	0.39%	0.60%
17	0.72%	0.66%	0.82%	0.29%	0.00%	0.51%	0.42%	0.44%	0.39%	0.65%
18	0.53%	0.54%	0.84%	0.27%	0.00%	0.45%	0.52%	0.30%	0.43%	0.60%
19	0.24%	0.60%	0.79%	0.30%	0.00%	0.40%	0.47%	0.31%	0.36%	0.74%
20	0.41%	0.66%	0.80%	0.29%	0.00%	0.42%	0.45%	0.25%	0.33%	1.02%
21	0.44%	0.45%	0.68%	0.23%	0.00%	0.40%	0.48%	0.26%	0.27%	1.04%
22	0.44%	0.42%	0.60%	0.19%	0.25%	0.40%	0.43%	0.28%	0.20%	1.00%
23	0.44%	0.42%	0.61%	0.17%	0.23%	0.41%	0.36%	0.27%	0.17%	1.04%
24	0.44%	0.37%	0.52%	0.11%	0.27%	0.42%	0.39%	0.30%	0.09%	0.65%
25	0.40%	0.37%	0.51%	0.12%	0.33%	0.36%	0.42%	0.30%	0.04%	0.49%
26	0.38%	0.35%	0.47%	0.11%	0.37%	0.32%	0.13%	0.24%	0.02%	0.39%
27	0.30%	0.34%	0.42%	0.08%	0.36%	0.32%	0.14%	0.15%	0.01%	0.40%
28	0.25%	0.30%	0.40%	0.09%	0.36%	0.28%	0.14%	0.10%	0.02%	0.40%
29	0.25%	0.28%	0.36%	0.08%	0.38%	0.27%	0.15%	0.06%	0.02%	0.35%
30	0.18%	0.26%	0.33%	0.07%	0.37%	0.24%	0.11%	0.05%	0.01%	0.29%
31	0.08%	0.24%	0.34%	0.07%	0.37%	0.24%	0.06%	0.07%	0.01%	0.27%
32	0.12%	0.30%	0.29%	0.06%	0.36%	0.21%	0.02%	0.09%	0.02%	0.22%
33	0.10%	0.21%	0.28%	0.07%	0.36%	0.18%	0.07%	0.10%	0.01%	0.20%
34	0.06%	0.20%	0.23%	0.06%	0.33%	0.17%	0.20%	0.15%	0.01%	0.17%
35	0.05%	0.20%	0.25%	0.07%	0.34%	0.17%	0.17%	0.13%	0.04%	0.11%
36	0.03%	0.17%	0.20%	0.06%	0.30%	0.15%	0.16%	0.13%	0.08%	0.07%
37	0.05%	0.15%	0.18%	0.06%	0.29%	0.14%	0.15%	0.13%	0.09%	0.00%

Table B.3. PAH in oil and CEWAF

Chemical	Endicott	CEWAF				
	mg/kg	Ctl1	L1.38 mg/L	L2 96 mg/L	L3 240 mg/L	L4 600 mg/L
Naphthalene	1.02E+03	3.90E-01	4.11E+01	8.45E+01	1.85E+02	2.46E+02
C1-Naphthalene	2.17E+03	1.00E-20	1.23E+02	1.99E+02	3.08E+02	3.66E+02
C2-Naphthalenes	2.36E+03	6.09E-03	2.25E+01	3.07E+01	4.28E+01	5.57E+01
C3-Naphthalenes	1.61E+03	5.20E-03	6.67E+00	8.67E+00	1.18E+01	1.52E+01
C4-Naphthalenes	7.98E+02	1.00E-20	1.55E+00	2.16E+00	3.30E+00	4.70E+00
Biphenyl	3.42E+02	2.05E-03	5.99E+00	9.67E+00	1.30E+01	1.37E+01
Dibenzofuran	1.52E+02	1.61E-03	2.20E+00	3.33E+00	4.45E+00	4.85E+00
Acenaphthylene	8.93E+00	5.74E-04	3.85E-02	4.60E-02	6.45E-02	8.59E-02
Acenaphthene	3.60E+01	5.84E-04	3.85E-01	5.32E-01	6.96E-01	7.91E-01
Fluorene	1.42E+02	1.90E-03	1.96E+00	2.80E+00	3.60E+00	3.85E+00
C1-Fluorenes	3.05E+02	1.00E-20	1.81E+00	2.32E+00	3.11E+00	3.70E+00
C2-Fluorenes	4.33E+02	1.00E-20	9.16E-01	1.23E+00	1.90E+00	2.59E+00
C3-Fluorenes	3.91E+02	1.00E-20	4.48E-01	6.38E-01	1.00E+00	1.74E+00
Anthracene	0.00E+00	3.77E-04	9.28E-03	1.26E-02	3.20E-02	3.24E-02
Phenanthrene	3.70E+02	5.78E-03	2.98E+00	3.91E+00	5.38E+00	6.27E+00
C1-Phenanthrenes	7.57E+02	2.13E-03	2.26E+00	3.06E+00	4.65E+00	6.06E+00
C2-Phenanthrenes	7.98E+02	3.04E-03	1.10E+00	1.57E+00	2.44E+00	3.76E+00
C3-Phenanthrenes	5.27E+02	1.00E-20	3.92E-01	5.35E-01	9.08E-01	1.54E+00
C4-Phenanthrenes	2.08E+02	1.00E-20	1.31E-01	1.67E-01	2.35E-01	4.21E-01
Retene	0.00E+00	1.00E-20	1.00E-20	1.00E-20	1.00E-20	1.00E-20
Dibenzothiophene	3.33E+02	7.43E-04	2.69E+00	3.54E+00	4.79E+00	5.50E+00
C1-Dibenzothiophenes	5.90E+02	1.04E-03	1.73E+00	2.32E+00	3.53E+00	4.63E+00
C2-Dibenzothiophenes	6.88E+02	2.75E-03	8.26E-01	1.20E+00	1.89E+00	2.92E+00
C3-Dibenzothiophenes	5.54E+02	1.00E-20	3.80E-01	5.29E-01	8.49E-01	1.60E+00
C4-Dibenzothiophenes	2.94E+02	1.00E-20	2.01E-01	2.98E-01	4.67E-01	1.61E+00
Benzo(b)fluorene	0.00E+00	1.00E-20	1.00E-20	1.00E-20	1.00E-20	1.00E-20
Fluoranthene	6.22E+00	1.73E-03	1.61E-02	2.26E-02	3.32E-02	4.92E-02
Pyrene	2.05E+01	1.12E-02	4.14E-02	5.81E-02	8.64E-02	1.33E-01
C1-Fluoranthenes/Pyrenes	1.25E+02	1.00E-20	1.44E-01	2.07E-01	3.02E-01	4.48E-01
C2-Fluoranthenes/Pyrenes	2.02E+02	1.00E-20	1.56E-01	2.11E-01	3.18E-01	5.41E-01
C3-Fluoranthenes/Pyrenes	2.34E+02	1.00E-20	1.20E-01	1.52E-01	2.49E-01	4.68E-01
C4-Fluoranthenes/Pyrenes	1.84E+02	1.00E-20	6.82E-02	8.93E-02	1.39E-01	2.90E-01
Naphthobenzothiophenes	9.90E+01	2.86E-04	9.68E-02	1.41E-01	2.02E-01	3.27E-01
C1-Naphthobenzothiophenes	2.61E+02	1.00E-20	1.44E-01	1.85E-01	2.70E-01	5.48E-01
C2-Naphthobenzothiophenes	3.41E+02	1.00E-20	1.07E-01	1.35E-01	2.29E-01	5.47E-01
C3-Naphthobenzothiophenes	2.43E+02	1.00E-20	4.74E-02	5.21E-02	7.20E-02	2.12E-01

Table continued						
C4-Naphthobenzothiophenes	1.58E+02	1.00E-20	3.01E-02	4.19E-02	5.67E-02	1.55E-01
Benz[a]anthracene	3.10E+00	5.05E-04	4.15E-03	4.83E-03	7.00E-03	1.05E-02
Chrysene	7.09E+01	1.36E-03	8.99E-02	1.22E-01	1.68E-01	2.50E-01
C1-Chrysenes	1.19E+02	1.00E-20	8.94E-02	1.19E-01	1.54E-01	2.86E-01
C2-Chrysenes	1.49E+02	1.00E-20	7.94E-02	1.05E-01	1.26E-01	2.49E-01
C3-Chrysenes	1.74E+02	1.00E-20	8.79E-02	1.15E-01	1.43E-01	3.32E-01
C4-Chrysenes	1.07E+02	1.00E-20	1.00E-20	1.00E-20	1.00E-20	1.66E-01
Benzo[b]fluoranthene	1.10E+01	6.77E-04	6.98E-03	8.22E-03	1.16E-02	2.38E-02
Benzo[k]fluoranthene	0.00E+00	5.54E-04	1.00E-20	1.00E-20	1.00E-20	1.00E-20
Benzo[a]fluoranthene	0.00E+00	1.00E-20	1.00E-20	1.00E-20	1.00E-20	1.00E-20
Benzo[e]pyrene	2.17E+01	1.00E-20	1.37E-02	1.78E-02	2.33E-02	4.71E-02
Benzo[a]pyrene	2.74E+00	1.00E-20	1.32E-03	1.56E-03	1.94E-03	4.16E-03
Perylene	2.11E+00	1.00E-20	1.00E-20	1.00E-20	1.00E-20	1.00E-20
Indeno[1,2,3-cd]pyrene	1.21E+00	5.38E-04	1.00E-20	1.00E-20	1.44E-03	2.98E-03
Dibenz[ah]anthracene	1.92E+00	1.00E-20	8.84E-04	8.83E-04	1.88E-03	2.97E-03
Benzo[g,h,i]perylene	6.77E+00	4.26E-04	2.74E-03	3.33E-03	4.09E-03	9.44E-03

Table B.4. BE measurements, top table Dmagna results

Loading (mg/L)	Chemically Dispersed (CD) (1:10 DOR) 30-Oct-13	Loading (mg/L)	Physically Dispersed (PD) 5-Nov-13	Passively Dosed (PSVD) 4-Dec-13	Chemically Dispersed (CD) (1:10 DOR) 11-Dec-13
0 (control)	nd	0 (control)	nd	nd	nd
4	3.05	38	11.4	8.54	11.2
	2.51		12.2	8.86	9.81
mean	**2.78**	mean	**11.8**	**8.70**	**10.5**
20	8.79	96	19.1	12.5	20.2
	9.28		19.6	13.2	18.5
mean	**9.04**	mean	**19.4**	**12.9**	**19.4**
100	19.9	240	23.2	19.0	24.2
	20.8		20.8	19.2	26.9
mean	**20.4**	mean	**22.0**	**19.1**	**25.6**
500	39.8	600	30.6	25.0	33.7
	41.7		29.5	23.3	34.1
mean	**40.8**	mean	**30.1**	**24.2**	**33.9**

Table B.4 continued

Seawater tests with mysids **Fresh Endicott**

Loading (mg/L)	Chemically Dispersed (CD) (1:20 DOR)		Passively Dosed (PSVD)		Physically Dispersed (PD)	
	30-Apr-14	2-May-14	4-Jun-14	6-Jun-14	24-Jun-14	27-Jun-14
	Day 0 (new)	Day 2 (old)	Day 0 (new)	Day 2 (old)	Day 0 (new)	Day 2 (old)
0 (control)	nd	nd	nd	nd	nd	nd
5	3.38	2.90	1.23	0.986	3.59	2.78
	3.59	2.67	1.25	1.30	4.23	4.26
mean	**3.49**	**2.79**	**1.24**	**1.14**	**3.91**	**3.52**
17	7.57	5.77	3.55	3.12	7.79	6.62
	7.35	5.12	3.48	3.82	7.55	7.16
mean	**7.46**	**5.45**	**3.52**	**3.47**	**7.67**	**6.89**
56	14.6	9.27	7.32	5.40	13.0	10.8
	15.6	9.72	6.97	5.28	13.0	10.4
mean	**15.1**	**9.50**	**7.15**	**5.34**	**13.0**	**10.6**
185	27.9	21.0	14.3	9.75	19.7	15.0
	25.5	20.8	13.4	11.4	18.9	15.3
mean	**26.7**	**20.9**	**13.9**	**10.6**	**19.3**	**15.2**

Table B.5. Dissolved PAH measurements

Freshwater testing with daphnids

fresh crude oil

Chemical	4 mg/L		20 mg/L		100 mg/L		500 mg/L	
	rep 1	rep 2	rep 1	rep 2	rep 1	rep 2	rep 1	rep 2
naphthalene	3.21	3.25	24.2	24.3	108	110	249	244
acenaphthylene	0.233	0.242	0.632	0.657	0.950	0.944	1.11	1.02
acenaphthene	0.067	0.076	0.200	0.216	0.356	0.379	0.455	0.428
fluorene	0.612	0.617	2.53	2.62	3.56	3.65	4.63	4.41
me-fluorene	0.832	0.859	1.85	1.89	2.28	2.33	2.41	2.28
phenanthrene	1.42	1.41	4.10	4.28	6.90	6.85	9.56	9.68
anthracene	nd	nd	nd	nd	nd	0.037	nd	nd
fluoranthene	nd	nd	nd	nd	0.027	0.025	0.043	nd
pyrene	nd	nd	nd	nd	nd	nd	nd	nd
me-pyrene	nd	nd	0.010	0.013	nd	nd	nd	0.138
benzo[a]anthracene	nd	nd	nd	nd	nd	nd	nd	nd
chrysene	0.038	0.035	0.057	0.060	0.09	0.094	0.083	0.078
benzo[b&k]fluoranthene	nd	nd	nd	nd	nd	nd	nd	nd
benzo[a]pyrene	0.02	nd	nd	nd	nd	nd	nd	nd
indeno(1,2,3cd) pyrene	0.052	0.041	0.040	0.043	0.063	0.062	0.090	0.071
dibenzo(a,h)anthracene	0.039	0.031	0.018	0.015	0.050	0.053	0.092	0.064
benzo(ghi)perylene	0.037	0.024	nd	0.018	0.040	0.046	nd	nd

Table Continued. **Seawater testing with mysids**

fresh crude oil

	5 mg/L		17 mg/L		56 mg/L		185 mg/L	
	rep 1	rep 2	rep 1	rep 2	rep 1	rep 2	rep 1	rep 2
naphthalene	4.11	4.00	15.7	17.5	54.2	61.1	145	153
acenaphthylene	0.171	0.097	0.229	0.255	0.308	0.831	0.397	1.02
acenaphthene	0.064	0.076	0.179	0.185	0.267	0.302	0.440	0.462
fluorene	0.989	0.979	1.97	1.91	2.93	3.24	4.37	4.42
me-fluorene	0.709	0.631	0.977	0.981	1.27	1.38	1.68	1.93
phenanthrene	1.04	1.10	2.16	2.19	2.92	3.18	6.22	6.42
anthracene	0.008	0.013	0.012	0.014	0.009	0.010	nd	0.021
fluoranthene	nd	nd	nd	nd	nd	nd	nd	0.019
pyrene	nd	nd	0.027	0.019	0.023	0.029	0.032	0.054
me-pyrene	nd	nd	nd	nd	nd	nd	0.085	0.082
benzo[a]anthracene	nd	nd	nd	nd	nd	nd	nd	nd
chrysene	0.020	0.035	0.021	0.036	0.020	0.020	0.046	0.048
benzo[b&k]fluoranthene	nd	nd	nd	nd	nd	nd	nd	nd
benzo[a]pyrene	nd	nd	nd	nd	nd	nd	nd	nd
indeno(1,2,3cd) pyrene	nd	nd	nd	nd	nd	0.023	0.035	0.033
dibenzo(a,h)anthracene	nd	nd	nd	nd	nd	nd	nd	nd
benzo(ghi)perylene	nd	nd	nd	nd	nd	nd	0.036	0.053

Table B.6. Effects data

Biological results following oil exposures
mortality at 48 h with intermediate observations

Freshwater tests with *Daphnia magna*
fresh crude oil

Treatment Level	Obs. (Hours)	CEWAF	PDWAF	PsvWAF
		Mortality (%)	Mortality (%)	Mortality (%)
Control	2	0	0	0
	6	0	0	0
	24	0	0	0
	48	0	0	0
38 mg/L	2	0	0	0
	6	0	0	0
	24	0	0	0
	48	25	0	20
96 mg/L	2	0	0	0
	6	0	0	0
	24	0	0	0
	48	60	5	20
240 mg/L	2	0	0	0
	6	0	0	0
	24	0	0	0
	48	100	35	45
600 mg/L	2	0	0	0
	6	0	0	0
	24	20	5	0
	48	100	80	80

Table B.6 continued
Saltwater tests with *Mysidopsis bahia*
Fresh crude oil

Treatment Level	Obs. (Hours)	CEWAF	PDWAF	PsvWAF
		Mortality (%)	Mortality (%)	Mortality (%)
Control	2	0	0	0
	17	0	0	0
	24	0	0	0
	48	0	0	0
5 mg/L	2	0	0	0
	17	0	0	0
	24	0	0	0
	48	15	35	0
17 mg/L	2	0	0	0
	17	0	0	0
	24	5	10	0
	48	65	100	15
56 mg/L	2	0	0	0
	17	25	10	0
	24	25	80	0
	48	100	100	40
185 mg/L	2	0	0	0
	17	80	80	40
	24	80	100	90
	48	100	100	100

Appendix C

CHAPTER 3 SUPPLEMENTAL INFORMATION

Table C.1. Effects data

Species	t_obs (d)	Survival (fraction)	Cw (mg/L)	Chemical	Source
D. rerio	2	0.5	79	OHP	Butler2016
D. rerio	4	0.4	79	OHP	Butler2016
D. rerio	2	0.7	242	OHP	Butler2016
D. rerio	4	0.1	242	OHP	Butler2016
D. rerio	2	0.15	682	OHP	Butler2016
D. rerio	4	0	682	OHP	Butler2016
D. rerio	0	1	32	PHE	Butler2016
D. rerio	4	0.94	32	PHE	Butler2016
D. rerio	0	1	105	PHE	Butler2016
D. rerio	3	0.94	105	PHE	Butler2016
D. rerio	4	0.75	105	PHE	Butler2016
D. rerio	0	1	423	PHE	Butler2016
D. rerio	2	0.94	423	PHE	Butler2016
D. rerio	3	0.88	423	PHE	Butler2016
D. rerio	4	0.59	423	PHE	Butler2016
D. rerio	2	1	36	PHE	Butler2016
D. rerio	4	1	36	PHE	Butler2016
D. rerio	2	1	70	PHE	Butler2016
D. rerio	4	1	70	PHE	Butler2016
D. rerio	2	1	159	PHE	Butler2016
D. rerio	4	1	159	PHE	Butler2016
D. rerio	2	0.4	415	PHE	Butler2016
D. rerio	4	0.4	415	PHE	Butler2016
D. rerio	4	0	948	PHE	Butler2016

Table continued

D. rerio	0	1	60	meNAP	Butler2016
D. rerio	0	1	277	meNAP	Butler2016
D. rerio	3	0.95	277	meNAP	Butler2016
D. rerio	0	1	1227	meNAP	Butler2016
D. rerio	2	0.44	1227	meNAP	Butler2016
D. rerio	3	0.29	1227	meNAP	Butler2016
D. rerio	4	0.24	1227	meNAP	Butler2016
D. rerio	2	1	118	meNAP	Butler2016
D. rerio	4	1	118	meNAP	Butler2016
D. rerio	2	1	204	meNAP	Butler2016
D. rerio	4	1	204	meNAP	Butler2016
D. rerio	2	1	401	meNAP	Butler2016
D. rerio	4	1	401	meNAP	Butler2016
D. rerio	2	1	913	meNAP	Butler2016
D. rerio	4	0.9	913	meNAP	Butler2016
D. rerio	2	1	1716	meNAP	Butler2016
D. rerio	4	0.55	1716	meNAP	Butler2016
D. rerio	2	1	419	NAP	Butler2016
D. rerio	4	1	419	NAP	Butler2016
D. rerio	2	1	875	NAP	Butler2016
D. rerio	4	1	875	NAP	Butler2016
D. rerio	2	1	2183	NAP	Butler2016
D. rerio	4	1	2183	NAP	Butler2016
D. rerio	2	0.85	5401	NAP	Butler2016
D. rerio	4	0.85	5401	NAP	Butler2016
D. rerio	2	0	18059	NAP	Butler2016
D. rerio	4	0	18059	NAP	Butler2016
D. rerio	2	1	230	BPH	Butler2016
D. rerio	4	1	230	BPH	Butler2016
D. rerio	2	1	338	BPH	Butler2016
D. rerio	4	0.9	338	BPH	Butler2016
D. rerio	2	0.9	955	BPH	Butler2016
D. rerio	4	0.75	955	BPH	Butler2016
D. rerio	2	0.95	1647	BPH	Butler2016
D. rerio	4	0.45	1647	BPH	Butler2016
D. rerio	2	0	3882	BPH	Butler2016
D. rerio	4	0	3882	BPH	Butler2016
D. rerio	2	1	9	PYR	Butler2016

Table continued

D. rerio	4	1	9	PYR	Butler2016
D. rerio	2	1	18	PYR	Butler2016
D. rerio	4	1	18	PYR	Butler2016
D. rerio	2	1	35	PYR	Butler2016
D. rerio	4	0.95	35	PYR	Butler2016
D. rerio	2	0.95	70	PYR	Butler2016
D. rerio	4	0.9	70	PYR	Butler2016
D. rerio	2	1	140	PYR	Butler2016
D. rerio	4	0.6	140	PYR	Butler2016
O. mykiss	0	1	0.01	PHE_5deg	EMBSI2006
O. mykiss	0.010417	1	0.01	PHE_5deg	EMBSI2006
O. mykiss	0.03125	1	0.01	PHE_5deg	EMBSI2006
O. mykiss	0.052083	1	0.01	PHE_5deg	EMBSI2006
O. mykiss	0.072917	1	0.01	PHE_5deg	EMBSI2006
O. mykiss	0.09375	1	0.01	PHE_5deg	EMBSI2006
O. mykiss	0.135417	1	0.01	PHE_5deg	EMBSI2006
O. mykiss	0.177083	1	0.01	PHE_5deg	EMBSI2006
O. mykiss	1	1	0.01	PHE_5deg	EMBSI2006
O. mykiss	2	1	0.01	PHE_5deg	EMBSI2006
O. mykiss	3	1	0.01	PHE_5deg	EMBSI2006
O. mykiss	4	1	0.01	PHE_5deg	EMBSI2006
O. mykiss	0	1	0.2	PHE_5deg	EMBSI2006
O. mykiss	0.010417	1	0.2	PHE_5deg	EMBSI2006
O. mykiss	0.03125	1	0.2	PHE_5deg	EMBSI2006
O. mykiss	0.052083	1	0.2	PHE_5deg	EMBSI2006
O. mykiss	0.072917	1	0.2	PHE_5deg	EMBSI2006
O. mykiss	0.09375	1	0.2	PHE_5deg	EMBSI2006
O. mykiss	0.135417	1	0.2	PHE_5deg	EMBSI2006
O. mykiss	0.177083	1	0.2	PHE_5deg	EMBSI2006
O. mykiss	1	1	0.2	PHE_5deg	EMBSI2006
O. mykiss	2	0.75	0.2	PHE_5deg	EMBSI2006
O. mykiss	3	0	0.2	PHE_5deg	EMBSI2006
O. mykiss	4	0	0.2	PHE_5deg	EMBSI2006
O. mykiss	0	1	0.56	PHE_5deg	EMBSI2006
O. mykiss	0.010417	1	0.56	PHE_5deg	EMBSI2006
O. mykiss	0.03125	1	0.56	PHE_5deg	EMBSI2006
O. mykiss	0.052083	1	0.56	PHE_5deg	EMBSI2006
O. mykiss	0.072917	1	0.56	PHE_5deg	EMBSI2006

Table continued

O. mykiss	0.09375	1	0.56	PHE_5deg	EMBSI2006
O. mykiss	0.135417	1	0.56	PHE_5deg	EMBSI2006
O. mykiss	0.177083	1	0.56	PHE_5deg	EMBSI2006
O. mykiss	1	0	0.56	PHE_5deg	EMBSI2006
O. mykiss	2	0	0.56	PHE_5deg	EMBSI2006
O. mykiss	3	0	0.56	PHE_5deg	EMBSI2006
O. mykiss	4	0	0.56	PHE_5deg	EMBSI2006
O. mykiss	0	1	0.01	PHE_18deg	EMBSI2006
O. mykiss	0.010417	1	0.01	PHE_18deg	EMBSI2006
O. mykiss	0.03125	1	0.01	PHE_18deg	EMBSI2006
O. mykiss	0.052083	1	0.01	PHE_18deg	EMBSI2006
O. mykiss	0.072917	1	0.01	PHE_18deg	EMBSI2006
O. mykiss	0.09375	1	0.01	PHE_18deg	EMBSI2006
O. mykiss	0.135417	1	0.01	PHE_18deg	EMBSI2006
O. mykiss	0.177083	1	0.01	PHE_18deg	EMBSI2006
O. mykiss	1	1	0.01	PHE_18deg	EMBSI2006
O. mykiss	2	1	0.01	PHE_18deg	EMBSI2006
O. mykiss	3	1	0.01	PHE_18deg	EMBSI2006
O. mykiss	4	1	0.01	PHE_18deg	EMBSI2006
O. mykiss	0	1	0.2	PHE_18deg	EMBSI2006
O. mykiss	0.010417	1	0.2	PHE_18deg	EMBSI2006
O. mykiss	0.03125	1	0.2	PHE_18deg	EMBSI2006
O. mykiss	0.052083	1	0.2	PHE_18deg	EMBSI2006
O. mykiss	0.072917	1	0.2	PHE_18deg	EMBSI2006
O. mykiss	0.09375	1	0.2	PHE_18deg	EMBSI2006
O. mykiss	0.135417	1	0.2	PHE_18deg	EMBSI2006
O. mykiss	0.177083	1	0.2	PHE_18deg	EMBSI2006
O. mykiss	1	0.875	0.2	PHE_18deg	EMBSI2006
O. mykiss	2	0.75	0.2	PHE_18deg	EMBSI2006
O. mykiss	3	0.625	0.2	PHE_18deg	EMBSI2006
O. mykiss	4	0.5	0.2	PHE_18deg	EMBSI2006
O. mykiss	0	1	0.56	PHE_18deg	EMBSI2006
O. mykiss	0.010417	1	0.56	PHE_18deg	EMBSI2006
O. mykiss	0.03125	1	0.56	PHE_18deg	EMBSI2006
O. mykiss	0.052083	1	0.56	PHE_18deg	EMBSI2006
O. mykiss	0.072917	1	0.56	PHE_18deg	EMBSI2006
O. mykiss	0.09375	0.875	0.56	PHE_18deg	EMBSI2006
O. mykiss	0.135417	0.75	0.56	PHE_18deg	EMBSI2006

Table continued

O. mykiss	0.177083	0.75	0.56	PHE_18deg	EMBSI2006
O. mykiss	1	0	0.56	PHE_18deg	EMBSI2006
O. mykiss	2	0	0.56	PHE_18deg	EMBSI2006
O. mykiss	3	0	0.56	PHE_18deg	EMBSI2006
O. mykiss	4	0	0.56	PHE_18deg	EMBSI2006
O. mykiss	0	1	0.001	meNAP_5deg	EMBSI2006
O. mykiss	0.010417	1	0.001	meNAP_5deg	EMBSI2006
O. mykiss	0.03125	1	0.001	meNAP_5deg	EMBSI2006
O. mykiss	0.041667	1	0.001	meNAP_5deg	EMBSI2006
O. mykiss	0.052083	1	0.001	meNAP_5deg	EMBSI2006
O. mykiss	0.072917	1	0.001	meNAP_5deg	EMBSI2006
O. mykiss	0.114583	1	0.001	meNAP_5deg	EMBSI2006
O. mykiss	0.15625	1	0.001	meNAP_5deg	EMBSI2006
O. mykiss	0.197917	1	0.001	meNAP_5deg	EMBSI2006
O. mykiss	1	1	0.001	meNAP_5deg	EMBSI2006
O. mykiss	2	1	0.001	meNAP_5deg	EMBSI2006
O. mykiss	3	1	0.001	meNAP_5deg	EMBSI2006
O. mykiss	4	1	0.001	meNAP_5deg	EMBSI2006
O. mykiss	0	1	0.111	meNAP_5deg	EMBSI2006
O. mykiss	0.010417	1	0.111	meNAP_5deg	EMBSI2006
O. mykiss	0.03125	1	0.111	meNAP_5deg	EMBSI2006
O. mykiss	0.041667	1	0.111	meNAP_5deg	EMBSI2006
O. mykiss	0.052083	1	0.111	meNAP_5deg	EMBSI2006
O. mykiss	0.072917	1	0.111	meNAP_5deg	EMBSI2006
O. mykiss	0.114583	1	0.111	meNAP_5deg	EMBSI2006
O. mykiss	0.15625	1	0.111	meNAP_5deg	EMBSI2006
O. mykiss	0.197917	1	0.111	meNAP_5deg	EMBSI2006
O. mykiss	1	1	0.111	meNAP_5deg	EMBSI2006
O. mykiss	2	1	0.111	meNAP_5deg	EMBSI2006
O. mykiss	3	1	0.111	meNAP_5deg	EMBSI2006
O. mykiss	4	0.625	0.111	meNAP_5deg	EMBSI2006
O. mykiss	0	1	0.361	meNAP_5deg	EMBSI2006
O. mykiss	0.010417	1	0.361	meNAP_5deg	EMBSI2006
O. mykiss	0.03125	1	0.361	meNAP_5deg	EMBSI2006
O. mykiss	0.041667	1	0.361	meNAP_5deg	EMBSI2006
O. mykiss	0.052083	1	0.361	meNAP_5deg	EMBSI2006
O. mykiss	0.072917	1	0.361	meNAP_5deg	EMBSI2006
O. mykiss	0.114583	1	0.361	meNAP_5deg	EMBSI2006

Table continued

O. mykiss	0.15625	1	0.361	meNAP_5deg	EMBSI2006
O. mykiss	0.197917	1	0.361	meNAP_5deg	EMBSI2006
O. mykiss	1	1	0.361	meNAP_5deg	EMBSI2006
O. mykiss	2	1	0.361	meNAP_5deg	EMBSI2006
O. mykiss	3	1	0.361	meNAP_5deg	EMBSI2006
O. mykiss	4	0.875	0.361	meNAP_5deg	EMBSI2006
O. mykiss	0	1	3.06	meNAP_5deg	EMBSI2006
O. mykiss	0.010417	1	3.06	meNAP_5deg	EMBSI2006
O. mykiss	0.03125	1	3.06	meNAP_5deg	EMBSI2006
O. mykiss	0.041667	1	3.06	meNAP_5deg	EMBSI2006
O. mykiss	0.052083	1	3.06	meNAP_5deg	EMBSI2006
O. mykiss	0.072917	1	3.06	meNAP_5deg	EMBSI2006
O. mykiss	0.114583	1	3.06	meNAP_5deg	EMBSI2006
O. mykiss	0.15625	1	3.06	meNAP_5deg	EMBSI2006
O. mykiss	0.197917	1	3.06	meNAP_5deg	EMBSI2006
O. mykiss	1	0	3.06	meNAP_5deg	EMBSI2006
O. mykiss	2	0	3.06	meNAP_5deg	EMBSI2006
O. mykiss	3	0	3.06	meNAP_5deg	EMBSI2006
O. mykiss	4	0	3.06	meNAP_5deg	EMBSI2006
O. mykiss	0	1	17.9	meNAP_5deg	EMBSI2006
O. mykiss	0.010417	1	17.9	meNAP_5deg	EMBSI2006
O. mykiss	0.03125	0.625	17.9	meNAP_5deg	EMBSI2006
O. mykiss	0.041667	0.625	17.9	meNAP_5deg	EMBSI2006
O. mykiss	0.052083	0.625	17.9	meNAP_5deg	EMBSI2006
O. mykiss	0.072917	0.625	17.9	meNAP_5deg	EMBSI2006
O. mykiss	0.114583	0.625	17.9	meNAP_5deg	EMBSI2006
O. mykiss	0.15625	0.625	17.9	meNAP_5deg	EMBSI2006
O. mykiss	0.197917	0	17.9	meNAP_5deg	EMBSI2006
O. mykiss	1	0	17.9	meNAP_5deg	EMBSI2006
O. mykiss	2	0	17.9	meNAP_5deg	EMBSI2006
O. mykiss	3	0	17.9	meNAP_5deg	EMBSI2006
O. mykiss	4	0	17.9	meNAP_5deg	EMBSI2006
O. mykiss	0	1	0.001	meNAP_18deg	EMBSI2006
O. mykiss	0.010417	1	0.001	meNAP_18deg	EMBSI2006
O. mykiss	0.03125	1	0.001	meNAP_18deg	EMBSI2006
O. mykiss	0.041667	1	0.001	meNAP_18deg	EMBSI2006
O. mykiss	0.052083	1	0.001	meNAP_18deg	EMBSI2006
O. mykiss	0.072917	1	0.001	meNAP_18deg	EMBSI2006

Table continued

O. mykiss	0.114583	1	0.001	meNAP_18deg	EMBSI2006
O. mykiss	0.15625	1	0.001	meNAP_18deg	EMBSI2006
O. mykiss	0.197917	1	0.001	meNAP_18deg	EMBSI2006
O. mykiss	1	1	0.001	meNAP_18deg	EMBSI2006
O. mykiss	2	1	0.001	meNAP_18deg	EMBSI2006
O. mykiss	3	1	0.001	meNAP_18deg	EMBSI2006
O. mykiss	4	1	0.001	meNAP_18deg	EMBSI2006
O. mykiss	0	1	0.139	meNAP_18deg	EMBSI2006
O. mykiss	0.010417	1	0.139	meNAP_18deg	EMBSI2006
O. mykiss	0.03125	1	0.139	meNAP_18deg	EMBSI2006
O. mykiss	0.041667	1	0.139	meNAP_18deg	EMBSI2006
O. mykiss	0.052083	1	0.139	meNAP_18deg	EMBSI2006
O. mykiss	0.072917	1	0.139	meNAP_18deg	EMBSI2006
O. mykiss	0.114583	1	0.139	meNAP_18deg	EMBSI2006
O. mykiss	0.15625	1	0.139	meNAP_18deg	EMBSI2006
O. mykiss	0.197917	1	0.139	meNAP_18deg	EMBSI2006
O. mykiss	1	1	0.139	meNAP_18deg	EMBSI2006
O. mykiss	2	1	0.139	meNAP_18deg	EMBSI2006
O. mykiss	3	1	0.139	meNAP_18deg	EMBSI2006
O. mykiss	4	1	0.139	meNAP_18deg	EMBSI2006
O. mykiss	0	1	0.669	meNAP_18deg	EMBSI2006
O. mykiss	0.010417	1	0.669	meNAP_18deg	EMBSI2006
O. mykiss	0.03125	1	0.669	meNAP_18deg	EMBSI2006
O. mykiss	0.041667	1	0.669	meNAP_18deg	EMBSI2006
O. mykiss	0.052083	1	0.669	meNAP_18deg	EMBSI2006
O. mykiss	0.072917	1	0.669	meNAP_18deg	EMBSI2006
O. mykiss	0.114583	1	0.669	meNAP_18deg	EMBSI2006
O. mykiss	0.15625	1	0.669	meNAP_18deg	EMBSI2006
O. mykiss	0.197917	1	0.669	meNAP_18deg	EMBSI2006
O. mykiss	1	0.75	0.669	meNAP_18deg	EMBSI2006
O. mykiss	2	0.75	0.669	meNAP_18deg	EMBSI2006
O. mykiss	3	0.75	0.669	meNAP_18deg	EMBSI2006
O. mykiss	4	0.75	0.669	meNAP_18deg	EMBSI2006
O. mykiss	0	1	2.63	meNAP_18deg	EMBSI2006
O. mykiss	0.010417	1	2.63	meNAP_18deg	EMBSI2006
O. mykiss	0.03125	1	2.63	meNAP_18deg	EMBSI2006
O. mykiss	0.041667	1	2.63	meNAP_18deg	EMBSI2006
O. mykiss	0.052083	1	2.63	meNAP_18deg	EMBSI2006

Table continued

O. mykiss	0.072917	1	2.63	meNAP_18deg	EMBSI2006
O. mykiss	0.114583	1	2.63	meNAP_18deg	EMBSI2006
O. mykiss	0.15625	1	2.63	meNAP_18deg	EMBSI2006
O. mykiss	0.197917	1	2.63	meNAP_18deg	EMBSI2006
O. mykiss	1	0	2.63	meNAP_18deg	EMBSI2006
O. mykiss	2	0	2.63	meNAP_18deg	EMBSI2006
O. mykiss	3	0	2.63	meNAP_18deg	EMBSI2006
O. mykiss	4	0	2.63	meNAP_18deg	EMBSI2006
O. mykiss	0	1	18.6	meNAP_18deg	EMBSI2006
O. mykiss	0.010417	1	18.6	meNAP_18deg	EMBSI2006
O. mykiss	0.03125	0.625	18.6	meNAP_18deg	EMBSI2006
O. mykiss	0.041667	0.625	18.6	meNAP_18deg	EMBSI2006
O. mykiss	0.052083	0.625	18.6	meNAP_18deg	EMBSI2006
O. mykiss	0.072917	0.625	18.6	meNAP_18deg	EMBSI2006
O. mykiss	0.114583	0	18.6	meNAP_18deg	EMBSI2006
O. mykiss	0.15625	0	18.6	meNAP_18deg	EMBSI2006
O. mykiss	0.197917	0	18.6	meNAP_18deg	EMBSI2006
O. mykiss	1	0	18.6	meNAP_18deg	EMBSI2006
O. mykiss	2	0	18.6	meNAP_18deg	EMBSI2006
O. mykiss	3	0	18.6	meNAP_18deg	EMBSI2006
O. mykiss	4	0	18.6	meNAP_18deg	EMBSI2006
O. mykiss	0	1	1.00E-03	XYL_5deg	EMBSI2006
O. mykiss	0.020833	1	1.00E-03	XYL_5deg	EMBSI2006
O. mykiss	0.041667	1	1.00E-03	XYL_5deg	EMBSI2006
O. mykiss	0.125	1	1.00E-03	XYL_5deg	EMBSI2006
O. mykiss	0.208333	1	1.00E-03	XYL_5deg	EMBSI2006
O. mykiss	1	1	1.00E-03	XYL_5deg	EMBSI2006
O. mykiss	2	1	1.00E-03	XYL_5deg	EMBSI2006
O. mykiss	3	1	1.00E-03	XYL_5deg	EMBSI2006
O. mykiss	4	1	1.00E-03	XYL_5deg	EMBSI2006
O. mykiss	0	1	1.81	XYL_5deg	EMBSI2006
O. mykiss	0.020833	1	1.81	XYL_5deg	EMBSI2006
O. mykiss	0.041667	1	1.81	XYL_5deg	EMBSI2006
O. mykiss	0.125	1	1.81	XYL_5deg	EMBSI2006
O. mykiss	0.208333	1	1.81	XYL_5deg	EMBSI2006
O. mykiss	1	1	1.81	XYL_5deg	EMBSI2006
O. mykiss	2	1	1.81	XYL_5deg	EMBSI2006
O. mykiss	3	1	1.81	XYL_5deg	EMBSI2006

Table continued

O. mykiss	4	1	1.81	XYL_5deg	EMBSI2006
O. mykiss	0	1	5.15	XYL_5deg	EMBSI2006
O. mykiss	0.020833	1	5.15	XYL_5deg	EMBSI2006
O. mykiss	0.041667	1	5.15	XYL_5deg	EMBSI2006
O. mykiss	0.125	1	5.15	XYL_5deg	EMBSI2006
O. mykiss	0.208333	1	5.15	XYL_5deg	EMBSI2006
O. mykiss	1	1	5.15	XYL_5deg	EMBSI2006
O. mykiss	2	0.75	5.15	XYL_5deg	EMBSI2006
O. mykiss	3	0.583333	5.15	XYL_5deg	EMBSI2006
O. mykiss	4	0.583333	5.15	XYL_5deg	EMBSI2006
O. mykiss	0	1	10.56	XYL_5deg	EMBSI2006
O. mykiss	0.020833	1	10.56	XYL_5deg	EMBSI2006
O. mykiss	0.041667	1	10.56	XYL_5deg	EMBSI2006
O. mykiss	0.125	1	10.56	XYL_5deg	EMBSI2006
O. mykiss	0.208333	0.916667	10.56	XYL_5deg	EMBSI2006
O. mykiss	1	0.416667	10.56	XYL_5deg	EMBSI2006
O. mykiss	2	0.25	10.56	XYL_5deg	EMBSI2006
O. mykiss	3	0.25	10.56	XYL_5deg	EMBSI2006
O. mykiss	4	0.25	10.56	XYL_5deg	EMBSI2006
O. mykiss	0	1	25.85	XYL_5deg	EMBSI2006
O. mykiss	0.020833	1	25.85	XYL_5deg	EMBSI2006
O. mykiss	0.041667	1	25.85	XYL_5deg	EMBSI2006
O. mykiss	0.125	0.833333	25.85	XYL_5deg	EMBSI2006
O. mykiss	0.208333	0	25.85	XYL_5deg	EMBSI2006
O. mykiss	1	0	25.85	XYL_5deg	EMBSI2006
O. mykiss	2	0	25.85	XYL_5deg	EMBSI2006
O. mykiss	3	0	25.85	XYL_5deg	EMBSI2006
O. mykiss	4	0	25.85	XYL_5deg	EMBSI2006
O. mykiss	0	1	67.65	XYL_5deg	EMBSI2006
O. mykiss	0.020833	1	67.65	XYL_5deg	EMBSI2006
O. mykiss	0.041667	0	67.65	XYL_5deg	EMBSI2006
O. mykiss	0.125	0	67.65	XYL_5deg	EMBSI2006
O. mykiss	0.208333	0	67.65	XYL_5deg	EMBSI2006
O. mykiss	1	0	67.65	XYL_5deg	EMBSI2006
O. mykiss	2	0	67.65	XYL_5deg	EMBSI2006
O. mykiss	3	0	67.65	XYL_5deg	EMBSI2006
O. mykiss	4	0	67.65	XYL_5deg	EMBSI2006
O. mykiss	0	1	1.00E-03	XYL_18deg	EMBSI2006

Table continued

O. mykiss	0.010417	1	1.00E-03	XYL_18deg	EMBSI2006
O. mykiss	0.020833	1	1.00E-03	XYL_18deg	EMBSI2006
O. mykiss	0.041667	1	1.00E-03	XYL_18deg	EMBSI2006
O. mykiss	0.125	1	1.00E-03	XYL_18deg	EMBSI2006
O. mykiss	0.208333	1	1.00E-03	XYL_18deg	EMBSI2006
O. mykiss	1	1	1.00E-03	XYL_18deg	EMBSI2006
O. mykiss	2	1	1.00E-03	XYL_18deg	EMBSI2006
O. mykiss	3	1	1.00E-03	XYL_18deg	EMBSI2006
O. mykiss	4	1	1.00E-03	XYL_18deg	EMBSI2006
O. mykiss	0	1	1.81	XYL_18deg	EMBSI2006
O. mykiss	0.010417	1	1.81	XYL_18deg	EMBSI2006
O. mykiss	0.020833	1	1.81	XYL_18deg	EMBSI2006
O. mykiss	0.041667	1	1.81	XYL_18deg	EMBSI2006
O. mykiss	0.125	1	1.81	XYL_18deg	EMBSI2006
O. mykiss	0.208333	1	1.81	XYL_18deg	EMBSI2006
O. mykiss	1	1	1.81	XYL_18deg	EMBSI2006
O. mykiss	2	1	1.81	XYL_18deg	EMBSI2006
O. mykiss	3	1	1.81	XYL_18deg	EMBSI2006
O. mykiss	4	1	1.81	XYL_18deg	EMBSI2006
O. mykiss	0	1	5.15	XYL_18deg	EMBSI2006
O. mykiss	0.010417	1	5.15	XYL_18deg	EMBSI2006
O. mykiss	0.020833	1	5.15	XYL_18deg	EMBSI2006
O. mykiss	0.041667	1	5.15	XYL_18deg	EMBSI2006
O. mykiss	0.125	1	5.15	XYL_18deg	EMBSI2006
O. mykiss	0.208333	1	5.15	XYL_18deg	EMBSI2006
O. mykiss	1	1	5.15	XYL_18deg	EMBSI2006
O. mykiss	2	1	5.15	XYL_18deg	EMBSI2006
O. mykiss	3	1	5.15	XYL_18deg	EMBSI2006
O. mykiss	4	1	5.15	XYL_18deg	EMBSI2006
O. mykiss	0	1	10.56	XYL_18deg	EMBSI2006
O. mykiss	0.010417	1	10.56	XYL_18deg	EMBSI2006
O. mykiss	0.020833	1	10.56	XYL_18deg	EMBSI2006
O. mykiss	0.041667	1	10.56	XYL_18deg	EMBSI2006
O. mykiss	0.125	0.916667	10.56	XYL_18deg	EMBSI2006
O. mykiss	0.208333	0.75	10.56	XYL_18deg	EMBSI2006
O. mykiss	1	0.5	10.56	XYL_18deg	EMBSI2006
O. mykiss	2	0.416667	10.56	XYL_18deg	EMBSI2006
O. mykiss	3	0.416667	10.56	XYL_18deg	EMBSI2006

Table continued

O. mykiss	4	0.333333	10.56	XYL_18deg	EMBSI2006
O. mykiss	0	1	25.85	XYL_18deg	EMBSI2006
O. mykiss	0.010417	1	25.85	XYL_18deg	EMBSI2006
O. mykiss	0.020833	0.916667	25.85	XYL_18deg	EMBSI2006
O. mykiss	0.041667	0.25	25.85	XYL_18deg	EMBSI2006
O. mykiss	0.125	0	25.85	XYL_18deg	EMBSI2006
O. mykiss	0.208333	0	25.85	XYL_18deg	EMBSI2006
O. mykiss	1	0	25.85	XYL_18deg	EMBSI2006
O. mykiss	2	0	25.85	XYL_18deg	EMBSI2006
O. mykiss	3	0	25.85	XYL_18deg	EMBSI2006
O. mykiss	4	0	25.85	XYL_18deg	EMBSI2006
O. mykiss	0	1	67.65	XYL_18deg	EMBSI2006
O. mykiss	0.010417	0	67.65	XYL_18deg	EMBSI2006
O. mykiss	0.020833	0	67.65	XYL_18deg	EMBSI2006
O. mykiss	0.041667	0	67.65	XYL_18deg	EMBSI2006
O. mykiss	0.125	0	67.65	XYL_18deg	EMBSI2006
O. mykiss	0.208333	0	67.65	XYL_18deg	EMBSI2006
O. mykiss	1	0	67.65	XYL_18deg	EMBSI2006
O. mykiss	2	0	67.65	XYL_18deg	EMBSI2006
O. mykiss	3	0	67.65	XYL_18deg	EMBSI2006
O. mykiss	4	0	67.65	XYL_18deg	EMBSI2006
Sablefish	0.041667	1	1.00E-03	TOL	API/UNCW
Sablefish	0.125	1	1.00E-03	TOL	API/UNCW
Sablefish	0.25	1	1.00E-03	TOL	API/UNCW
Sablefish	1	1	1.00E-03	TOL	API/UNCW
Sablefish	1.25	1	1.00E-03	TOL	API/UNCW
Sablefish	2	1	1.00E-03	TOL	API/UNCW
Sablefish	2.25	1	1.00E-03	TOL	API/UNCW
Sablefish	3	1	1.00E-03	TOL	API/UNCW
Sablefish	3.25	1	1.00E-03	TOL	API/UNCW
Sablefish	4	1	1.00E-03	TOL	API/UNCW
Sablefish	0.041667	1	1.33	TOL	API/UNCW
Sablefish	0.125	1	1.33	TOL	API/UNCW
Sablefish	0.25	1	1.33	TOL	API/UNCW
Sablefish	1	1	1.33	TOL	API/UNCW
Sablefish	1.25	1	1.33	TOL	API/UNCW
Sablefish	2	1	1.33	TOL	API/UNCW
Sablefish	2.25	1	1.33	TOL	API/UNCW

Table continued

Sablefish	3	1	1.33	TOL	API/UNCW
Sablefish	3.25	1	1.33	TOL	API/UNCW
Sablefish	4	1	1.33	TOL	API/UNCW
Sablefish	0.041667	1	2.88	TOL	API/UNCW
Sablefish	0.125	1	2.88	TOL	API/UNCW
Sablefish	0.25	1	2.88	TOL	API/UNCW
Sablefish	1	1	2.88	TOL	API/UNCW
Sablefish	1.25	1	2.88	TOL	API/UNCW
Sablefish	2	1	2.88	TOL	API/UNCW
Sablefish	2.25	1	2.88	TOL	API/UNCW
Sablefish	3	1	2.88	TOL	API/UNCW
Sablefish	3.25	1	2.88	TOL	API/UNCW
Sablefish	4	1	2.88	TOL	API/UNCW
Sablefish	0.041667	1	6.66	TOL	API/UNCW
Sablefish	0.125	1	6.66	TOL	API/UNCW
Sablefish	0.25	1	6.66	TOL	API/UNCW
Sablefish	1	1	6.66	TOL	API/UNCW
Sablefish	1.25	0.583333	6.66	TOL	API/UNCW
Sablefish	2	0.583333	6.66	TOL	API/UNCW
Sablefish	2.25	0.416667	6.66	TOL	API/UNCW
Sablefish	3	0.333333	6.66	TOL	API/UNCW
Sablefish	3.25	0.25	6.66	TOL	API/UNCW
Sablefish	4	0.166667	6.66	TOL	API/UNCW
Sablefish	0.041667	1	10.6	TOL	API/UNCW
Sablefish	0.125	0.75	10.6	TOL	API/UNCW
Sablefish	0.25	0.333333	10.6	TOL	API/UNCW
Sablefish	1	0	10.6	TOL	API/UNCW
Sablefish	1.25	0	10.6	TOL	API/UNCW
Sablefish	2	0	10.6	TOL	API/UNCW
Sablefish	2.25	0	10.6	TOL	API/UNCW
Sablefish	3	0	10.6	TOL	API/UNCW
Sablefish	3.25	0	10.6	TOL	API/UNCW
Sablefish	4	0	10.6	TOL	API/UNCW
Sablefish	0.041667	1	1.00E-03	PHE	API/UNCW
Sablefish	0.125	1	1.00E-03	PHE	API/UNCW
Sablefish	0.25	1	1.00E-03	PHE	API/UNCW
Sablefish	1	1	1.00E-03	PHE	API/UNCW
Sablefish	1.25	1	1.00E-03	PHE	API/UNCW

Table continued

Sablefish	2	1	1.00E-03	PHE	API/UNCW
Sablefish	2.25	1	1.00E-03	PHE	API/UNCW
Sablefish	3	1	1.00E-03	PHE	API/UNCW
Sablefish	3.25	1	1.00E-03	PHE	API/UNCW
Sablefish	4	1	1.00E-03	PHE	API/UNCW
Sablefish	0.041667	1	0.02	PHE	API/UNCW
Sablefish	0.125	1	0.02	PHE	API/UNCW
Sablefish	0.25	1	0.02	PHE	API/UNCW
Sablefish	1	1	0.02	PHE	API/UNCW
Sablefish	1.25	1	0.02	PHE	API/UNCW
Sablefish	2	1	0.02	PHE	API/UNCW
Sablefish	2.25	1	0.02	PHE	API/UNCW
Sablefish	3	1	0.02	PHE	API/UNCW
Sablefish	3.25	1	0.02	PHE	API/UNCW
Sablefish	4	1	0.02	PHE	API/UNCW
Sablefish	0.041667	1	0.1	PHE	API/UNCW
Sablefish	0.125	1	0.1	PHE	API/UNCW
Sablefish	0.25	1	0.1	PHE	API/UNCW
Sablefish	1	0.75	0.1	PHE	API/UNCW
Sablefish	1.25	0.75	0.1	PHE	API/UNCW
Sablefish	2	0.75	0.1	PHE	API/UNCW
Sablefish	2.25	0.666667	0.1	PHE	API/UNCW
Sablefish	3	0.666667	0.1	PHE	API/UNCW
Sablefish	3.25	0.666667	0.1	PHE	API/UNCW
Sablefish	4	0.416667	0.1	PHE	API/UNCW
Sablefish	0.041667	1	0.32	PHE	API/UNCW
Sablefish	0.125	1	0.32	PHE	API/UNCW
Sablefish	0.25	1	0.32	PHE	API/UNCW
Sablefish	1	0.833333	0.32	PHE	API/UNCW
Sablefish	1.25	0.666667	0.32	PHE	API/UNCW
Sablefish	2	0.25	0.32	PHE	API/UNCW
Sablefish	2.25	0.25	0.32	PHE	API/UNCW
Sablefish	3	0.083333	0.32	PHE	API/UNCW
Sablefish	3.25	0	0.32	PHE	API/UNCW
Sablefish	4	0	0.32	PHE	API/UNCW
Sablefish	0.041667	1	2.3	PHE	API/UNCW
Sablefish	0.125	1	2.3	PHE	API/UNCW
Sablefish	0.25	1	2.3	PHE	API/UNCW

Table continued

Sablefish	1	0.583333	2.3	PHE	API/UNCW
Sablefish	1.25	0.416667	2.3	PHE	API/UNCW
Sablefish	2	0	2.3	PHE	API/UNCW
Sablefish	2.25	0	2.3	PHE	API/UNCW
Sablefish	3	0	2.3	PHE	API/UNCW
Sablefish	3.25	0	2.3	PHE	API/UNCW
Sablefish	4	0	2.3	PHE	API/UNCW
Sablefish	0.041667	1	4.3	PHE	API/UNCW
Sablefish	0.125	1	4.3	PHE	API/UNCW
Sablefish	0.25	1	4.3	PHE	API/UNCW
Sablefish	1	0.666667	4.3	PHE	API/UNCW
Sablefish	1.25	0.333333	4.3	PHE	API/UNCW
Sablefish	2	0	4.3	PHE	API/UNCW
Sablefish	2.25	0	4.3	PHE	API/UNCW
Sablefish	3	0	4.3	PHE	API/UNCW
Sablefish	3.25	0	4.3	PHE	API/UNCW
Sablefish	4	0	4.3	PHE	API/UNCW
Sablefish	0.041667	1	1.00E-03	meNAP	API/UNCW
Sablefish	0.125	1	1.00E-03	meNAP	API/UNCW
Sablefish	0.25	1	1.00E-03	meNAP	API/UNCW
Sablefish	1	1	1.00E-03	meNAP	API/UNCW
Sablefish	1.25	1	1.00E-03	meNAP	API/UNCW
Sablefish	2	1	1.00E-03	meNAP	API/UNCW
Sablefish	2.25	1	1.00E-03	meNAP	API/UNCW
Sablefish	3	1	1.00E-03	meNAP	API/UNCW
Sablefish	3.25	1	1.00E-03	meNAP	API/UNCW
Sablefish	4	1	1.00E-03	meNAP	API/UNCW
Sablefish	0.041667	1	0.13	meNAP	API/UNCW
Sablefish	0.125	1	0.13	meNAP	API/UNCW
Sablefish	0.25	1	0.13	meNAP	API/UNCW
Sablefish	1	1	0.13	meNAP	API/UNCW
Sablefish	1.25	1	0.13	meNAP	API/UNCW
Sablefish	2	0.916667	0.13	meNAP	API/UNCW
Sablefish	2.25	0.916667	0.13	meNAP	API/UNCW
Sablefish	3	0.916667	0.13	meNAP	API/UNCW
Sablefish	3.25	0.916667	0.13	meNAP	API/UNCW
Sablefish	4	0.916667	0.13	meNAP	API/UNCW
Sablefish	0.041667	1	0.37	meNAP	API/UNCW

Table continued

Sablefish	0.125	1	0.37	meNAP	API/UNCW
Sablefish	0.25	1	0.37	meNAP	API/UNCW
Sablefish	1	1	0.37	meNAP	API/UNCW
Sablefish	1.25	1	0.37	meNAP	API/UNCW
Sablefish	2	0.916667	0.37	meNAP	API/UNCW
Sablefish	2.25	0.916667	0.37	meNAP	API/UNCW
Sablefish	3	0.916667	0.37	meNAP	API/UNCW
Sablefish	3.25	0.916667	0.37	meNAP	API/UNCW
Sablefish	4	0.916667	0.37	meNAP	API/UNCW
Sablefish	0.041667	1	1.6	meNAP	API/UNCW
Sablefish	0.125	1	1.6	meNAP	API/UNCW
Sablefish	0.25	1	1.6	meNAP	API/UNCW
Sablefish	1	0	1.6	meNAP	API/UNCW
Sablefish	1.25	0	1.6	meNAP	API/UNCW
Sablefish	2	0	1.6	meNAP	API/UNCW
Sablefish	2.25	0	1.6	meNAP	API/UNCW
Sablefish	3	0	1.6	meNAP	API/UNCW
Sablefish	3.25	0	1.6	meNAP	API/UNCW
Sablefish	4	0	1.6	meNAP	API/UNCW
Sablefish	0.041667	1	4.2	meNAP	API/UNCW
Sablefish	0.125	1	4.2	meNAP	API/UNCW
Sablefish	0.25	1	4.2	meNAP	API/UNCW
Sablefish	1	0	4.2	meNAP	API/UNCW
Sablefish	1.25	0	4.2	meNAP	API/UNCW
Sablefish	2	0	4.2	meNAP	API/UNCW
Sablefish	2.25	0	4.2	meNAP	API/UNCW
Sablefish	3	0	4.2	meNAP	API/UNCW
Sablefish	3.25	0	4.2	meNAP	API/UNCW
Sablefish	4	0	4.2	meNAP	API/UNCW
P. promelas	1	1	0.01	t-butylstyrene	EPA
P. promelas	2	1	0.01	t-butylstyrene	EPA
P. promelas	3	1	0.01	t-butylstyrene	EPA
P. promelas	4	1	0.01	t-butylstyrene	EPA
P. promelas	1	1	0.0653	t-butylstyrene	EPA
P. promelas	2	1	0.0653	t-butylstyrene	EPA
P. promelas	3	1	0.0653	t-butylstyrene	EPA
P. promelas	4	1	0.0653	t-butylstyrene	EPA
P. promelas	1	1	0.22	t-butylstyrene	EPA

Table continued

P. promelas	2	1	0.22	t-butylstyrene	EPA
P. promelas	3	0.95	0.22	t-butylstyrene	EPA
P. promelas	4	0.95	0.22	t-butylstyrene	EPA
P. promelas	1	1	0.23	t-butylstyrene	EPA
P. promelas	2	0.95	0.23	t-butylstyrene	EPA
P. promelas	3	0.95	0.23	t-butylstyrene	EPA
P. promelas	4	0.9	0.23	t-butylstyrene	EPA
P. promelas	1	1	0.321	t-butylstyrene	EPA
P. promelas	2	1	0.321	t-butylstyrene	EPA
P. promelas	3	1	0.321	t-butylstyrene	EPA
P. promelas	4	0.9	0.321	t-butylstyrene	EPA
P. promelas	1	0.9	0.764	t-butylstyrene	EPA
P. promelas	2	0.8	0.764	t-butylstyrene	EPA
P. promelas	3	0.35	0.764	t-butylstyrene	EPA
P. promelas	4	0.1	0.764	t-butylstyrene	EPA
P. promelas	1	1	0.001	Acenaphthene	EPA
P. promelas	2	1	0.001	Acenaphthene	EPA
P. promelas	3	1	0.001	Acenaphthene	EPA
P. promelas	4	1	0.001	Acenaphthene	EPA
P. promelas	1	1	0.01	Acenaphthene	EPA
P. promelas	2	1	0.01	Acenaphthene	EPA
P. promelas	3	1	0.01	Acenaphthene	EPA
P. promelas	4	1	0.01	Acenaphthene	EPA
P. promelas	1	1	0.2	Acenaphthene	EPA
P. promelas	2	1	0.2	Acenaphthene	EPA
P. promelas	3	1	0.2	Acenaphthene	EPA
P. promelas	4	1	0.2	Acenaphthene	EPA
P. promelas	1	1	0.23	Acenaphthene	EPA
P. promelas	2	1	0.23	Acenaphthene	EPA
P. promelas	3	1	0.23	Acenaphthene	EPA
P. promelas	4	1	0.23	Acenaphthene	EPA
P. promelas	1	1	0.42	Acenaphthene	EPA
P. promelas	2	1	0.42	Acenaphthene	EPA
P. promelas	3	1	0.42	Acenaphthene	EPA
P. promelas	4	1	0.42	Acenaphthene	EPA
P. promelas	1	1	0.44	Acenaphthene	EPA
P. promelas	2	1	0.44	Acenaphthene	EPA
P. promelas	3	1	0.44	Acenaphthene	EPA

Table continued

P. promelas	4	1	0.44	Acenaphthene	EPA
P. promelas	1	1	0.77	Acenaphthene	EPA
P. promelas	2	1	0.77	Acenaphthene	EPA
P. promelas	3	1	0.77	Acenaphthene	EPA
P. promelas	4	1	0.77	Acenaphthene	EPA
P. promelas	1	1	0.83	Acenaphthene	EPA
P. promelas	2	1	0.83	Acenaphthene	EPA
P. promelas	3	1	0.83	Acenaphthene	EPA
P. promelas	4	1	0.83	Acenaphthene	EPA
P. promelas	1	1	1.32	Acenaphthene	EPA
P. promelas	2	1	1.32	Acenaphthene	EPA
P. promelas	3	1	1.32	Acenaphthene	EPA
P. promelas	4	0.96	1.32	Acenaphthene	EPA
P. promelas	1	1	1.33	Acenaphthene	EPA
P. promelas	2	1	1.33	Acenaphthene	EPA
P. promelas	3	1	1.33	Acenaphthene	EPA
P. promelas	4	1	1.33	Acenaphthene	EPA
P. promelas	1	0.92	2.26	Acenaphthene	EPA
P. promelas	2	0.84	2.26	Acenaphthene	EPA
P. promelas	3	0.24	2.26	Acenaphthene	EPA
P. promelas	4	0.08	2.26	Acenaphthene	EPA
P. promelas	1	0.96	2.18	Acenaphthene	EPA
P. promelas	2	0.76	2.18	Acenaphthene	EPA
P. promelas	3	0.2	2.18	Acenaphthene	EPA
P. promelas	4	0.04	2.18	Acenaphthene	EPA
P. promelas	1	1	0.001	Naphthalene	EPA
P. promelas	2	1	0.001	Naphthalene	EPA
P. promelas	3	1	0.001	Naphthalene	EPA
P. promelas	4	1	0.001	Naphthalene	EPA
P. promelas	1	1	0.01	Naphthalene	EPA
P. promelas	2	1	0.01	Naphthalene	EPA
P. promelas	3	1	0.01	Naphthalene	EPA
P. promelas	4	1	0.01	Naphthalene	EPA
P. promelas	1	1	4.74	Naphthalene	EPA
P. promelas	2	1	4.74	Naphthalene	EPA
P. promelas	3	1	4.74	Naphthalene	EPA
P. promelas	4	1	4.74	Naphthalene	EPA
P. promelas	1	1	3.92	Naphthalene	EPA

Table continued

P. promelas	2	1	3.92	Naphthalene	EPA
P. promelas	3	1	3.92	Naphthalene	EPA
P. promelas	4	1	3.92	Naphthalene	EPA
P. promelas	1	0.88	6.57	Naphthalene	EPA
P. promelas	2	0.32	6.57	Naphthalene	EPA
P. promelas	3	0.24	6.57	Naphthalene	EPA
P. promelas	4	0.24	6.57	Naphthalene	EPA
P. promelas	1	0.96	5.52	Naphthalene	EPA
P. promelas	2	0.68	5.52	Naphthalene	EPA
P. promelas	3	0.56	5.52	Naphthalene	EPA
P. promelas	4	0.56	5.52	Naphthalene	EPA
P. promelas	1	0	10.4	Naphthalene	EPA
P. promelas	2	0	10.4	Naphthalene	EPA
P. promelas	3	0	10.4	Naphthalene	EPA
P. promelas	4	0	10.4	Naphthalene	EPA
P. promelas	1	0.12	10.2	Naphthalene	EPA
P. promelas	2	0	10.2	Naphthalene	EPA
P. promelas	3	0	10.2	Naphthalene	EPA
P. promelas	4	0	10.2	Naphthalene	EPA
P. promelas	1	1	0.001	toluene	EPA
P. promelas	2	1	0.001	toluene	EPA
P. promelas	3	1	0.001	toluene	EPA
P. promelas	4	1	0.001	toluene	EPA
P. promelas	1	0.9	12.1	toluene	EPA
P. promelas	2	0.8	12.1	toluene	EPA
P. promelas	3	0.65	12.1	toluene	EPA
P. promelas	4	0.55	12.1	toluene	EPA
P. promelas	1	1	17.8	toluene	EPA
P. promelas	2	0.9	17.8	toluene	EPA
P. promelas	3	0.75	17.8	toluene	EPA
P. promelas	4	0.7	17.8	toluene	EPA
P. promelas	1	0.85	28.5	toluene	EPA
P. promelas	2	0.75	28.5	toluene	EPA
P. promelas	3	0.7	28.5	toluene	EPA
P. promelas	4	0.65	28.5	toluene	EPA
P. promelas	1	0.55	47.1	toluene	EPA
P. promelas	2	0	47.1	toluene	EPA
P. promelas	3	0	47.1	toluene	EPA

Table continued

P. promelas	4	0	47.1	toluene	EPA
P. promelas	1	0	66.1	toluene	EPA
P. promelas	2	0	66.1	toluene	EPA
P. promelas	3	0	66.1	toluene	EPA
P. promelas	4	0	66.1	toluene	EPA
P. promelas	1	1	0.01	toluene	EPA
P. promelas	2	1	0.01	toluene	EPA
P. promelas	3	1	0.01	toluene	EPA
P. promelas	4	1	0.01	toluene	EPA
P. promelas	1	1	8.3	toluene	EPA
P. promelas	2	1	8.3	toluene	EPA
P. promelas	3	1	8.3	toluene	EPA
P. promelas	4	1	8.3	toluene	EPA
P. promelas	1	1	12.6	toluene	EPA
P. promelas	2	1	12.6	toluene	EPA
P. promelas	3	0.95	12.6	toluene	EPA
P. promelas	4	0.95	12.6	toluene	EPA
P. promelas	1	1	17.5	toluene	EPA
P. promelas	2	0.95	17.5	toluene	EPA
P. promelas	3	0.65	17.5	toluene	EPA
P. promelas	4	0.4	17.5	toluene	EPA
P. promelas	1	0.9	30.6	toluene	EPA
P. promelas	2	0.85	30.6	toluene	EPA
P. promelas	3	0.85	30.6	toluene	EPA
P. promelas	4	0.85	30.6	toluene	EPA
P. promelas	1	0.55	41.4	toluene	EPA
P. promelas	2	0.45	41.4	toluene	EPA
P. promelas	3	0.4	41.4	toluene	EPA
P. promelas	4	0.4	41.4	toluene	EPA
P. promelas	1	1	0.001	ethylbenzene	EPA
P. promelas	2	1	0.001	ethylbenzene	EPA
P. promelas	3	1	0.001	ethylbenzene	EPA
P. promelas	4	1	0.001	ethylbenzene	EPA
P. promelas	1	1	0.01	ethylbenzene	EPA
P. promelas	2	1	0.01	ethylbenzene	EPA
P. promelas	3	1	0.01	ethylbenzene	EPA
P. promelas	4	1	0.01	ethylbenzene	EPA
P. promelas	1	1	2.71	ethylbenzene	EPA

Table continued

P. promelas	2	1	2.71	ethylbenzene	EPA
P. promelas	3	1	2.71	ethylbenzene	EPA
P. promelas	4	1	2.71	ethylbenzene	EPA
P. promelas	1	1	3.33	ethylbenzene	EPA
P. promelas	2	1	3.33	ethylbenzene	EPA
P. promelas	3	1	3.33	ethylbenzene	EPA
P. promelas	4	1	3.33	ethylbenzene	EPA
P. promelas	1	1	5.26	ethylbenzene	EPA
P. promelas	2	1	5.26	ethylbenzene	EPA
P. promelas	3	1	5.26	ethylbenzene	EPA
P. promelas	4	1	5.26	ethylbenzene	EPA
P. promelas	1	1	5.67	ethylbenzene	EPA
P. promelas	2	1	5.67	ethylbenzene	EPA
P. promelas	3	1	5.67	ethylbenzene	EPA
P. promelas	4	1	5.67	ethylbenzene	EPA
P. promelas	1	1	9	ethylbenzene	EPA
P. promelas	2	0.96	9	ethylbenzene	EPA
P. promelas	3	0.96	9	ethylbenzene	EPA
P. promelas	4	0.96	9	ethylbenzene	EPA
P. promelas	1	1	9.77	ethylbenzene	EPA
P. promelas	2	1	9.77	ethylbenzene	EPA
P. promelas	3	1	9.77	ethylbenzene	EPA
P. promelas	4	1	9.77	ethylbenzene	EPA
P. promelas	1	1	12.7	ethylbenzene	EPA
P. promelas	2	0.84	12.7	ethylbenzene	EPA
P. promelas	3	0.52	12.7	ethylbenzene	EPA
P. promelas	4	0.08	12.7	ethylbenzene	EPA
P. promelas	1	1	15.3	ethylbenzene	EPA
P. promelas	2	0.64	15.3	ethylbenzene	EPA
P. promelas	3	0.52	15.3	ethylbenzene	EPA
P. promelas	4	0.2	15.3	ethylbenzene	EPA
P. promelas	1	1	21.6	ethylbenzene	EPA
P. promelas	2	0	21.6	ethylbenzene	EPA
P. promelas	3	0	21.6	ethylbenzene	EPA
P. promelas	4	0	21.6	ethylbenzene	EPA
P. promelas	1	0.04	24.9	ethylbenzene	EPA
P. promelas	2	0	24.9	ethylbenzene	EPA
P. promelas	3	0	24.9	ethylbenzene	EPA

Table continued

P. promelas	4	0	24.9	ethylbenzene	EPA
P. promelas	1	1	0.002	ethylbenzene	EPA
P. promelas	2	1	0.002	ethylbenzene	EPA
P. promelas	3	1	0.002	ethylbenzene	EPA
P. promelas	4	1	0.002	ethylbenzene	EPA
P. promelas	1	1	0.02	ethylbenzene	EPA
P. promelas	2	1	0.02	ethylbenzene	EPA
P. promelas	3	1	0.02	ethylbenzene	EPA
P. promelas	4	1	0.02	ethylbenzene	EPA
P. promelas	1	1	1.14	ethylbenzene	EPA
P. promelas	2	1	1.14	ethylbenzene	EPA
P. promelas	3	1	1.14	ethylbenzene	EPA
P. promelas	4	1	1.14	ethylbenzene	EPA
P. promelas	1	1	1.05	ethylbenzene	EPA
P. promelas	2	1	1.05	ethylbenzene	EPA
P. promelas	3	1	1.05	ethylbenzene	EPA
P. promelas	4	1	1.05	ethylbenzene	EPA
P. promelas	1	0.8	1.58	ethylbenzene	EPA
P. promelas	2	0.8	1.58	ethylbenzene	EPA
P. promelas	3	0.8	1.58	ethylbenzene	EPA
P. promelas	4	0.7	1.58	ethylbenzene	EPA
P. promelas	1	1	2.37	ethylbenzene	EPA
P. promelas	2	1	2.37	ethylbenzene	EPA
P. promelas	3	1	2.37	ethylbenzene	EPA
P. promelas	4	1	2.37	ethylbenzene	EPA
P. promelas	1	1	7.06	ethylbenzene	EPA
P. promelas	2	1	7.06	ethylbenzene	EPA
P. promelas	3	1	7.06	ethylbenzene	EPA
P. promelas	4	1	7.06	ethylbenzene	EPA
P. promelas	1	1	6.23	ethylbenzene	EPA
P. promelas	2	1	6.23	ethylbenzene	EPA
P. promelas	3	1	6.23	ethylbenzene	EPA
P. promelas	4	1	6.23	ethylbenzene	EPA
P. promelas	1	0.3	13.8	ethylbenzene	EPA
P. promelas	2	0.3	13.8	ethylbenzene	EPA
P. promelas	3	0.3	13.8	ethylbenzene	EPA
P. promelas	4	0.2	13.8	ethylbenzene	EPA
P. promelas	1	0	14.9	ethylbenzene	EPA

Table continued

P. promelas	2	0	14.9	ethylbenzene	EPA
P. promelas	3	0	14.9	ethylbenzene	EPA
P. promelas	4	0	14.9	ethylbenzene	EPA
P. promelas	1	0	29.3	ethylbenzene	EPA
P. promelas	2	0	29.3	ethylbenzene	EPA
P. promelas	3	0	29.3	ethylbenzene	EPA
P. promelas	4	0	29.3	ethylbenzene	EPA
P. promelas	1	0	28.5	ethylbenzene	EPA
P. promelas	2	0	28.5	ethylbenzene	EPA
P. promelas	3	0	28.5	ethylbenzene	EPA
P. promelas	4	0	28.5	ethylbenzene	EPA
P. promelas	0.125	1	0.001	p-xylene	EPA
P. promelas	0.25	1	0.001	p-xylene	EPA
P. promelas	1.083333	1	0.001	p-xylene	EPA
P. promelas	1.25	1	0.001	p-xylene	EPA
P. promelas	2	1	0.001	p-xylene	EPA
P. promelas	2.25	1	0.001	p-xylene	EPA
P. promelas	3	1	0.001	p-xylene	EPA
P. promelas	3.25	1	0.001	p-xylene	EPA
P. promelas	4	1	0.001	p-xylene	EPA
P. promelas	0.125	1	0.01	p-xylene	EPA
P. promelas	0.25	1	0.01	p-xylene	EPA
P. promelas	1.083333	1	0.01	p-xylene	EPA
P. promelas	1.25	1	0.01	p-xylene	EPA
P. promelas	2	1	0.01	p-xylene	EPA
P. promelas	2.25	1	0.01	p-xylene	EPA
P. promelas	3	1	0.01	p-xylene	EPA
P. promelas	3.25	1	0.01	p-xylene	EPA
P. promelas	4	1	0.01	p-xylene	EPA
P. promelas	0.125	1	2.64	p-xylene	EPA
P. promelas	0.25	1	2.64	p-xylene	EPA
P. promelas	1.083333	1	2.64	p-xylene	EPA
P. promelas	1.25	1	2.64	p-xylene	EPA
P. promelas	2	1	2.64	p-xylene	EPA
P. promelas	2.25	1	2.64	p-xylene	EPA
P. promelas	3	1	2.64	p-xylene	EPA
P. promelas	3.25	1	2.64	p-xylene	EPA
P. promelas	4	1	2.64	p-xylene	EPA

Table continued

P. promelas	0.125	1	2.54	p-xylene	EPA
P. promelas	0.25	1	2.54	p-xylene	EPA
P. promelas	1.083333	1	2.54	p-xylene	EPA
P. promelas	1.25	1	2.54	p-xylene	EPA
P. promelas	2	1	2.54	p-xylene	EPA
P. promelas	2.25	1	2.54	p-xylene	EPA
P. promelas	3	1	2.54	p-xylene	EPA
P. promelas	3.25	1	2.54	p-xylene	EPA
P. promelas	4	1	2.54	p-xylene	EPA
P. promelas	0.125	1	4.37	p-xylene	EPA
P. promelas	0.25	1	4.37	p-xylene	EPA
P. promelas	1.083333	1	4.37	p-xylene	EPA
P. promelas	1.25	1	4.37	p-xylene	EPA
P. promelas	2	1	4.37	p-xylene	EPA
P. promelas	2.25	1	4.37	p-xylene	EPA
P. promelas	3	1	4.37	p-xylene	EPA
P. promelas	3.25	1	4.37	p-xylene	EPA
P. promelas	4	1	4.37	p-xylene	EPA
P. promelas	0.125	1	4.02	p-xylene	EPA
P. promelas	0.25	1	4.02	p-xylene	EPA
P. promelas	1.083333	1	4.02	p-xylene	EPA
P. promelas	1.25	1	4.02	p-xylene	EPA
P. promelas	2	1	4.02	p-xylene	EPA
P. promelas	2.25	1	4.02	p-xylene	EPA
P. promelas	3	1	4.02	p-xylene	EPA
P. promelas	3.25	1	4.02	p-xylene	EPA
P. promelas	4	1	4.02	p-xylene	EPA
P. promelas	0.125	1	6.36	p-xylene	EPA
P. promelas	0.25	1	6.36	p-xylene	EPA
P. promelas	1.083333	1	6.36	p-xylene	EPA
P. promelas	1.25	1	6.36	p-xylene	EPA
P. promelas	2	1	6.36	p-xylene	EPA
P. promelas	2.25	1	6.36	p-xylene	EPA
P. promelas	3	1	6.36	p-xylene	EPA
P. promelas	3.25	1	6.36	p-xylene	EPA
P. promelas	4	1	6.36	p-xylene	EPA
P. promelas	0.125	1	6.19	p-xylene	EPA
P. promelas	0.25	1	6.19	p-xylene	EPA

Table continued

P. promelas	1.083333	1	6.19	p-xylene	EPA
P. promelas	1.25	1	6.19	p-xylene	EPA
P. promelas	2	1	6.19	p-xylene	EPA
P. promelas	2.25	1	6.19	p-xylene	EPA
P. promelas	3	1	6.19	p-xylene	EPA
P. promelas	3.25	1	6.19	p-xylene	EPA
P. promelas	4	1	6.19	p-xylene	EPA
P. promelas	0.125	1	9.93	p-xylene	EPA
P. promelas	0.25	1	9.93	p-xylene	EPA
P. promelas	1.083333	0.75	9.93	p-xylene	EPA
P. promelas	1.25	0.75	9.93	p-xylene	EPA
P. promelas	2	0.55	9.93	p-xylene	EPA
P. promelas	2.25	0.5	9.93	p-xylene	EPA
P. promelas	3	0.45	9.93	p-xylene	EPA
P. promelas	3.25	0.4	9.93	p-xylene	EPA
P. promelas	4	0.35	9.93	p-xylene	EPA
P. promelas	0.125	1	9.9	p-xylene	EPA
P. promelas	0.25	1	9.9	p-xylene	EPA
P. promelas	1.083333	0.9	9.9	p-xylene	EPA
P. promelas	1.25	0.9	9.9	p-xylene	EPA
P. promelas	2	0.85	9.9	p-xylene	EPA
P. promelas	2.25	0.8	9.9	p-xylene	EPA
P. promelas	3	0.8	9.9	p-xylene	EPA
P. promelas	3.25	0.55	9.9	p-xylene	EPA
P. promelas	4	0.15	9.9	p-xylene	EPA
P. promelas	0.125	0.9	17.6	p-xylene	EPA
P. promelas	0.25	0.8	17.6	p-xylene	EPA
P. promelas	1.083333	0.1	17.6	p-xylene	EPA
P. promelas	1.25	0.05	17.6	p-xylene	EPA
P. promelas	2	0.05	17.6	p-xylene	EPA
P. promelas	2.25	0.05	17.6	p-xylene	EPA
P. promelas	3	0.05	17.6	p-xylene	EPA
P. promelas	3.25	0.05	17.6	p-xylene	EPA
P. promelas	4	0.05	17.6	p-xylene	EPA
P. promelas	0.125	1	16.9	p-xylene	EPA
P. promelas	0.25	1	16.9	p-xylene	EPA
P. promelas	1.083333	0.55	16.9	p-xylene	EPA
P. promelas	1.25	0.55	16.9	p-xylene	EPA

Table continued

P. promelas	2	0.2	16.9	p-xylene	EPA
P. promelas	2.25	0.2	16.9	p-xylene	EPA
P. promelas	3	0.2	16.9	p-xylene	EPA
P. promelas	3.25	0.2	16.9	p-xylene	EPA
P. promelas	4	0.2	16.9	p-xylene	EPA
P. promelas	1	1	0.01	isopropylbenzene	EPA
P. promelas	2	1	0.01	isopropylbenzene	EPA
P. promelas	3	1	0.01	isopropylbenzene	EPA
P. promelas	4	1	0.01	isopropylbenzene	EPA
P. promelas	1	1	0.91	isopropylbenzene	EPA
P. promelas	2	1	0.91	isopropylbenzene	EPA
P. promelas	3	1	0.91	isopropylbenzene	EPA
P. promelas	4	1	0.91	isopropylbenzene	EPA
P. promelas	1	1	1.89	isopropylbenzene	EPA
P. promelas	2	1	1.89	isopropylbenzene	EPA
P. promelas	3	1	1.89	isopropylbenzene	EPA
P. promelas	4	1	1.89	isopropylbenzene	EPA
P. promelas	1	1	3.3	isopropylbenzene	EPA
P. promelas	2	1	3.3	isopropylbenzene	EPA
P. promelas	3	1	3.3	isopropylbenzene	EPA
P. promelas	4	1	3.3	isopropylbenzene	EPA
P. promelas	1	1	4.99	isopropylbenzene	EPA
P. promelas	2	1	4.99	isopropylbenzene	EPA
P. promelas	3	1	4.99	isopropylbenzene	EPA
P. promelas	4	0.95	4.99	isopropylbenzene	EPA
P. promelas	1	0.9	8.37	isopropylbenzene	EPA
P. promelas	2	0.65	8.37	isopropylbenzene	EPA
P. promelas	3	0	8.37	isopropylbenzene	EPA
P. promelas	4	0	8.37	isopropylbenzene	EPA
P. promelas	0.125	1	0.001	1,2,4-trimethylbenzene	EPA
P. promelas	2	1	0.001	1,2,4-trimethylbenzene	EPA
P. promelas	3	1	0.001	1,2,4-trimethylbenzene	EPA
P. promelas	4	1	0.001	1,2,4-trimethylbenzene	EPA
P. promelas	0.125	1	0.01	1,2,4-trimethylbenzene	EPA
P. promelas	2	1	0.01	1,2,4-trimethylbenzene	EPA
P. promelas	3	1	0.01	1,2,4-trimethylbenzene	EPA
P. promelas	4	1	0.01	1,2,4-trimethylbenzene	EPA
P. promelas	0.125	1	1.7	1,2,4-trimethylbenzene	EPA

Table continued

P. promelas	2	1	1.7	1,2,4-trimethylbenzene	EPA
P. promelas	3	1	1.7	1,2,4-trimethylbenzene	EPA
P. promelas	4	1	1.7	1,2,4-trimethylbenzene	EPA
P. promelas	0.125	1	1.49	1,2,4-trimethylbenzene	EPA
P. promelas	2	1	1.49	1,2,4-trimethylbenzene	EPA
P. promelas	3	1	1.49	1,2,4-trimethylbenzene	EPA
P. promelas	4	1	1.49	1,2,4-trimethylbenzene	EPA
P. promelas	0.125	1	3.05	1,2,4-trimethylbenzene	EPA
P. promelas	2	1	3.05	1,2,4-trimethylbenzene	EPA
P. promelas	3	1	3.05	1,2,4-trimethylbenzene	EPA
P. promelas	4	1	3.05	1,2,4-trimethylbenzene	EPA
P. promelas	0.125	1	2.64	1,2,4-trimethylbenzene	EPA
P. promelas	2	1	2.64	1,2,4-trimethylbenzene	EPA
P. promelas	3	1	2.64	1,2,4-trimethylbenzene	EPA
P. promelas	4	1	2.64	1,2,4-trimethylbenzene	EPA
P. promelas	0.125	1	4.58	1,2,4-trimethylbenzene	EPA
P. promelas	2	1	4.58	1,2,4-trimethylbenzene	EPA
P. promelas	3	1	4.58	1,2,4-trimethylbenzene	EPA
P. promelas	4	1	4.58	1,2,4-trimethylbenzene	EPA
P. promelas	0.125	1	4.18	1,2,4-trimethylbenzene	EPA
P. promelas	2	1	4.18	1,2,4-trimethylbenzene	EPA
P. promelas	3	1	4.18	1,2,4-trimethylbenzene	EPA
P. promelas	4	1	4.18	1,2,4-trimethylbenzene	EPA
P. promelas	0.125	1	8.52	1,2,4-trimethylbenzene	EPA
P. promelas	2	0.8	8.52	1,2,4-trimethylbenzene	EPA
P. promelas	3	0.76	8.52	1,2,4-trimethylbenzene	EPA
P. promelas	4	0.56	8.52	1,2,4-trimethylbenzene	EPA
P. promelas	0.125	1	7.66	1,2,4-trimethylbenzene	EPA
P. promelas	2	0.92	7.66	1,2,4-trimethylbenzene	EPA
P. promelas	3	0.76	7.66	1,2,4-trimethylbenzene	EPA
P. promelas	4	0.48	7.66	1,2,4-trimethylbenzene	EPA
P. promelas	0.125	0	12	1,2,4-trimethylbenzene	EPA
P. promelas	2	0	12	1,2,4-trimethylbenzene	EPA
P. promelas	3	0	12	1,2,4-trimethylbenzene	EPA
P. promelas	4	0	12	1,2,4-trimethylbenzene	EPA
P. promelas	0.125	0	11.8	1,2,4-trimethylbenzene	EPA
P. promelas	2	0	11.8	1,2,4-trimethylbenzene	EPA
P. promelas	3	0	11.8	1,2,4-trimethylbenzene	EPA

Table continued

P. promelas	4	0	11.8	1,2,4-trimethylbenzene	EPA
P. promelas	0.166667	1	0.001	1,3-diethylbenzene	EPA
P. promelas	1	1	0.001	1,3-diethylbenzene	EPA
P. promelas	1.25	1	0.001	1,3-diethylbenzene	EPA
P. promelas	2	1	0.001	1,3-diethylbenzene	EPA
P. promelas	2.25	1	0.001	1,3-diethylbenzene	EPA
P. promelas	3	1	0.001	1,3-diethylbenzene	EPA
P. promelas	3.25	1	0.001	1,3-diethylbenzene	EPA
P. promelas	4	1	0.001	1,3-diethylbenzene	EPA
P. promelas	0.166667	1	0.01	1,3-diethylbenzene	EPA
P. promelas	1	1	0.01	1,3-diethylbenzene	EPA
P. promelas	1.25	1	0.01	1,3-diethylbenzene	EPA
P. promelas	2	1	0.01	1,3-diethylbenzene	EPA
P. promelas	2.25	1	0.01	1,3-diethylbenzene	EPA
P. promelas	3	1	0.01	1,3-diethylbenzene	EPA
P. promelas	3.25	1	0.01	1,3-diethylbenzene	EPA
P. promelas	4	1	0.01	1,3-diethylbenzene	EPA
P. promelas	0.166667	1	0.91	1,3-diethylbenzene	EPA
P. promelas	1	1	0.91	1,3-diethylbenzene	EPA
P. promelas	1.25	1	0.91	1,3-diethylbenzene	EPA
P. promelas	2	1	0.91	1,3-diethylbenzene	EPA
P. promelas	2.25	1	0.91	1,3-diethylbenzene	EPA
P. promelas	3	1	0.91	1,3-diethylbenzene	EPA
P. promelas	3.25	1	0.91	1,3-diethylbenzene	EPA
P. promelas	4	1	0.91	1,3-diethylbenzene	EPA
P. promelas	0.166667	1	1.14	1,3-diethylbenzene	EPA
P. promelas	1	1	1.14	1,3-diethylbenzene	EPA
P. promelas	1.25	1	1.14	1,3-diethylbenzene	EPA
P. promelas	2	1	1.14	1,3-diethylbenzene	EPA
P. promelas	2.25	1	1.14	1,3-diethylbenzene	EPA
P. promelas	3	1	1.14	1,3-diethylbenzene	EPA
P. promelas	3.25	1	1.14	1,3-diethylbenzene	EPA
P. promelas	4	1	1.14	1,3-diethylbenzene	EPA
P. promelas	0.166667	1	1.73	1,3-diethylbenzene	EPA
P. promelas	1	1	1.73	1,3-diethylbenzene	EPA
P. promelas	1.25	0.96	1.73	1,3-diethylbenzene	EPA
P. promelas	2	0.96	1.73	1,3-diethylbenzene	EPA
P. promelas	2.25	0.96	1.73	1,3-diethylbenzene	EPA

Table continued

P. promelas	3	0.96	1.73	1,3-diethylbenzene	EPA
P. promelas	3.25	0.96	1.73	1,3-diethylbenzene	EPA
P. promelas	4	0.96	1.73	1,3-diethylbenzene	EPA
P. promelas	0.166667	1	1.96	1,3-diethylbenzene	EPA
P. promelas	1	1	1.96	1,3-diethylbenzene	EPA
P. promelas	1.25	1	1.96	1,3-diethylbenzene	EPA
P. promelas	2	1	1.96	1,3-diethylbenzene	EPA
P. promelas	2.25	1	1.96	1,3-diethylbenzene	EPA
P. promelas	3	1	1.96	1,3-diethylbenzene	EPA
P. promelas	3.25	1	1.96	1,3-diethylbenzene	EPA
P. promelas	4	1	1.96	1,3-diethylbenzene	EPA
P. promelas	0.166667	1	3	1,3-diethylbenzene	EPA
P. promelas	1	1	3	1,3-diethylbenzene	EPA
P. promelas	1.25	1	3	1,3-diethylbenzene	EPA
P. promelas	2	1	3	1,3-diethylbenzene	EPA
P. promelas	2.25	1	3	1,3-diethylbenzene	EPA
P. promelas	3	1	3	1,3-diethylbenzene	EPA
P. promelas	3.25	1	3	1,3-diethylbenzene	EPA
P. promelas	4	1	3	1,3-diethylbenzene	EPA
P. promelas	0.166667	1	3.32	1,3-diethylbenzene	EPA
P. promelas	1	1	3.32	1,3-diethylbenzene	EPA
P. promelas	1.25	1	3.32	1,3-diethylbenzene	EPA
P. promelas	2	1	3.32	1,3-diethylbenzene	EPA
P. promelas	2.25	1	3.32	1,3-diethylbenzene	EPA
P. promelas	3	1	3.32	1,3-diethylbenzene	EPA
P. promelas	3.25	1	3.32	1,3-diethylbenzene	EPA
P. promelas	4	1	3.32	1,3-diethylbenzene	EPA
P. promelas	0.166667	1	4.56	1,3-diethylbenzene	EPA
P. promelas	1	1	4.56	1,3-diethylbenzene	EPA
P. promelas	1.25	1	4.56	1,3-diethylbenzene	EPA
P. promelas	2	0.44	4.56	1,3-diethylbenzene	EPA
P. promelas	2.25	0.36	4.56	1,3-diethylbenzene	EPA
P. promelas	3	0.28	4.56	1,3-diethylbenzene	EPA
P. promelas	3.25	0.24	4.56	1,3-diethylbenzene	EPA
P. promelas	4	0	4.56	1,3-diethylbenzene	EPA
P. promelas	0.166667	1	5.72	1,3-diethylbenzene	EPA
P. promelas	1	0.88	5.72	1,3-diethylbenzene	EPA
P. promelas	1.25	0.88	5.72	1,3-diethylbenzene	EPA

Table continued

P. promelas	2	0.08	5.72	1,3-diethylbenzene	EPA
P. promelas	2.25	0.08	5.72	1,3-diethylbenzene	EPA
P. promelas	3	0.08	5.72	1,3-diethylbenzene	EPA
P. promelas	3.25	0.04	5.72	1,3-diethylbenzene	EPA
P. promelas	4	0.04	5.72	1,3-diethylbenzene	EPA
P. promelas	0.166667	0.92	8.04	1,3-diethylbenzene	EPA
P. promelas	1	0	8.04	1,3-diethylbenzene	EPA
P. promelas	1.25	0	8.04	1,3-diethylbenzene	EPA
P. promelas	2	0	8.04	1,3-diethylbenzene	EPA
P. promelas	2.25	0	8.04	1,3-diethylbenzene	EPA
P. promelas	3	0	8.04	1,3-diethylbenzene	EPA
P. promelas	3.25	0	8.04	1,3-diethylbenzene	EPA
P. promelas	4	0	8.04	1,3-diethylbenzene	EPA
P. promelas	0.166667	0.76	9.37	1,3-diethylbenzene	EPA
P. promelas	1	0	9.37	1,3-diethylbenzene	EPA
P. promelas	1.25	0	9.37	1,3-diethylbenzene	EPA
P. promelas	2	0	9.37	1,3-diethylbenzene	EPA
P. promelas	2.25	0	9.37	1,3-diethylbenzene	EPA
P. promelas	3	0	9.37	1,3-diethylbenzene	EPA
P. promelas	3.25	0	9.37	1,3-diethylbenzene	EPA
P. promelas	4	0	9.37	1,3-diethylbenzene	EPA
P. promelas	1	1	0.001	n-amylbenzene	EPA
P. promelas	2	1	0.001	n-amylbenzene	EPA
P. promelas	3	1	0.001	n-amylbenzene	EPA
P. promelas	4	1	0.001	n-amylbenzene	EPA
P. promelas	1	1	0.01	n-amylbenzene	EPA
P. promelas	2	1	0.01	n-amylbenzene	EPA
P. promelas	3	1	0.01	n-amylbenzene	EPA
P. promelas	4	1	0.01	n-amylbenzene	EPA
P. promelas	1	1	1.18	n-amylbenzene	EPA
P. promelas	2	1	1.18	n-amylbenzene	EPA
P. promelas	3	1	1.18	n-amylbenzene	EPA
P. promelas	4	1	1.18	n-amylbenzene	EPA
P. promelas	1	1	1.13	n-amylbenzene	EPA
P. promelas	2	1	1.13	n-amylbenzene	EPA
P. promelas	3	0.96	1.13	n-amylbenzene	EPA
P. promelas	4	0.96	1.13	n-amylbenzene	EPA
P. promelas	1	1	2.1	n-amylbenzene	EPA

Table continued

P. promelas	2	0.96	2.1	n-amylbenzene	EPA
P. promelas	3	0.52	2.1	n-amylbenzene	EPA
P. promelas	4	0.36	2.1	n-amylbenzene	EPA
P. promelas	1	1	1.82	n-amylbenzene	EPA
P. promelas	2	0.96	1.82	n-amylbenzene	EPA
P. promelas	3	0.6	1.82	n-amylbenzene	EPA
P. promelas	4	0.16	1.82	n-amylbenzene	EPA
P. promelas	1	0.96	3.45	n-amylbenzene	EPA
P. promelas	2	0.08	3.45	n-amylbenzene	EPA
P. promelas	3	0	3.45	n-amylbenzene	EPA
P. promelas	4	0	3.45	n-amylbenzene	EPA
P. promelas	1	0.96	3.17	n-amylbenzene	EPA
P. promelas	2	0	3.17	n-amylbenzene	EPA
P. promelas	3	0	3.17	n-amylbenzene	EPA
P. promelas	4	0	3.17	n-amylbenzene	EPA
P. promelas	1	0.04	5.39	n-amylbenzene	EPA
P. promelas	2	0	5.39	n-amylbenzene	EPA
P. promelas	3	0	5.39	n-amylbenzene	EPA
P. promelas	4	0	5.39	n-amylbenzene	EPA
P. promelas	1	0	4.75	n-amylbenzene	EPA
P. promelas	2	0	4.75	n-amylbenzene	EPA
P. promelas	3	0	4.75	n-amylbenzene	EPA
P. promelas	4	0	4.75	n-amylbenzene	EPA
P. promelas	1	0	9.29	n-amylbenzene	EPA
P. promelas	2	0	9.29	n-amylbenzene	EPA
P. promelas	3	0	9.29	n-amylbenzene	EPA
P. promelas	4	0	9.29	n-amylbenzene	EPA
P. promelas	1	0	8.56	n-amylbenzene	EPA
P. promelas	2	0	8.56	n-amylbenzene	EPA
P. promelas	3	0	8.56	n-amylbenzene	EPA
P. promelas	4	0	8.56	n-amylbenzene	EPA
P. promelas	1	1	0.001	benzene	EPA
P. promelas	2	1	0.001	benzene	EPA
P. promelas	3	1	0.001	benzene	EPA
P. promelas	4	1	0.001	benzene	EPA
P. promelas	1	1	0.01	benzene	EPA
P. promelas	2	1	0.01	benzene	EPA
P. promelas	3	1	0.01	benzene	EPA

Table continued

P. promelas	4	1	0.01	benzene	EPA
P. promelas	1	1	3.26	benzene	EPA
P. promelas	2	1	3.26	benzene	EPA
P. promelas	3	1	3.26	benzene	EPA
P. promelas	4	1	3.26	benzene	EPA
P. promelas	1	1	4.38	benzene	EPA
P. promelas	2	1	4.38	benzene	EPA
P. promelas	3	1	4.38	benzene	EPA
P. promelas	4	1	4.38	benzene	EPA
P. promelas	1	1	6.47	benzene	EPA
P. promelas	2	1	6.47	benzene	EPA
P. promelas	3	1	6.47	benzene	EPA
P. promelas	4	1	6.47	benzene	EPA
P. promelas	1	1	5.42	benzene	EPA
P. promelas	2	1	5.42	benzene	EPA
P. promelas	3	1	5.42	benzene	EPA
P. promelas	4	1	5.42	benzene	EPA
P. promelas	1	0.4	19.1	benzene	EPA
P. promelas	2	0.3	19.1	benzene	EPA
P. promelas	3	0.3	19.1	benzene	EPA
P. promelas	4	0.2	19.1	benzene	EPA
P. promelas	1	0.3	17.5	benzene	EPA
P. promelas	2	0.3	17.5	benzene	EPA
P. promelas	3	0.2	17.5	benzene	EPA
P. promelas	4	0.1	17.5	benzene	EPA
P. promelas	1	0.5	33	benzene	EPA
P. promelas	2	0.5	33	benzene	EPA
P. promelas	3	0.3	33	benzene	EPA
P. promelas	4	0.2	33	benzene	EPA
P. promelas	1	0.4	31.2	benzene	EPA
P. promelas	2	0.3	31.2	benzene	EPA
P. promelas	3	0.1	31.2	benzene	EPA
P. promelas	4	0	31.2	benzene	EPA
P. promelas	1	0	64.4	benzene	EPA
P. promelas	2	0	64.4	benzene	EPA
P. promelas	3	0	64.4	benzene	EPA
P. promelas	4	0	64.4	benzene	EPA
P. promelas	1	0	57.2	benzene	EPA

Table continued

P. promelas	2	0	57.2	benzene	EPA
P. promelas	3	0	57.2	benzene	EPA
P. promelas	4	0	57.2	benzene	EPA
P. promelas	1	1	0.02	benzene	EPA
P. promelas	2	1	0.02	benzene	EPA
P. promelas	3	1	0.02	benzene	EPA
P. promelas	4	1	0.02	benzene	EPA
P. promelas	1	1	10.7	benzene	EPA
P. promelas	2	1	10.7	benzene	EPA
P. promelas	3	1	10.7	benzene	EPA
P. promelas	4	1	10.7	benzene	EPA
P. promelas	1	1	16	benzene	EPA
P. promelas	2	1	16	benzene	EPA
P. promelas	3	1	16	benzene	EPA
P. promelas	4	1	16	benzene	EPA
P. promelas	1	1	25.4	benzene	EPA
P. promelas	2	0.65	25.4	benzene	EPA
P. promelas	3	0.2	25.4	benzene	EPA
P. promelas	4	0	25.4	benzene	EPA
P. promelas	1	0.75	45.8	benzene	EPA
P. promelas	2	0.75	45.8	benzene	EPA
P. promelas	3	0.55	45.8	benzene	EPA
P. promelas	4	0.35	45.8	benzene	EPA
P. promelas	1	0	84.9	benzene	EPA
P. promelas	2	0	84.9	benzene	EPA
P. promelas	3	0	84.9	benzene	EPA
P. promelas	4	0	84.9	benzene	EPA
P. promelas	1	1	0.01	cyclohexane	EPA
P. promelas	2	1	0.01	cyclohexane	EPA
P. promelas	3	1	0.01	cyclohexane	EPA
P. promelas	4	1	0.01	cyclohexane	EPA
P. promelas	1	1	2	cyclohexane	EPA
P. promelas	2	1	2	cyclohexane	EPA
P. promelas	3	1	2	cyclohexane	EPA
P. promelas	4	1	2	cyclohexane	EPA
P. promelas	1	0.9	3.52	cyclohexane	EPA
P. promelas	2	0.9	3.52	cyclohexane	EPA
P. promelas	3	0.9	3.52	cyclohexane	EPA

Table continued

P. promelas	4	0.9	3.52	cyclohexane	EPA
P. promelas	1	1	4.84	cyclohexane	EPA
P. promelas	2	0.9	4.84	cyclohexane	EPA
P. promelas	3	0.7	4.84	cyclohexane	EPA
P. promelas	4	0.4	4.84	cyclohexane	EPA
P. promelas	1	0	6.96	cyclohexane	EPA
P. promelas	2	0	6.96	cyclohexane	EPA
P. promelas	3	0	6.96	cyclohexane	EPA
P. promelas	4	0	6.96	cyclohexane	EPA
P. promelas	1	0	8.86	cyclohexane	EPA
P. promelas	2	0	8.86	cyclohexane	EPA
P. promelas	3	0	8.86	cyclohexane	EPA
P. promelas	4	0	8.86	cyclohexane	EPA
P. promelas	1	1	0.001	o-xylene	EPA
P. promelas	2	1	0.001	o-xylene	EPA
P. promelas	3	1	0.001	o-xylene	EPA
P. promelas	4	1	0.001	o-xylene	EPA
P. promelas	1	1	0.01	o-xylene	EPA
P. promelas	2	1	0.01	o-xylene	EPA
P. promelas	3	1	0.01	o-xylene	EPA
P. promelas	4	1	0.01	o-xylene	EPA
P. promelas	1	1	1.64	o-xylene	EPA
P. promelas	2	1	1.64	o-xylene	EPA
P. promelas	3	1	1.64	o-xylene	EPA
P. promelas	4	1	1.64	o-xylene	EPA
P. promelas	1	1	1.77	o-xylene	EPA
P. promelas	2	1	1.77	o-xylene	EPA
P. promelas	3	1	1.77	o-xylene	EPA
P. promelas	4	1	1.77	o-xylene	EPA
P. promelas	1	1	2.57	o-xylene	EPA
P. promelas	2	1	2.57	o-xylene	EPA
P. promelas	3	1	2.57	o-xylene	EPA
P. promelas	4	1	2.57	o-xylene	EPA
P. promelas	1	1	2.76	o-xylene	EPA
P. promelas	2	1	2.76	o-xylene	EPA
P. promelas	3	1	2.76	o-xylene	EPA
P. promelas	4	1	2.76	o-xylene	EPA
P. promelas	1	1	5.42	o-xylene	EPA

Table continued

P. promelas	2	1	5.42	o-xylene	EPA
P. promelas	3	1	5.42	o-xylene	EPA
P. promelas	4	1	5.42	o-xylene	EPA
P. promelas	1	1	5.98	o-xylene	EPA
P. promelas	2	1	5.98	o-xylene	EPA
P. promelas	3	1	5.98	o-xylene	EPA
P. promelas	4	1	5.98	o-xylene	EPA
P. promelas	1	1	11.4	o-xylene	EPA
P. promelas	2	1	11.4	o-xylene	EPA
P. promelas	3	1	11.4	o-xylene	EPA
P. promelas	4	1	11.4	o-xylene	EPA
P. promelas	1	1	12.2	o-xylene	EPA
P. promelas	2	1	12.2	o-xylene	EPA
P. promelas	3	1	12.2	o-xylene	EPA
P. promelas	4	1	12.2	o-xylene	EPA
P. promelas	1	0	21.7	o-xylene	EPA
P. promelas	2	0	21.7	o-xylene	EPA
P. promelas	3	0	21.7	o-xylene	EPA
P. promelas	4	0	21.7	o-xylene	EPA
P. promelas	1	0	24	o-xylene	EPA
P. promelas	2	0	24	o-xylene	EPA
P. promelas	3	0	24	o-xylene	EPA
P. promelas	4	0	24	o-xylene	EPA
P. promelas	1	1	0.02	o-xylene	EPA
P. promelas	2	1	0.02	o-xylene	EPA
P. promelas	3	1	0.02	o-xylene	EPA
P. promelas	4	1	0.02	o-xylene	EPA
P. promelas	1	1	3.79	o-xylene	EPA
P. promelas	2	1	3.79	o-xylene	EPA
P. promelas	3	1	3.79	o-xylene	EPA
P. promelas	4	1	3.79	o-xylene	EPA
P. promelas	1	1	6.67	o-xylene	EPA
P. promelas	2	1	6.67	o-xylene	EPA
P. promelas	3	1	6.67	o-xylene	EPA
P. promelas	4	1	6.67	o-xylene	EPA
P. promelas	1	1	9.43	o-xylene	EPA
P. promelas	2	1	9.43	o-xylene	EPA
P. promelas	3	1	9.43	o-xylene	EPA

Table continued

P. promelas	4	1	9.43	o-xylene	EPA
P. promelas	1	1	14	o-xylene	EPA
P. promelas	2	1	14	o-xylene	EPA
P. promelas	3	1	14	o-xylene	EPA
P. promelas	4	1	14	o-xylene	EPA
P. promelas	1	0.1	19.2	o-xylene	EPA
P. promelas	2	0.1	19.2	o-xylene	EPA
P. promelas	3	0.1	19.2	o-xylene	EPA
P. promelas	4	0	19.2	o-xylene	EPA
P. promelas	1	1	0.01	m-xylene	EPA
P. promelas	2	1	0.01	m-xylene	EPA
P. promelas	3	1	0.01	m-xylene	EPA
P. promelas	4	1	0.01	m-xylene	EPA
P. promelas	1	1	2.71	m-xylene	EPA
P. promelas	2	1	2.71	m-xylene	EPA
P. promelas	3	1	2.71	m-xylene	EPA
P. promelas	4	1	2.71	m-xylene	EPA
P. promelas	1	1	5.22	m-xylene	EPA
P. promelas	2	1	5.22	m-xylene	EPA
P. promelas	3	1	5.22	m-xylene	EPA
P. promelas	4	1	5.22	m-xylene	EPA
P. promelas	1	1	9.76	m-xylene	EPA
P. promelas	2	1	9.76	m-xylene	EPA
P. promelas	3	1	9.76	m-xylene	EPA
P. promelas	4	1	9.76	m-xylene	EPA
P. promelas	1	0.8	14.9	m-xylene	EPA
P. promelas	2	0.55	14.9	m-xylene	EPA
P. promelas	3	0.55	14.9	m-xylene	EPA
P. promelas	4	0.55	14.9	m-xylene	EPA
P. promelas	1	0	27.4	m-xylene	EPA
P. promelas	2	0	27.4	m-xylene	EPA
P. promelas	3	0	27.4	m-xylene	EPA
P. promelas	4	0	27.4	m-xylene	EPA
P. promelas	1	1	0.02	m-xylene	EPA
P. promelas	2	1	0.02	m-xylene	EPA
P. promelas	3	1	0.02	m-xylene	EPA
P. promelas	4	1	0.02	m-xylene	EPA
P. promelas	1	1	1.11	m-xylene	EPA

Table continued

P. promelas	2	1	1.11	m-xylene	EPA
P. promelas	3	1	1.11	m-xylene	EPA
P. promelas	4	1	1.11	m-xylene	EPA
P. promelas	1	1	2.47	m-xylene	EPA
P. promelas	2	1	2.47	m-xylene	EPA
P. promelas	3	1	2.47	m-xylene	EPA
P. promelas	4	1	2.47	m-xylene	EPA
P. promelas	1	1	3.89	m-xylene	EPA
P. promelas	2	1	3.89	m-xylene	EPA
P. promelas	3	1	3.89	m-xylene	EPA
P. promelas	4	1	3.89	m-xylene	EPA
P. promelas	1	1	7.88	m-xylene	EPA
P. promelas	2	1	7.88	m-xylene	EPA
P. promelas	3	1	7.88	m-xylene	EPA
P. promelas	4	1	7.88	m-xylene	EPA
P. promelas	1	0.45	14.95	m-xylene	EPA
P. promelas	2	0.4	14.95	m-xylene	EPA
P. promelas	3	0.4	14.95	m-xylene	EPA
P. promelas	4	0.4	14.95	m-xylene	EPA
P. promelas	0.125	1	0.01	hexane	EPA
P. promelas	1	1	0.01	hexane	EPA
P. promelas	2	1	0.01	hexane	EPA
P. promelas	3	1	0.01	hexane	EPA
P. promelas	4	1	0.01	hexane	EPA
P. promelas	0.125	1	0.96	hexane	EPA
P. promelas	1	1	0.96	hexane	EPA
P. promelas	2	1	0.96	hexane	EPA
P. promelas	3	1	0.96	hexane	EPA
P. promelas	4	1	0.96	hexane	EPA
P. promelas	0.125	1	1.85	hexane	EPA
P. promelas	1	0.8	1.85	hexane	EPA
P. promelas	2	0.8	1.85	hexane	EPA
P. promelas	3	0.8	1.85	hexane	EPA
P. promelas	4	0.8	1.85	hexane	EPA
P. promelas	0.125	1	2.59	hexane	EPA
P. promelas	1	0.8	2.59	hexane	EPA
P. promelas	2	0.6	2.59	hexane	EPA
P. promelas	3	0.6	2.59	hexane	EPA

Table continued

P. promelas	4	0.6	2.59	hexane	EPA
P. promelas	0.125	1	4.02	hexane	EPA
P. promelas	1	0	4.02	hexane	EPA
P. promelas	2	0	4.02	hexane	EPA
P. promelas	3	0	4.02	hexane	EPA
P. promelas	4	0	4.02	hexane	EPA
P. promelas	0.125	0	4.99	hexane	EPA
P. promelas	1	0	4.99	hexane	EPA
P. promelas	2	0	4.99	hexane	EPA
P. promelas	3	0	4.99	hexane	EPA
P. promelas	4	0	4.99	hexane	EPA
A. bahia	0	1	0.001	ACE	Horne1983
A. bahia	0	1	0.07	ACE	Horne1983
A. bahia	0	1	0.12	ACE	Horne1983
A. bahia	0	1	0.17	ACE	Horne1983
A. bahia	0	1	0.28	ACE	Horne1983
A. bahia	0	1	0.33	ACE	Horne1983
A. bahia	1	0.95	0.001	ACE	Horne1983
A. bahia	1	1	0.07	ACE	Horne1983
A. bahia	1	1	0.12	ACE	Horne1983
A. bahia	1	0.95	0.17	ACE	Horne1983
A. bahia	1	0.95	0.28	ACE	Horne1983
A. bahia	1	1	0.33	ACE	Horne1983
A. bahia	2	0.95	0.001	ACE	Horne1983
A. bahia	2	1	0.07	ACE	Horne1983
A. bahia	2	1	0.12	ACE	Horne1983
A. bahia	2	0.95	0.17	ACE	Horne1983
A. bahia	2	0.85	0.28	ACE	Horne1983
A. bahia	2	0.6	0.33	ACE	Horne1983
A. bahia	3	0.95	0.001	ACE	Horne1983
A. bahia	3	0.95	0.07	ACE	Horne1983
A. bahia	3	1	0.12	ACE	Horne1983
A. bahia	3	0.95	0.17	ACE	Horne1983
A. bahia	3	0.75	0.28	ACE	Horne1983
A. bahia	3	0.2	0.33	ACE	Horne1983
A. bahia	4	0.95	0.001	ACE	Horne1983
A. bahia	4	0.9	0.07	ACE	Horne1983
A. bahia	4	0.95	0.12	ACE	Horne1983

Table continued

A. bahia	4	0.9	0.17	ACE	Horne1983
A. bahia	4	0.5	0.28	ACE	Horne1983
A. bahia	4	0.15	0.33	ACE	Horne1983
A. bahia	0	1	0.001	ACE	Horne1983
A. bahia	0	1	0.1	ACE	Horne1983
A. bahia	0	1	0.13	ACE	Horne1983
A. bahia	0	1	0.24	ACE	Horne1983
A. bahia	0	1	0.34	ACE	Horne1983
A. bahia	0	1	0.51	ACE	Horne1983
A. bahia	1	1	0.001	ACE	Horne1983
A. bahia	1	1	0.1	ACE	Horne1983
A. bahia	1	1	0.13	ACE	Horne1983
A. bahia	1	0.97	0.24	ACE	Horne1983
A. bahia	1	0.97	0.34	ACE	Horne1983
A. bahia	1	0.93	0.51	ACE	Horne1983
A. bahia	4	1	0.001	ACE	Horne1983
A. bahia	4	1	0.1	ACE	Horne1983
A. bahia	4	1	0.13	ACE	Horne1983
A. bahia	4	0.97	0.24	ACE	Horne1983
A. bahia	4	0.97	0.34	ACE	Horne1983
A. bahia	4	0.37	0.51	ACE	Horne1983
M. beryllina	0	1	0.001	ACE	Horne1983
M. beryllina	0	1	1.5	ACE	Horne1983
M. beryllina	0	1	1.67	ACE	Horne1983
M. beryllina	0	1	2	ACE	Horne1983
M. beryllina	0	1	2.33	ACE	Horne1983
M. beryllina	0	1	2.7	ACE	Horne1983
M. beryllina	1	0.95	0.001	ACE	Horne1983
M. beryllina	1	1	1.5	ACE	Horne1983
M. beryllina	1	1	1.67	ACE	Horne1983
M. beryllina	1	0.95	2	ACE	Horne1983
M. beryllina	1	0.95	2.33	ACE	Horne1983
M. beryllina	1	1	2.7	ACE	Horne1983
M. beryllina	2	0.95	0.001	ACE	Horne1983
M. beryllina	2	1	1.5	ACE	Horne1983
M. beryllina	2	1	1.67	ACE	Horne1983
M. beryllina	2	0.95	2	ACE	Horne1983
M. beryllina	2	0.85	2.33	ACE	Horne1983

Table continued

M. beryllina	2	0.6	2.7	ACE	Horne1983
M. beryllina	3	0.95	0.001	ACE	Horne1983
M. beryllina	3	0.95	1.5	ACE	Horne1983
M. beryllina	3	1	1.67	ACE	Horne1983
M. beryllina	3	0.95	2	ACE	Horne1983
M. beryllina	3	0.75	2.33	ACE	Horne1983
M. beryllina	3	0.2	2.7	ACE	Horne1983
M. beryllina	4	0.95	0.001	ACE	Horne1983
M. beryllina	4	0.9	1.5	ACE	Horne1983
M. beryllina	4	0.95	1.67	ACE	Horne1983
M. beryllina	4	0.9	2	ACE	Horne1983
M. beryllina	4	0.5	2.33	ACE	Horne1983
M. beryllina	4	0.15	2.7	ACE	Horne1983
N. arenacoedentata	0	1	0.001	ACE	Horne1983
N. arenacoedentata	0	1	2.61	ACE	Horne1983
N. arenacoedentata	0	1	3.07	ACE	Horne1983
N. arenacoedentata	0	1	3.61	ACE	Horne1983
N. arenacoedentata	0	1	4.25	ACE	Horne1983
N. arenacoedentata	0	1	5	ACE	Horne1983
N. arenacoedentata	1	1	0.001	ACE	Horne1983
N. arenacoedentata	1	1	2.61	ACE	Horne1983
N. arenacoedentata	1	0.95	3.07	ACE	Horne1983
N. arenacoedentata	1	0.9	3.61	ACE	Horne1983
N. arenacoedentata	1	1	4.25	ACE	Horne1983
N. arenacoedentata	1	0.95	5	ACE	Horne1983
N. arenacoedentata	2	1	0.001	ACE	Horne1983
N. arenacoedentata	2	0.8	2.61	ACE	Horne1983
N. arenacoedentata	2	0.9	3.07	ACE	Horne1983
N. arenacoedentata	2	0.5	3.61	ACE	Horne1983
N. arenacoedentata	2	0.55	4.25	ACE	Horne1983
N. arenacoedentata	2	0.65	5	ACE	Horne1983
N. arenacoedentata	3	1	0.001	ACE	Horne1983
N. arenacoedentata	3	0.8	2.61	ACE	Horne1983
N. arenacoedentata	3	0.85	3.07	ACE	Horne1983
N. arenacoedentata	3	0.4	3.61	ACE	Horne1983
N. arenacoedentata	3	0.5	4.25	ACE	Horne1983
N. arenacoedentata	3	0.25	5	ACE	Horne1983
N. arenacoedentata	4	0.95	0.001	ACE	Horne1983

Table continued

N. arenacoedentata	4	0.8	2.61	ACE	Horne1983
N. arenacoedentata	4	0.65	3.07	ACE	Horne1983
N. arenacoedentata	4	0.4	3.61	ACE	Horne1983
N. arenacoedentata	4	0.45	4.25	ACE	Horne1983
N. arenacoedentata	4	0.2	5	ACE	Horne1983
C. septemspinosus	0	1	0.001	ACE	Horne1983
C. septemspinosus	0	1	0.07	ACE	Horne1983
C. septemspinosus	0	1	0.1	ACE	Horne1983
C. septemspinosus	0	1	0.14	ACE	Horne1983
C. septemspinosus	0	1	0.19	ACE	Horne1983
C. septemspinosus	0	1	0.28	ACE	Horne1983
C. septemspinosus	0	1	0.4	ACE	Horne1983
C. septemspinosus	1	1	0.001	ACE	Horne1983
C. septemspinosus	1	0.95	0.07	ACE	Horne1983
C. septemspinosus	1	0.95	0.1	ACE	Horne1983
C. septemspinosus	1	0.95	0.14	ACE	Horne1983
C. septemspinosus	1	1	0.19	ACE	Horne1983
C. septemspinosus	1	0.8	0.28	ACE	Horne1983
C. septemspinosus	1	0.25	0.4	ACE	Horne1983
C. septemspinosus	2	1	0.001	ACE	Horne1983
C. septemspinosus	2	0.95	0.07	ACE	Horne1983
C. septemspinosus	2	0.95	0.1	ACE	Horne1983
C. septemspinosus	2	0.95	0.14	ACE	Horne1983
C. septemspinosus	2	0.8	0.19	ACE	Horne1983
C. septemspinosus	2	0.8	0.28	ACE	Horne1983
C. septemspinosus	2	0.25	0.4	ACE	Horne1983
C. septemspinosus	3	1	0.001	ACE	Horne1983
C. septemspinosus	3	0.9	0.07	ACE	Horne1983
C. septemspinosus	3	0.85	0.1	ACE	Horne1983
C. septemspinosus	3	0.85	0.14	ACE	Horne1983
C. septemspinosus	3	0.75	0.19	ACE	Horne1983
C. septemspinosus	3	0.8	0.28	ACE	Horne1983
C. septemspinosus	3	0.15	0.4	ACE	Horne1983
C. septemspinosus	4	0.95	0.001	ACE	Horne1983
C. septemspinosus	4	0.9	0.07	ACE	Horne1983
C. septemspinosus	4	0.75	0.1	ACE	Horne1983
C. septemspinosus	4	0.55	0.14	ACE	Horne1983
C. septemspinosus	4	0.7	0.19	ACE	Horne1983

Table continued

C. septemspinosus	4	0.6	0.28	ACE	Horne1983
C. septemspinosus	4	0.15	0.4	ACE	Horne1983
G. annulatus	0	1	0.001	ACE	Horne1983
G. annulatus	0	1	0.4	ACE	Horne1983
G. annulatus	0	1	0.5	ACE	Horne1983
G. annulatus	0	1	0.6	ACE	Horne1983
G. annulatus	0	1	0.78	ACE	Horne1983
G. annulatus	0	1	0.95	ACE	Horne1983
G. annulatus	0	1	1.2	ACE	Horne1983
G. annulatus	1	0.9	0.001	ACE	Horne1983
G. annulatus	1	1	0.4	ACE	Horne1983
G. annulatus	1	0.95	0.5	ACE	Horne1983
G. annulatus	1	0.9	0.6	ACE	Horne1983
G. annulatus	1	0.75	0.78	ACE	Horne1983
G. annulatus	1	0.5	0.95	ACE	Horne1983
G. annulatus	1	0.65	1.2	ACE	Horne1983
G. annulatus	2	0.8	0.001	ACE	Horne1983
G. annulatus	2	1	0.4	ACE	Horne1983
G. annulatus	2	0.95	0.5	ACE	Horne1983
G. annulatus	2	0.9	0.6	ACE	Horne1983
G. annulatus	2	0.7	0.78	ACE	Horne1983
G. annulatus	2	0.35	0.95	ACE	Horne1983
G. annulatus	2	0.55	1.2	ACE	Horne1983
G. annulatus	3	0.8	0.001	ACE	Horne1983
G. annulatus	3	1	0.4	ACE	Horne1983
G. annulatus	3	0.95	0.5	ACE	Horne1983
G. annulatus	3	0.9	0.6	ACE	Horne1983
G. annulatus	3	0.6	0.78	ACE	Horne1983
G. annulatus	3	0.35	0.95	ACE	Horne1983
G. annulatus	3	0.5	1.2	ACE	Horne1983
G. annulatus	4	0.8	0.001	ACE	Horne1983
G. annulatus	4	1	0.4	ACE	Horne1983
G. annulatus	4	0.95	0.5	ACE	Horne1983
G. annulatus	4	0.85	0.6	ACE	Horne1983
G. annulatus	4	0.6	0.78	ACE	Horne1983
G. annulatus	4	0.3	0.95	ACE	Horne1983
G. annulatus	4	0.45	1.2	ACE	Horne1983
A. tonsa	0	1	0.001	ACE	Horne1983

Table continued

A. tonsa	0	1	0.082	ACE	Horne1983
A. tonsa	0	1	1.024	ACE	Horne1983
A. tonsa	0	1	1.28	ACE	Horne1983
A. tonsa	0	1	1.6	ACE	Horne1983
A. tonsa	0	1	2	ACE	Horne1983
A. tonsa	0	1	2.5	ACE	Horne1983
A. tonsa	1	0.95	0.001	ACE	Horne1983
A. tonsa	1	0.85	0.082	ACE	Horne1983
A. tonsa	1	0.85	1.024	ACE	Horne1983
A. tonsa	1	0.55	1.28	ACE	Horne1983
A. tonsa	1	0.95	1.6	ACE	Horne1983
A. tonsa	1	0.4	2	ACE	Horne1983
A. tonsa	1	0.4	2.5	ACE	Horne1983
A. tonsa	2	0.9	0.001	ACE	Horne1983
A. tonsa	2	0.6	0.082	ACE	Horne1983
A. tonsa	2	0.8	1.024	ACE	Horne1983
A. tonsa	2	0.55	1.28	ACE	Horne1983
A. tonsa	2	0.95	1.6	ACE	Horne1983
A. tonsa	2	0.35	2	ACE	Horne1983
A. tonsa	2	0.35	2.5	ACE	Horne1983
A. tonsa	3	0.8	0.001	ACE	Horne1983
A. tonsa	3	0.55	0.082	ACE	Horne1983
A. tonsa	3	0.8	1.024	ACE	Horne1983
A. tonsa	3	0.5	1.28	ACE	Horne1983
A. tonsa	3	0.95	1.6	ACE	Horne1983
A. tonsa	3	0.25	2	ACE	Horne1983
A. tonsa	3	0.2	2.5	ACE	Horne1983
A. tonsa	4	0.8	0.001	ACE	Horne1983
A. tonsa	4	0.55	0.082	ACE	Horne1983
A. tonsa	4	0.8	1.024	ACE	Horne1983
A. tonsa	4	0.45	1.28	ACE	Horne1983
A. tonsa	4	0.95	1.6	ACE	Horne1983
A. tonsa	4	0.25	2	ACE	Horne1983
A. tonsa	4	0.2	2.5	ACE	Horne1983
P. maria	0	1	0.001	ACE	Horne1983
P. maria	0	1	0.288	ACE	Horne1983
P. maria	0	1	0.48	ACE	Horne1983
P. maria	0	1	0.799	ACE	Horne1983

Table continued

P. maria	0	1	1.332	ACE	Horne1983
P. maria	0	1	2.22	ACE	Horne1983
P. maria	0	1	3.7	ACE	Horne1983
P. maria	1	1	0.001	ACE	Horne1983
P. maria	1	1	0.288	ACE	Horne1983
P. maria	1	0.85	0.48	ACE	Horne1983
P. maria	1	0.95	0.799	ACE	Horne1983
P. maria	1	0.85	1.332	ACE	Horne1983
P. maria	1	0.75	2.22	ACE	Horne1983
P. maria	1	0.6	3.7	ACE	Horne1983
P. maria	2	0.9	0.001	ACE	Horne1983
P. maria	2	0.95	0.288	ACE	Horne1983
P. maria	2	0.85	0.48	ACE	Horne1983
P. maria	2	0.8	0.799	ACE	Horne1983
P. maria	2	0.7	1.332	ACE	Horne1983
P. maria	2	0.35	2.22	ACE	Horne1983
P. maria	2	0.25	3.7	ACE	Horne1983
P. maria	3	0.9	0.001	ACE	Horne1983
P. maria	3	0.95	0.288	ACE	Horne1983
P. maria	3	0.7	0.48	ACE	Horne1983
P. maria	3	0.5	0.799	ACE	Horne1983
P. maria	3	0.15	1.332	ACE	Horne1983
P. maria	3	0.05	2.22	ACE	Horne1983
P. maria	3	0	3.7	ACE	Horne1983
P. maria	4	0.9	0.001	ACE	Horne1983
P. maria	4	0.75	0.288	ACE	Horne1983
P. maria	4	0.55	0.48	ACE	Horne1983
P. maria	4	0.35	0.799	ACE	Horne1983
P. maria	4	0.15	1.332	ACE	Horne1983
P. maria	4	0.05	2.22	ACE	Horne1983
P. maria	4	0	3.7	ACE	Horne1983
G. minor	0	1	0.001	ACE	Horne1983
G. minor	0	1	0.288	ACE	Horne1983
G. minor	0	1	0.48	ACE	Horne1983
G. minor	0	1	0.799	ACE	Horne1983
G. minor	0	1	1.332	ACE	Horne1983
G. minor	0	1	2.22	ACE	Horne1983
G. minor	0	1	3.7	ACE	Horne1983

Table continued

G. minor	1	1	0.001	ACE	Horne1983
G. minor	1	1	0.288	ACE	Horne1983
G. minor	1	1	0.48	ACE	Horne1983
G. minor	1	0.95	0.799	ACE	Horne1983
G. minor	1	0.95	1.332	ACE	Horne1983
G. minor	1	0.65	2.22	ACE	Horne1983
G. minor	1	0.15	3.7	ACE	Horne1983
G. minor	2	1	0.001	ACE	Horne1983
G. minor	2	1	0.288	ACE	Horne1983
G. minor	2	1	0.48	ACE	Horne1983
G. minor	2	0.95	0.799	ACE	Horne1983
G. minor	2	0.3	1.332	ACE	Horne1983
G. minor	2	0.1	2.22	ACE	Horne1983
G. minor	2	0	3.7	ACE	Horne1983
G. minor	3	1	0.001	ACE	Horne1983
G. minor	3	1	0.288	ACE	Horne1983
G. minor	3	1	0.48	ACE	Horne1983
G. minor	3	0.85	0.799	ACE	Horne1983
G. minor	3	0.1	1.332	ACE	Horne1983
G. minor	3	0	2.22	ACE	Horne1983
G. minor	3	0	3.7	ACE	Horne1983
G. minor	4	1	0.001	ACE	Horne1983
G. minor	4	1	0.288	ACE	Horne1983
G. minor	4	0.95	0.48	ACE	Horne1983
G. minor	4	0.65	0.799	ACE	Horne1983
G. minor	4	0	1.332	ACE	Horne1983
G. minor	4	0	2.22	ACE	Horne1983
G. minor	4	0	3.7	ACE	Horne1983
A. bahia	1	1	0.031	FLA	Turner1982
A. bahia	1	1	0.016	FLA	Turner1982
A. bahia	1	1	0.007	FLA	Turner1982
A. bahia	1	1	0.0029	FLA	Turner1982
A. bahia	1	1	0.0013	FLA	Turner1982
A. bahia	1	1	0.0001	FLA	Turner1982
A. bahia	1	0	0.078	FLA	Turner1982
A. bahia	1	1	0.04	FLA	Turner1982
A. bahia	1	1	0.022	FLA	Turner1982
A. bahia	1	1	0.01	FLA	Turner1982

Table continued

A. bahia	1	1	0.006	FLA	Turner1982
A. bahia	1	1	0.0002	FLA	Turner1982
A. bahia	1	0.65	0.077	FLA	Turner1982
A. bahia	1	0.95	0.043	FLA	Turner1982
A. bahia	1	1	0.02	FLA	Turner1982
A. bahia	1	1	0.013	FLA	Turner1982
A. bahia	1	1	0.008	FLA	Turner1982
A. bahia	1	1	0.0003	FLA	Turner1982
A. bahia	2	0.75	0.031	FLA	Turner1982
A. bahia	2	0.95	0.016	FLA	Turner1982
A. bahia	2	1	0.007	FLA	Turner1982
A. bahia	2	1	0.0029	FLA	Turner1982
A. bahia	2	1	0.0013	FLA	Turner1982
A. bahia	2	1	0.0001	FLA	Turner1982
A. bahia	2	0	0.078	FLA	Turner1982
A. bahia	2	0.85	0.04	FLA	Turner1982
A. bahia	2	1	0.022	FLA	Turner1982
A. bahia	2	1	0.01	FLA	Turner1982
A. bahia	2	1	0.006	FLA	Turner1982
A. bahia	2	1	0.0002	FLA	Turner1982
A. bahia	2	0.5	0.077	FLA	Turner1982
A. bahia	2	0.95	0.043	FLA	Turner1982
A. bahia	2	1	0.02	FLA	Turner1982
A. bahia	2	1	0.013	FLA	Turner1982
A. bahia	2	1	0.008	FLA	Turner1982
A. bahia	2	1	0.0003	FLA	Turner1982
A. bahia	3	0.2	0.031	FLA	Turner1982
A. bahia	3	0.95	0.016	FLA	Turner1982
A. bahia	3	1	0.007	FLA	Turner1982
A. bahia	3	1	0.0029	FLA	Turner1982
A. bahia	3	0.95	0.0013	FLA	Turner1982
A. bahia	3	1	0.0001	FLA	Turner1982
A. bahia	3	0	0.078	FLA	Turner1982
A. bahia	3	0.8	0.04	FLA	Turner1982
A. bahia	3	1	0.022	FLA	Turner1982
A. bahia	3	0.95	0.01	FLA	Turner1982
A. bahia	3	1	0.006	FLA	Turner1982
A. bahia	3	1	0.0002	FLA	Turner1982

Table continued

A. bahia	3	0	0.077	FLA	Turner1982
A. bahia	3	0.9	0.043	FLA	Turner1982
A. bahia	3	0.95	0.02	FLA	Turner1982
A. bahia	3	0.95	0.013	FLA	Turner1982
A. bahia	3	1	0.008	FLA	Turner1982
A. bahia	3	1	0.0003	FLA	Turner1982
A. bahia	4	0.05	0.031	FLA	Turner1982
A. bahia	4	0.9	0.016	FLA	Turner1982
A. bahia	4	1	0.007	FLA	Turner1982
A. bahia	4	1	0.0029	FLA	Turner1982
A. bahia	4	0.95	0.0013	FLA	Turner1982
A. bahia	4	0.95	0.0001	FLA	Turner1982
A. bahia	4	0	0.078	FLA	Turner1982
A. bahia	4	0.7	0.04	FLA	Turner1982
A. bahia	4	1	0.022	FLA	Turner1982
A. bahia	4	0.95	0.01	FLA	Turner1982
A. bahia	4	1	0.006	FLA	Turner1982
A. bahia	4	0.95	0.0002	FLA	Turner1982
A. bahia	4	0	0.077	FLA	Turner1982
A. bahia	4	0.5	0.043	FLA	Turner1982
A. bahia	4	0.9	0.02	FLA	Turner1982
A. bahia	4	0.95	0.013	FLA	Turner1982
A. bahia	4	1	0.008	FLA	Turner1982
A. bahia	4	1	0.0003	FLA	Turner1982
A. bahia	1	0.25	0.29	ACE	Turner1982
A. bahia	1	1	0.14	ACE	Turner1982
A. bahia	1	1	0.074	ACE	Turner1982
A. bahia	1	1	0.06	ACE	Turner1982
A. bahia	1	1	0.02	ACE	Turner1982
A. bahia	1	1	0.001	ACE	Turner1982
A. bahia	1	0.45	0.39	ACE	Turner1982
A. bahia	1	1	0.18	ACE	Turner1982
A. bahia	1	1	0.072	ACE	Turner1982
A. bahia	1	1	0.03	ACE	Turner1982
A. bahia	1	1	0.014	ACE	Turner1982
A. bahia	1	1	0.002	ACE	Turner1982
A. bahia	2	0.2	0.29	ACE	Turner1982
A. bahia	2	0.95	0.14	ACE	Turner1982

Table continued

A. bahia	2	0.95	0.074	ACE	Turner1982
A. bahia	2	1	0.06	ACE	Turner1982
A. bahia	2	1	0.02	ACE	Turner1982
A. bahia	2	1	0.001	ACE	Turner1982
A. bahia	2	0.2	0.39	ACE	Turner1982
A. bahia	2	0.9	0.18	ACE	Turner1982
A. bahia	2	1	0.072	ACE	Turner1982
A. bahia	2	1	0.03	ACE	Turner1982
A. bahia	2	1	0.014	ACE	Turner1982
A. bahia	2	1	0.002	ACE	Turner1982
A. bahia	3	0.05	0.29	ACE	Turner1982
A. bahia	3	0.9	0.14	ACE	Turner1982
A. bahia	3	0.95	0.074	ACE	Turner1982
A. bahia	3	1	0.06	ACE	Turner1982
A. bahia	3	1	0.02	ACE	Turner1982
A. bahia	3	0.95	0.001	ACE	Turner1982
A. bahia	3	0.1	0.39	ACE	Turner1982
A. bahia	3	0.75	0.18	ACE	Turner1982
A. bahia	3	0.95	0.072	ACE	Turner1982
A. bahia	3	1	0.03	ACE	Turner1982
A. bahia	3	1	0.014	ACE	Turner1982
A. bahia	3	1	0.002	ACE	Turner1982
A. bahia	4	0	0.29	ACE	Turner1982
A. bahia	4	0.8	0.14	ACE	Turner1982
A. bahia	4	0.9	0.074	ACE	Turner1982
A. bahia	4	1	0.06	ACE	Turner1982
A. bahia	4	1	0.02	ACE	Turner1982
A. bahia	4	0.95	0.001	ACE	Turner1982
A. bahia	4	0	0.39	ACE	Turner1982
A. bahia	4	0.75	0.18	ACE	Turner1982
A. bahia	4	0.9	0.072	ACE	Turner1982
A. bahia	4	0.966667	0.03	ACE	Turner1982
A. bahia	4	1	0.014	ACE	Turner1982
A. bahia	4	1	0.002	ACE	Turner1982
P. promelas	1	0.533333	2.7	ACE	Turner1982
P. promelas	1	0.9	1.7	ACE	Turner1982
P. promelas	1	1	1.4	ACE	Turner1982
P. promelas	1	1	0.6	ACE	Turner1982

Table continued

P. promelas	1	1	0.36	ACE	Turner1982
P. promelas	1	1	0.001	ACE	Turner1982
P. promelas	1	1	1.41	ACE	Turner1982
P. promelas	1	1	0.71	ACE	Turner1982
P. promelas	1	1	0.45	ACE	Turner1982
P. promelas	1	1	0.29	ACE	Turner1982
P. promelas	1	1	0.16	ACE	Turner1982
P. promelas	1	1	0.1	ACE	Turner1982
P. promelas	1	1	0.002	ACE	Turner1982
P. promelas	2	0.05	2.7	ACE	Turner1982
P. promelas	2	0.6	1.7	ACE	Turner1982
P. promelas	2	1	1.4	ACE	Turner1982
P. promelas	2	1	0.6	ACE	Turner1982
P. promelas	2	1	0.36	ACE	Turner1982
P. promelas	2	1	0.001	ACE	Turner1982
P. promelas	2	1	1.41	ACE	Turner1982
P. promelas	2	1	0.71	ACE	Turner1982
P. promelas	2	1	0.45	ACE	Turner1982
P. promelas	2	1	0.29	ACE	Turner1982
P. promelas	2	1	0.16	ACE	Turner1982
P. promelas	2	1	0.1	ACE	Turner1982
P. promelas	2	1	0.002	ACE	Turner1982
P. promelas	3	0	2.7	ACE	Turner1982
P. promelas	3	0	1.7	ACE	Turner1982
P. promelas	3	0.9	1.4	ACE	Turner1982
P. promelas	3	1	0.6	ACE	Turner1982
P. promelas	3	1	0.36	ACE	Turner1982
P. promelas	3	1	0.001	ACE	Turner1982
P. promelas	3	1	1.41	ACE	Turner1982
P. promelas	3	1	0.71	ACE	Turner1982
P. promelas	3	1	0.45	ACE	Turner1982
P. promelas	3	1	0.29	ACE	Turner1982
P. promelas	3	1	0.16	ACE	Turner1982
P. promelas	3	1	0.1	ACE	Turner1982
P. promelas	3	1	0.002	ACE	Turner1982
P. promelas	4	0	2.7	ACE	Turner1982
P. promelas	4	0	1.7	ACE	Turner1982
P. promelas	4	0.75	1.4	ACE	Turner1982

Table continued

P. promelas	4	1	0.6	ACE	Turner1982
P. promelas	4	1	0.36	ACE	Turner1982
P. promelas	4	1	0.001	ACE	Turner1982
P. promelas	4	1	1.41	ACE	Turner1982
P. promelas	4	1	0.71	ACE	Turner1982
P. promelas	4	1	0.45	ACE	Turner1982
P. promelas	4	1	0.29	ACE	Turner1982
P. promelas	4	1	0.16	ACE	Turner1982
P. promelas	4	1	0.1	ACE	Turner1982
P. promelas	4	1	0.002	ACE	Turner1982
C. dubia	1	1	0.02	FLU	EMBSI 2013
C. dubia	2	1	0.02	FLU	EMBSI 2013
C. dubia	3	1	0.02	FLU	EMBSI 2013
C. dubia	4	1	0.02	FLU	EMBSI 2013
C. dubia	1	1	0.05	FLU	EMBSI 2013
C. dubia	2	1	0.05	FLU	EMBSI 2013
C. dubia	3	1	0.05	FLU	EMBSI 2013
C. dubia	4	1	0.05	FLU	EMBSI 2013
C. dubia	1	1	0.128	FLU	EMBSI 2013
C. dubia	2	1	0.128	FLU	EMBSI 2013
C. dubia	3	1	0.128	FLU	EMBSI 2013
C. dubia	4	1	0.128	FLU	EMBSI 2013
C. dubia	1	1	0.257	FLU	EMBSI 2013
C. dubia	2	1	0.257	FLU	EMBSI 2013
C. dubia	3	1	0.257	FLU	EMBSI 2013
C. dubia	4	1	0.257	FLU	EMBSI 2013
C. dubia	1	0.9	0.536	FLU	EMBSI 2013
C. dubia	2	0.7	0.536	FLU	EMBSI 2013
C. dubia	3	0.6	0.536	FLU	EMBSI 2013
C. dubia	4	0.5	0.536	FLU	EMBSI 2013
C. dubia	1	1	0.0011	mePYR	EMBSI 2013
C. dubia	2	1	0.0011	mePYR	EMBSI 2013
C. dubia	3	1	0.0011	mePYR	EMBSI 2013
C. dubia	4	1	0.0011	mePYR	EMBSI 2013
C. dubia	1	1	0.0027	mePYR	EMBSI 2013
C. dubia	2	1	0.0027	mePYR	EMBSI 2013
C. dubia	3	1	0.0027	mePYR	EMBSI 2013
C. dubia	4	1	0.0027	mePYR	EMBSI 2013

Table continued

C. dubia	1	1	0.0068	mePYR	EMBSI 2013
C. dubia	2	1	0.0068	mePYR	EMBSI 2013
C. dubia	3	1	0.0068	mePYR	EMBSI 2013
C. dubia	4	1	0.0068	mePYR	EMBSI 2013
C. dubia	1	1	0.017	mePYR	EMBSI 2013
C. dubia	2	1	0.017	mePYR	EMBSI 2013
C. dubia	3	1	0.017	mePYR	EMBSI 2013
C. dubia	4	0.9	0.017	mePYR	EMBSI 2013
C. dubia	1	1	0.048	mePYR	EMBSI 2013
C. dubia	2	1	0.048	mePYR	EMBSI 2013
C. dubia	3	0.9	0.048	mePYR	EMBSI 2013
C. dubia	4	0.9	0.048	mePYR	EMBSI 2013
C. dubia	1	0.8	0.184	mePYR	EMBSI 2013
C. dubia	2	0	0.184	mePYR	EMBSI 2013
C. dubia	3	0	0.184	mePYR	EMBSI 2013
C. dubia	4	0	0.184	mePYR	EMBSI 2013
C. dubia	1	1	0.184	meHexene	EMBSI 2013
C. dubia	2	1	0.184	meHexene	EMBSI 2013
C. dubia	3	1	0.184	meHexene	EMBSI 2013
C. dubia	4	1	0.184	meHexene	EMBSI 2013
C. dubia	1	1	0.317	meHexene	EMBSI 2013
C. dubia	2	1	0.317	meHexene	EMBSI 2013
C. dubia	3	1	0.317	meHexene	EMBSI 2013
C. dubia	4	1	0.317	meHexene	EMBSI 2013
C. dubia	1	1	0.917	meHexene	EMBSI 2013
C. dubia	2	1	0.917	meHexene	EMBSI 2013
C. dubia	3	1	0.917	meHexene	EMBSI 2013
C. dubia	4	1	0.917	meHexene	EMBSI 2013
C. dubia	1	1	1.55	meHexene	EMBSI 2013
C. dubia	2	0.9	1.55	meHexene	EMBSI 2013
C. dubia	3	0.8	1.55	meHexene	EMBSI 2013
C. dubia	4	0.8	1.55	meHexene	EMBSI 2013
C. dubia	1	0.9	5.02	meHexene	EMBSI 2013
C. dubia	2	0	5.02	meHexene	EMBSI 2013
C. dubia	3	0	5.02	meHexene	EMBSI 2013
C. dubia	4	0	5.02	meHexene	EMBSI 2013
C. finmarchus	0	1	0.0011	meNAP	Jager2017
C. finmarchus	1	1	0.0011	meNAP	Jager2017

Table continued

C. finmarchus	2	1	0.0011	meNAP	Jager2017
C. finmarchus	3	1	0.0011	meNAP	Jager2017
C. finmarchus	4	1	0.0011	meNAP	Jager2017
C. finmarchus	0	1	1.03	meNAP	Jager2017
C. finmarchus	1	1	1.03	meNAP	Jager2017
C. finmarchus	2	1	1.03	meNAP	Jager2017
C. finmarchus	3	1	1.03	meNAP	Jager2017
C. finmarchus	4	0.982143	1.03	meNAP	Jager2017
C. finmarchus	0	1	1.97	meNAP	Jager2017
C. finmarchus	1	1	1.97	meNAP	Jager2017
C. finmarchus	2	1	1.97	meNAP	Jager2017
C. finmarchus	3	1	1.97	meNAP	Jager2017
C. finmarchus	4	0.928571	1.97	meNAP	Jager2017
C. finmarchus	0	1	4.83	meNAP	Jager2017
C. finmarchus	1	1	4.83	meNAP	Jager2017
C. finmarchus	2	1	4.83	meNAP	Jager2017
C. finmarchus	3	0.928571	4.83	meNAP	Jager2017
C. finmarchus	4	0.75	4.83	meNAP	Jager2017
C. finmarchus	0	1	10.3	meNAP	Jager2017
C. finmarchus	1	0.892857	10.3	meNAP	Jager2017
C. finmarchus	2	0.357143	10.3	meNAP	Jager2017
C. finmarchus	3	0.035714	10.3	meNAP	Jager2017
C. finmarchus	4	0	10.3	meNAP	Jager2017
C. finmarchus	0	1	29.3	meNAP	Jager2017
C. finmarchus	1	0	29.3	meNAP	Jager2017
C. finmarchus	2	0	29.3	meNAP	Jager2017
C. finmarchus	3	0	29.3	meNAP	Jager2017
C. finmarchus	4	0	29.3	meNAP	Jager2017
O. mykiss	0.083333	1	0.001	meNAP	SmFs_18d
O. mykiss	0.166667	1	0.001	meNAP	SmFs_18d
O. mykiss	0.25	1	0.001	meNAP	SmFs_18d
O. mykiss	0.333333	1	0.001	meNAP	SmFs_18d
O. mykiss	1	1	0.001	meNAP	SmFs_18d
O. mykiss	2	1	0.001	meNAP	SmFs_18d
O. mykiss	3	1	0.001	meNAP	SmFs_18d
O. mykiss	4	1	0.001	meNAP	SmFs_18d
O. mykiss	0.083333	1	0.35125	meNAP	SmFs_18d
O. mykiss	0.166667	1	0.35125	meNAP	SmFs_18d

Table continued

O. mykiss	0.25	1	0.35125	meNAP	SmFs_18d
O. mykiss	0.333333	1	0.35125	meNAP	SmFs_18d
O. mykiss	1	1	0.35125	meNAP	SmFs_18d
O. mykiss	2	1	0.35125	meNAP	SmFs_18d
O. mykiss	3	1	0.35125	meNAP	SmFs_18d
O. mykiss	4	1	0.35125	meNAP	SmFs_18d
O. mykiss	0.083333	1	1.19	meNAP	SmFs_18d
O. mykiss	0.166667	1	1.19	meNAP	SmFs_18d
O. mykiss	0.25	1	1.19	meNAP	SmFs_18d
O. mykiss	0.333333	1	1.19	meNAP	SmFs_18d
O. mykiss	1	1	1.19	meNAP	SmFs_18d
O. mykiss	2	1	1.19	meNAP	SmFs_18d
O. mykiss	3	1	1.19	meNAP	SmFs_18d
O. mykiss	4	1	1.19	meNAP	SmFs_18d
O. mykiss	0.083333	1	3.6175	meNAP	SmFs_18d
O. mykiss	0.166667	1	3.6175	meNAP	SmFs_18d
O. mykiss	0.25	1	3.6175	meNAP	SmFs_18d
O. mykiss	0.333333	0.857143	3.6175	meNAP	SmFs_18d
O. mykiss	1	0.071429	3.6175	meNAP	SmFs_18d
O. mykiss	2	0	3.6175	meNAP	SmFs_18d
O. mykiss	3	0	3.6175	meNAP	SmFs_18d
O. mykiss	4	0	3.6175	meNAP	SmFs_18d
O. mykiss	0.083333	0.357143	11.45	meNAP	SmFs_18d
O. mykiss	0.166667	0	11.45	meNAP	SmFs_18d
O. mykiss	0.25	0	11.45	meNAP	SmFs_18d
O. mykiss	0.333333	0	11.45	meNAP	SmFs_18d
O. mykiss	1	0	11.45	meNAP	SmFs_18d
O. mykiss	2	0	11.45	meNAP	SmFs_18d
O. mykiss	3	0	11.45	meNAP	SmFs_18d
O. mykiss	4	0	11.45	meNAP	SmFs_18d
O. mykiss	0.083333	1	0.001	meNAP	LgFs_18d
O. mykiss	0.166667	1	0.001	meNAP	LgFs_18d
O. mykiss	0.25	1	0.001	meNAP	LgFs_18d
O. mykiss	1	1	0.001	meNAP	LgFs_18d
O. mykiss	2	1	0.001	meNAP	LgFs_18d
O. mykiss	3	1	0.001	meNAP	LgFs_18d
O. mykiss	4	1	0.001	meNAP	LgFs_18d
O. mykiss	0.083333	1	0.36775	meNAP	LgFs_18d

Table continued

O. mykiss	0.166667	1	0.36775	meNAP	LgFs_18d
O. mykiss	0.25	1	0.36775	meNAP	LgFs_18d
O. mykiss	1	1	0.36775	meNAP	LgFs_18d
O. mykiss	2	1	0.36775	meNAP	LgFs_18d
O. mykiss	3	1	0.36775	meNAP	LgFs_18d
O. mykiss	4	1	0.36775	meNAP	LgFs_18d
O. mykiss	0.083333	1	1.24	meNAP	LgFs_18d
O. mykiss	0.166667	1	1.24	meNAP	LgFs_18d
O. mykiss	0.25	1	1.24	meNAP	LgFs_18d
O. mykiss	1	1	1.24	meNAP	LgFs_18d
O. mykiss	2	1	1.24	meNAP	LgFs_18d
O. mykiss	3	1	1.24	meNAP	LgFs_18d
O. mykiss	4	1	1.24	meNAP	LgFs_18d
O. mykiss	0.083333	1	3.5425	meNAP	LgFs_18d
O. mykiss	0.166667	1	3.5425	meNAP	LgFs_18d
O. mykiss	0.25	1	3.5425	meNAP	LgFs_18d
O. mykiss	1	0.214286	3.5425	meNAP	LgFs_18d
O. mykiss	2	0	3.5425	meNAP	LgFs_18d
O. mykiss	3	0	3.5425	meNAP	LgFs_18d
O. mykiss	4	0	3.5425	meNAP	LgFs_18d
O. mykiss	0.083333	1	11.6	meNAP	LgFs_18d
O. mykiss	0.166667	0.5	11.6	meNAP	LgFs_18d
O. mykiss	0.25	0.142857	11.6	meNAP	LgFs_18d
O. mykiss	1	0	11.6	meNAP	LgFs_18d
O. mykiss	2	0	11.6	meNAP	LgFs_18d
O. mykiss	3	0	11.6	meNAP	LgFs_18d
O. mykiss	4	0	11.6	meNAP	LgFs_18d
O. mykiss	0.083333	1	0.001	meNAP	SmFs_10d
O. mykiss	0.166667	1	0.001	meNAP	SmFs_10d
O. mykiss	0.25	1	0.001	meNAP	SmFs_10d
O. mykiss	1	1	0.001	meNAP	SmFs_10d
O. mykiss	2	1	0.001	meNAP	SmFs_10d
O. mykiss	3	1	0.001	meNAP	SmFs_10d
O. mykiss	4	1	0.001	meNAP	SmFs_10d
O. mykiss	0.083333	1	0.3405	meNAP	SmFs_10d
O. mykiss	0.166667	1	0.3405	meNAP	SmFs_10d
O. mykiss	0.25	1	0.3405	meNAP	SmFs_10d
O. mykiss	1	1	0.3405	meNAP	SmFs_10d

Table continued

O. mykiss	2	1	0.3405	meNAP	SmFs_10d
O. mykiss	3	1	0.3405	meNAP	SmFs_10d
O. mykiss	4	1	0.3405	meNAP	SmFs_10d
O. mykiss	0.083333	1	1.10175	meNAP	SmFs_10d
O. mykiss	0.166667	1	1.10175	meNAP	SmFs_10d
O. mykiss	0.25	1	1.10175	meNAP	SmFs_10d
O. mykiss	1	1	1.10175	meNAP	SmFs_10d
O. mykiss	2	1	1.10175	meNAP	SmFs_10d
O. mykiss	3	1	1.10175	meNAP	SmFs_10d
O. mykiss	4	1	1.10175	meNAP	SmFs_10d
O. mykiss	0.083333	1	3.345	meNAP	SmFs_10d
O. mykiss	0.166667	0.5	3.345	meNAP	SmFs_10d
O. mykiss	0.25	0.285714	3.345	meNAP	SmFs_10d
O. mykiss	1	0	3.345	meNAP	SmFs_10d
O. mykiss	2	0	3.345	meNAP	SmFs_10d
O. mykiss	3	0	3.345	meNAP	SmFs_10d
O. mykiss	4	0	3.345	meNAP	SmFs_10d
O. mykiss	0.083333	1	9.9075	meNAP	SmFs_10d
O. mykiss	0.166667	0.071429	9.9075	meNAP	SmFs_10d
O. mykiss	0.25	0	9.9075	meNAP	SmFs_10d
O. mykiss	1	0	9.9075	meNAP	SmFs_10d
O. mykiss	2	0	9.9075	meNAP	SmFs_10d
O. mykiss	3	0	9.9075	meNAP	SmFs_10d
O. mykiss	4	0	9.9075	meNAP	SmFs_10d
O. mykiss	0.083333	1	0.001	meNAP	LgFs_10d
O. mykiss	0.166667	1	0.001	meNAP	LgFs_10d
O. mykiss	0.25	1	0.001	meNAP	LgFs_10d
O. mykiss	1	1	0.001	meNAP	LgFs_10d
O. mykiss	2	1	0.001	meNAP	LgFs_10d
O. mykiss	3	1	0.001	meNAP	LgFs_10d
O. mykiss	4	1	0.001	meNAP	LgFs_10d
O. mykiss	0.083333	1	0.3395	meNAP	LgFs_10d
O. mykiss	0.166667	1	0.3395	meNAP	LgFs_10d
O. mykiss	0.25	1	0.3395	meNAP	LgFs_10d
O. mykiss	1	1	0.3395	meNAP	LgFs_10d
O. mykiss	2	1	0.3395	meNAP	LgFs_10d
O. mykiss	3	1	0.3395	meNAP	LgFs_10d
O. mykiss	4	1	0.3395	meNAP	LgFs_10d

Table continued

O. mykiss	0.083333	1	1.105	meNAP	LgFs_10d
O. mykiss	0.166667	1	1.105	meNAP	LgFs_10d
O. mykiss	0.25	1	1.105	meNAP	LgFs_10d
O. mykiss	1	1	1.105	meNAP	LgFs_10d
O. mykiss	2	1	1.105	meNAP	LgFs_10d
O. mykiss	3	1	1.105	meNAP	LgFs_10d
O. mykiss	4	1	1.105	meNAP	LgFs_10d
O. mykiss	0.083333	1	2.9225	meNAP	LgFs_10d
O. mykiss	0.166667	1	2.9225	meNAP	LgFs_10d
O. mykiss	0.25	1	2.9225	meNAP	LgFs_10d
O. mykiss	1	0.5	2.9225	meNAP	LgFs_10d
O. mykiss	2	0	2.9225	meNAP	LgFs_10d
O. mykiss	3	0	2.9225	meNAP	LgFs_10d
O. mykiss	4	0	2.9225	meNAP	LgFs_10d
O. mykiss	0.083333	1	10.3375	meNAP	LgFs_10d
O. mykiss	0.166667	0.642857	10.3375	meNAP	LgFs_10d
O. mykiss	0.25	0	10.3375	meNAP	LgFs_10d
O. mykiss	1	0	10.3375	meNAP	LgFs_10d
O. mykiss	2	0	10.3375	meNAP	LgFs_10d
O. mykiss	3	0	10.3375	meNAP	LgFs_10d
O. mykiss	4	0	10.3375	meNAP	LgFs_10d
D. magna	0.083333	1	0.001	meNAP	Dm_18d
D. magna	0.166667	1	0.001	meNAP	Dm_18d
D. magna	0.25	1	0.001	meNAP	Dm_18d
D. magna	1	1	0.001	meNAP	Dm_18d
D. magna	2	1	0.001	meNAP	Dm_18d
D. magna	0.083333	1	0.3635	meNAP	Dm_18d
D. magna	0.166667	1	0.3635	meNAP	Dm_18d
D. magna	0.25	1	0.3635	meNAP	Dm_18d
D. magna	1	1	0.3635	meNAP	Dm_18d
D. magna	2	1	0.3635	meNAP	Dm_18d
D. magna	0.083333	1	1.06	meNAP	Dm_18d
D. magna	0.166667	1	1.06	meNAP	Dm_18d
D. magna	0.25	1	1.06	meNAP	Dm_18d
D. magna	1	1	1.06	meNAP	Dm_18d
D. magna	2	1	1.06	meNAP	Dm_18d
D. magna	0.083333	1	3.8025	meNAP	Dm_18d
D. magna	0.166667	0.85	3.8025	meNAP	Dm_18d

Table continued

D. magna	0.25	0.85	3.8025	meNAP	Dm_18d
D. magna	1	0.35	3.8025	meNAP	Dm_18d
D. magna	2	0.05	3.8025	meNAP	Dm_18d
D. magna	0.083333	0	10.9	meNAP	Dm_18d
D. magna	0.166667	0	10.9	meNAP	Dm_18d
D. magna	0.25	0	10.9	meNAP	Dm_18d
D. magna	1	0	10.9	meNAP	Dm_18d
D. magna	2	0	10.9	meNAP	Dm_18d
L. variegatus	0.083333	1	0.001	meNAP	Wm_18d
L. variegatus	0.166667	1	0.001	meNAP	Wm_18d
L. variegatus	0.25	1	0.001	meNAP	Wm_18d
L. variegatus	1	1	0.001	meNAP	Wm_18d
L. variegatus	2	1	0.001	meNAP	Wm_18d
L. variegatus	3	1	0.001	meNAP	Wm_18d
L. variegatus	4	1	0.001	meNAP	Wm_18d
L. variegatus	0.083333	1	0.33525	meNAP	Wm_18d
L. variegatus	0.166667	1	0.33525	meNAP	Wm_18d
L. variegatus	0.25	1	0.33525	meNAP	Wm_18d
L. variegatus	1	1	0.33525	meNAP	Wm_18d
L. variegatus	2	1	0.33525	meNAP	Wm_18d
L. variegatus	3	1	0.33525	meNAP	Wm_18d
L. variegatus	4	1	0.33525	meNAP	Wm_18d
L. variegatus	0.083333	1	1.17	meNAP	Wm_18d
L. variegatus	0.166667	1	1.17	meNAP	Wm_18d
L. variegatus	0.25	1	1.17	meNAP	Wm_18d
L. variegatus	1	1	1.17	meNAP	Wm_18d
L. variegatus	2	1	1.17	meNAP	Wm_18d
L. variegatus	3	1	1.17	meNAP	Wm_18d
L. variegatus	4	1	1.17	meNAP	Wm_18d
L. variegatus	0.083333	1	3.5125	meNAP	Wm_18d
L. variegatus	0.166667	1	3.5125	meNAP	Wm_18d
L. variegatus	0.25	1	3.5125	meNAP	Wm_18d
L. variegatus	1	1	3.5125	meNAP	Wm_18d
L. variegatus	2	1	3.5125	meNAP	Wm_18d
L. variegatus	3	0.75	3.5125	meNAP	Wm_18d
L. variegatus	4	0.05	3.5125	meNAP	Wm_18d
L. variegatus	0.083333	1	11.25	meNAP	Wm_18d
L. variegatus	0.166667	1	11.25	meNAP	Wm_18d

Table continued

L. variegatus	0.25	0.55	11.25	meNAP	Wm_18d
L. variegatus	1	0.45	11.25	meNAP	Wm_18d
L. variegatus	2	0.45	11.25	meNAP	Wm_18d
L. variegatus	3	0	11.25	meNAP	Wm_18d
L. variegatus	4	0	11.25	meNAP	Wm_18d